Superoscillations in the Quantum Harmonic Oscillator

Max Bussell

Physical Science Theoretical Physics Group
—— University of Kent ——

Thesis submitted to the University of Kent
for the degree of Master of Science in Physics by Research.

Principal Supervisor: Professor of Physics Paul Strange

—— March 2015 ——

ABSTRACT

A superoscillatory function is one that oscillates faster than its fastest Fourier component - A phenomenon created by subtle interference between Fourier components. In this thesis, the work of Professor Sir Michael Berry [1, 2] and Professor Sandu Popescu on superoscillations in free space [2] has been applied to the case of the quantum harmonic oscillator. Superoscillations in free space are seen to persist in time longer than expected and are also seen to reform periodically after times much greater than their disappearance - for the quantum harmonic oscillator superoscillations reform periodically faster. The time of disappearance, t_d, depends upon a larger set of variables, this is due to the added complexity of the quantum harmonic oscillator. The evolution of the wavepacket is investigated using an expansion in terms of eigenfunctions and in terms of the propagator using both an exact integration and a saddle point approximation. The creation and disappearance of superoscillations is shown to depend on the behaviour of the saddle points. The frequency of the quantum harmonic oscillator, ω, is found to be an extra control parameter which dictates the strength and duration of the superoscillations.

ACKNOWLEDGEMENTS

To begin I would like to thank my supervisor, Professor Paul Strange without whom none of this would have been possible. I first met Paul during my undergraduate degree, where I was inspired by his engaging and enjoyable lectures. When I began to consider postgraduate study, he was a clear choice for a supervisor who would provide challenging and exciting work. I have since grown accustom to the work environment he has created, be it a complex discussion about saddle coalescence or a slice of cake complimented by his whimsical mastery. I wish you the best of luck with your future research.

Next I would like to mention my fellow Physics researchers Greg Smith and Jack Herklots. At no point in time did either of them assist me with my work, wait that's not fair to Jack he helped a bit. But they did make the experience memorable. I particularity enjoyed the constant competition with Greg who seemed to enjoy loosing at Board games, Chess and Clay pigeon shooting. I hope you both will continue to work hard and achieve your doctorates.

A great deal of thanks need to go to my family who's continued support through out my studies has enabled me to be where I am today. My grand mothers Gladys Bussell and May Fitzgerald, have always been an inspiration for me to work hard and achieve my goals. My parents Tim and Jane Bussell who's dedication to my personal development has given me the best opportunity to realise and maximise my potential. And of course my little brother Jake who has been a great source of encouragement and distraction.

Lastly I would like to thank my girlfriend Mizuki Matsui for her infinite help in all things and for making me smile while working on this project.

DECLARATION

University of Kent
MSc-R work Candidate Declaration

Candidate Name: Max Bussell

Faculty: Faculty of Sciences

Thesis Title: Superoscillations in the Harmonic Oscillator

Declaration to be completed by the candidate:

I declare that no portion of this work referred to in this thesis has been submitted in support of an application for another degree or qualification of this or any other university or other institute of learning.

Signed: Date: April 17, 2016

COPYRIGHT

[1] This excludes material already printed in academic journals, for which the copyright belongs to said journal and publisher. Pages for which the author does not own the copyright are numbered differently from the rest of the thesis.

NOMENCLATURE

Greek Letters

δ - delta

η - eta

τ - tau

Γ - Gamma

λ - lambda

Λ - Lambda

π - pi

ψ - psi

Ψ - Psi

ϕ - phi

Φ - Phi

θ - theta

ω - omega

Ω - Omega

ξ - xi

Mathematical Symbols

$*$ - Complex conjugate

$\exp[x]$ - Exponential Function of the variable 'x'

$f(x)$ - A function of the variable 'x'

∞ - Infinity

$\int$ - Integral over

i - Denotes the imaginary part of an equation

Im - Imaginary numbers

$\lim_{r \to 0}$ - In the limit of the variable 'r' approaching the value 0

log - Natural logarithm

$\frac{\partial u}{\partial x}$ - Partial derivative of 'u' with respect to 'x'

Re - Real numbers

$\sum$ - Sum over

Physical Constants

π - 3.14159 (5.d.p)
h - Planck's Constant $= 6.63 \times 10^{-34} Js$
$\hbar$ - h-bar$= \frac{h}{2\pi}$

CONTENTS

Final word count: 27,728

LIST OF FIGURES

LIST OF TABLES

CHAPTER

ONE

INTRODUCTION

"For the things we have to learn before we can do,
we learn by doing."
Aristotle

Superoscillations are an interesting and seemingly paradoxical phenomenon. A function is said to be superoscillatory if at certain points in space it is oscillating much more rapidly than its fastest Fourier component [1]. Conventionally, a function would be expected to oscillate only as fast as the fastest Fourier contribution - given that a Fourier series builds a function as a set of super-positioned waves, the fastest component could be seen as the limiting factor to the speed of the oscillations. As is described in detail during this thesis, superoscillations are formed by subtle interactions between its components, creating a wave that at certain points in space is oscillating faster than this conventional limit. There is an inherent cost attributed to superoscillations - within the superoscillating area the magnitude of the oscillations is exponentially smaller than the conventional oscillations bordering them.

The purpose of this thesis is to provide an introduction to superoscillations, and to further the work of Professor Sir Michael Berry and Professor Sandu Popescu by applying their previous findings on the persistence of superoscillations in free space [2], to the quantum harmonic oscillator. Specifically this thesis will be looking for a disappearance time, t_d, for superoscillations in the quantum harmonic oscillator, as well as examining the expected periodic nature of the superoscillations.

Over the last 15 years their has been an increase in the amount of research committed to investigating superoscillations. To pay tribute to the researchers that have worked on this topic, here is a brief history of some papers and letters that have contributed to the topic; the aim being to offer some insight into what has been achieved. Following on from M. Berry's previously mentioned paper [1]. In 2002, P. J. S. G. Ferreira and A. Kempf showed how superoscillations could be used to compress data; finding that the energy used to create the necessary superoscillations exponentially increases with the size of the message [3]. Then in 2004, P. J. S. G. Ferreira and A. Kempf suggest that the quantum harmonic oscillator might be a potential starting point for constructing superoscillations experimentally, where the quantum harmonic oscillator is a kind of ground state of superoscillations. They also discuss the theoretical application of superoscillations to information theory. The compres-

sion of a signal is shown to be possible but as before the abhorrent energy cost that is associated with superoscillations is seen to exponentially increase with the length of the message [4]. 2005, M. S. Calder and A. Kempf present a very detailed paper on the design of superoscillations that have custom physical properties [5]. Followed by 2006, P. J. S. G. Ferreira and A. Kempf write a paper that shows that the energy needed to achieve superoscillations with N oscillations; again the energy is shown to exponentially increase with N [6]. In 2007, P. J. S. G. Ferreira and A. Kempf use the method of over sampling to construct superoscillations, finding that the inherent instability in oversampled reconstruction from communication theory translates into the difficulty of constructing superoscillations. The results highlights the difficulties to be expected with fine tuning when trying to experimentally create superoscillating wavefunctions [7]. During 2008 M. R. Dennis, A. C. Hamilton and J. Courtial show that the probability density function of intensity for superoscillations (D=2) is $1/3$ when all of the contributing waves have the same wavenumber [8]. As well as M. V. Berry and M. R. Dennis showing that the probability distributions of superoscillatory waves over large regions of Ddimensional space, increase from 0.293 for D = 1 to 0.394 as D $\rightarrow \infty$ [9]. This reinforces and extends the result of $1/3$ from the previously mentioned paper [8] for D = 2. In 2011 M. V. Berry and P. Shukla discuss how supershifts can be regarded as a consequence of superoscillations [10]. In 2013 M. V. Berry remarks in his study that is it possible to proper-gate sub-wavelength information using superoscillations. An initial source is seen to be propagated in a sequence of equally spaced points [11]. In 2014 M.V. Berry shows how using end-fire arrays (an antenna in the form of a set of radiation sources) uses superoscillations to achieve super-gain also referred to as super-directivity [12]. Also during 2014 M. V. Berry and N. Moiseyev offer a physical understanding of the supershifts associated with superoscillatory functions [13]. It is interesting to note that within many of most of these papers remarks are made about further study that could be undertaken. Here you can see that the theory of superoscillations has come a long way in such a short period of time, proof of the excitement that surrounds the subject. The culmination of all this study hints to an application of great significance, Super-resolution; that if achieved will mean one day, thanks to nanotechnology, a schoolboy will be able to screw a nano-array lens to his science class microscope and see a DNA molecule [14].

Chapter Two 'Mathematical Methods' briefly touches on a number of mathematical tools that are used within the main body of research. The topics covered consist of: Critical Points - introducing the idea of approximating specific integrals by evaluating them for the immediate vicinity of highly contributing points; Laplace's Method - the method for approximating integrals of a given form when the stationary point is a maxima; Saddle Point Method [15,16,17,18] - building on the ideas of the last two sections, explore the technique of deforming the path of integration on the complex plane to pass through saddle points, to gain an approximation for integrals of a given form; The Schrodinger Equation - looking at the basic equation of quantum mechanics and normalization; Quantum Harmonic Oscillator - a solution of the Schrodinger equation for the harmonic oscillator, making use of recursion relations and introducing Hermite polynomials; Completeness - a proof of orthogonality and c_n the weighting factor, that combines linear separable solutions into a general solution.

The following chapter 'Superoscillations' is a reproduction of Professor Sir Michael Berry's paper 'Faster Than Fourier' [1]. This was undertaken as an introduction to superoscillations, deriving the same results and using Matlab to recreate the figures presented in the paper. A lot of the underlying mathematics not shown in the paper has been included in this thesis, displaying the first use of the saddle point method that will be applied more rigorously throughout the study.

The ensuing chapter 'Time Dependent Superoscillations' recreates a paper by Professors Sir Michael Berry and Sandu Popescu, the 'Evolution of Quantum Superoscillations and Optical Super Resolution Without Evanescent Waves [2]. The persistence of superoscillations is analysed leading to a disappearance time, t_d, being found for the system in free space. The derivative focus of this thesis will be building upon the findings of this paper. At times it proved revealing to go into greater detail than was offered by the paper - by way of testing different Matlab codes, new figures were created with interpretations not discussed in the paper by doing this a good understanding of the phenomenon was obtained.

Chapter Five 'Time Dependent Superoscillations in the Quantum Harmonic Oscillator' encompasses the main body of mathematics for the research that can be considered a small extension of the physics presented in Professors Sir Michael Berry and Sandu Popescu's paper [2]. It explores how a superoscillatory wave function evolves over time within the quantum harmonic oscillator, four different methods are employed to investigate this phenomenon, where each method reveals a deeper understanding of the physical properties.

The next chapter 'Interpretation' presents the derivations of the previous one in graphical form along with interpretations of what they display. This chapter has been made separate from the mathematics to better organizes the findings. In the first section the methods, approximations and simplifications are all confirmed to be in agreement and maintain the essential structures that are being studied - strengthening the practises used in finding the time of disappearance, t_d. Next the structure of how the saddle point contributions change as time increases in discussed leading to a new time of disappearance, t_d, being found for this system, along with a function for the critical frequency, Ω_c, that acts as a limit for which frequencys allow superoscillations.

.

The result of this thesis is a greater understanding of superoscillations, specifically the broader knowledge of how they evolve within the quantum harmonic oscillator. The Periodic recurrence and disappearance is shown to be much quicker than the free particle. The Critical frequency provides a greater understanding of the added complexity of the quantum harmonic oscillator case. Many of the results are seen to collapse down to the same result as free space when $\omega \to 0$ this is as expected as ω arises from the potential, $V(x)$, which is the added complexity to the Schrodinger equation for the quantum harmonic oscillator.

CHAPTER

TWO

MATHEMATICAL METHODS

"Ce que nous connaissons est peu de chose; ce que nous ignorons est immense.
What we know is not much. What we do not know is immense."
Pierre-Simon Laplace

The purpose of this Chapter is to gain the mathematical tools necessary to commence research with superoscillations. The following sections have been written using the books: Asymptotic Expansions, A. Erdelyi, 1956 [15]; Asymtotic Expansions, E.T. Copson, 1965 [17]; Asymptotic Methods in Analysis, N. G. de Bruijn, 1981 [18]; Quantum Mechanics, D.J. Griffiths, 2005 [19]; Quantum Mechanics, L.E. Ballentine, 1990 [20]; Quantum Physics, R. Eisberg, R. Resnick, 1985 [21].

2.1 Critical Points

Critical points or stationary points are any point in the domain of a function where the derivative is zero. These points can be local minima or maxima or saddle points that can be defined by looking at the region around them. Given the integral,

$$\int_a^b \phi(x) \exp[Nf(x)]\, dx \qquad [2.1.1]$$

Assume that the function $f(x)$ has a maximum at x_0 - so that $f(x) < f(x_0)$ for all $x \neq x_0$. Then for large N, the modulus of the integrand will have a sharp maximum at a point very near x_0. Most of the contribution to the integral will arise from the immediate vicinity of this maximum. This is because the function is multiplied by a large number N. The difference between $Nf(x)$ and $Nf(x_0)$ will be the same, as the difference between $f(x)$ and $f(x_0)$.

$$\frac{Nf(x)}{Nf(x_0)} = \frac{f(x)}{f(x_0)} \qquad [2.1.2]$$

But for $\exp[Nf(x)]$ the affect of large N will mean at x_0 (the maximum) the function will be exponentially larger than at x. From this it can be seen that a significant contribution to the integral will come from the local points x in the region close to x_0. The integral can be evaluated approximately by expanding both $\phi(x)$ and $f(x)$ close to x_0 - this idea is the foundation of Laplace's Method.

If N and $f(x)$ are complex, and $\phi(x)$ and $f(x)$ are analytic functions of x, then it is often possible to deform the path of integration so that it passes through one, or several critical points at which

$f'(x) = 0$ - this adaptation is known as the Saddle Point Method for reasons that will become clear later.

2.2 Laplace's Method

Originating from the work of Pierre-Simon Laplace, Laplace's method is a technique used for estimating integrals of the form,

$$\int_a^b \exp[Nf(x)]\,dx \tag{2.2.1}$$

where a and b can be finite or infinite. Using the Taylor expansion about x_0,

$$f(x) = f(x_0) + f'(x_0)(x - x_0) + \frac{1}{2}f''(x_0)(x - x_0)^2 + O((x - x_0)^3) \tag{2.2.2}$$

where $O((x - x_0)^3)$ is the rest of the expansion of the order $(x - x_0)^3$. As x_0 is a maximum and is not an endpoint, it is a stationary point. Therefore $f'(x_0) = 0$ and the expansion becomes,

$$f(x) = f(x_0) - \frac{1}{2}|f''(x_0)|(x - x_0)^2 \tag{2.2.3}$$

Where the change to the negative of the modulus is made as $f''(x_0)$ is negative. Now substituting this into Equation [2.2.1],

$$\int_a^b \exp[Nf(x)]\,dx \approx \exp[Nf(x_0)] \int_a^b \exp[-N|f''(x_0)|(x - x_0)^2/2]\,dx \tag{2.2.4}$$

The assumption the limits are ∞ and $-\infty$, can be made as the exponential decays so rapidly away from x_0. The integral on the right side can now be identified as a Gaussian integral.

$$\int_{-\infty}^{\infty} \exp[N|f''(x_0)|(x - x_0)^2/2]\,dx = \sqrt{\frac{2\pi}{N|f''(x_0)|}} \tag{2.2.5}$$

By using Lapace's method the integral has now been approximated,

$$\int_a^b \exp[f(x)]\,dx \approx \sqrt{\frac{2\pi}{N|f''(x_0)|}}\exp[Nf(x_0)], \text{ as } N \to \infty \tag{2.2.6}$$

2.3 Saddle Point Method

The saddle point method as previously mentioned is an extension of Laplace's method. If the functions $f(x)$ and $\phi(x)$ are analytic and regular within a region of the complex plane, it is possible to find an asymptotic expansion of the integral,

$$\int \exp[Nf(x)]\,\phi(x)\,dx \tag{2.3.1}$$

It is necessary to begin by re-arranging a given integral into this form. Then deform the path of integration so that it passes through one or more saddle-points at which $f'(x) = 0$ and follows a path down into the valley of the complex plane - this is achieved as now described. As $f(x)$ is complex ($f = u + iv$), for a given set of saddle points where, x_0 is the highest - that is x_0 is the saddle-point where u has its greatest value. The neighbourhood of x_0 will contribute the dominant part of the integral as $N \to \infty$. Furthermore if there are several saddle-points of the same height, each will make a contribution of the same order of magnitude. For this introduction lets consider x_0 as the only saddle-point. Near x_0, $f(x)$ can be written as a Taylor series expansion,

$$f(x) = f(x_0) + a_2(x - x_0)^2 + a_3(x - x_0)^3 + ..., \qquad [2.3.2]$$

where $a_2 = \frac{1}{2}f''(x_0)$ and so on. The path of integration is chosen so that near x_0 it is a straight line where the second term in the series is real and negative. This selects a path that passes through the saddle and then down into the valley of the complex plane. In the power series Equation [2.3.2] above, the terms are of the orders $O(1),\ O(x^{-2}),\ O(x^{-3})$ respectively, and so,

$$\exp[Nf(x)] = \exp[Nf(x_0) + Na_2(x - x_0)^2]. \qquad [2.3.3]$$

The original integral [2.3.1] can now be written,

$$\phi(x_0)\exp[Nf(x_0)] \int \exp[Na_2(x - x_0)^2]\, dx \qquad [2.3.4]$$

Recall that when selecting the path of integration a_2 was said to be real and negative. If $a_2 = A\exp[ia]$, where $A > 0$ and $x = x_0 + r\exp[i\theta]$, then $a_2(x - x_0) = Ar^2\exp[i(a + 2\theta)]$ - which is real and negative when $\theta = \pm\frac{1}{2}\pi - \frac{1}{2}a$. This sets the path of integration through the saddle point and down into the valley of the complex plane. The expression [2.3.4] now becomes,

$$\phi(x_0)\exp[Nf(x_0)] \int \exp[-ANr^2 + \frac{1}{2}i(\pi - a)]\, dr. \qquad [2.3.5]$$

Now substituting $ANr^2 = u^2$,

$$\phi(x_0)\exp[Nf(x_0) + \frac{1}{2}i(\pi - a)]\frac{1}{\sqrt{AN}} \int_{-\infty}^{\infty} \exp(-u^2)\, du. \qquad [2.3.6]$$

Separating and evaluating the exponentials, where the right hand side is an Gaussian integral,

$$\phi(x_0)\exp[Nf(x_0)]\left(\frac{-1}{AN\exp[ia]}\right)^{\frac{1}{2}} \int_{-\infty}^{\infty} exp(-u^2)du = \phi(x_0)\exp[Nf(x_0)]\left(\frac{-\pi}{AN\exp[ia]}\right)^{\frac{1}{2}} \qquad [2.3.7]$$

Recall that using $A\exp[ia] = a_2$ and $a_2 = \frac{1}{2}f''(x_0)$, Equation [2.3.7] becomes,

$$\phi(x_0)\exp[Nf(x_0)]\left(\frac{-2\pi}{Nf''(x_0)}\right)^{\frac{1}{2}}. \qquad [2.3.8]$$

This is the asymptotic approximation to the integral [2.3.1] when there is only one saddle point.

If there are several saddle points the approximation will consist of many terms like [2.3.8].

2.4 The Schrodinger Equation

The Schrodinger Equation is the most fundamental equation of quantum mechanics. The one-dimensional form is,

$$i\hbar\frac{\partial\Psi}{\partial t} = -\frac{\hbar^2}{2m}\frac{\partial^2\Psi}{\partial x^2} + V\Psi, \qquad [2.4.1]$$

where V is the potential energy of the particle. The Schrodinger Equation is essentially a wave equation that gives solutions as wave functions $\Psi(x,t)$, when considering only the x dimension. Max Born devised a probabilistic interpretation of the wave function. Born showed that the absolute square value of the wave function,

$$P = |\Psi(x,t)|^2. \qquad [2.4.2]$$

gave the probability density for finding the particle at position, x, at time, t. So the probability of a particle within a region, R, at time, t is given by the integral,

$$P_R = \int_R |\Psi(x,t)|^2\,dx. \qquad [2.4.3]$$

Lets look at the Heisenberg uncertainty principle,

$$\Delta x\Delta p \geqslant \hbar/2. \qquad [2.4.4]$$

The relation highlights that there is a limitation on the accuracy to which a system can be described using position and momentum. The greater the precision of one the higher the inaccuracy of the other.

Now lets consider how to get $\psi(x,t)$. It is found as mentioned before by solving the Schrodinger Equation. If V (the potential) doesn't vary in t then equation can be solved using the method of separation of variables.

$$\psi(x,t) = \psi(x)\varphi(t) \qquad [2.4.5]$$

The Schrodinger equation can be written as,

$$i\hbar\psi\frac{d\varphi}{dt} = -\frac{\hbar^2}{2m}\frac{d^2\psi}{dx^2}\varphi + V\psi\varphi. \qquad [2.4.6]$$

Dividing through by $\psi\varphi$ gives,

$$i\hbar\frac{1}{\varphi}\frac{d\varphi}{dt} = -\frac{\hbar^2}{2m}\frac{1}{\psi}\frac{d^2\psi}{dx^2} + V. \qquad [2.4.7]$$

Now the LHS is a function of only t and the RHS only of x, this is only true as V is not a function of t. This means t must be constant otherwise they would not be equal. The Schrodinger equation

can now be written as,

$$-\frac{\hbar^2}{2m}\frac{d^2\psi}{dx^2} + V\psi = E\psi, \qquad [2.4.8]$$

where E is constant. This is called the time-independent Schrodinger equation. This is to say that, the time dependent part of the wave function is,

$$\varphi(t) = \exp[-iEt/\hbar], \qquad [2.4.9]$$

When $\phi(x)$ has been found, $\psi(x,t)$ can be written as,

$$\Psi(x,t) = \phi(x)\exp[-iEt/\hbar]. \qquad [2.4.10]$$

For the free particle the general solution is,

$$\psi(x) = A\exp[ikx] + B\exp[-kx]. \qquad [2.4.11]$$

Combining this with the time dependence as shown above gives the wave function,

$$\Psi(x,t) = A\exp\left[ik\left(x - \frac{\hbar k}{2m}t\right)\right] + B\exp\left[-ik\left(x + \frac{\hbar k}{2m}t\right)\right], \qquad [2.4.12]$$

where the energy of the free particle is

$$E = \frac{k^2\hbar^2}{2m}. \qquad [2.4.13]$$

Now k is defined as,

$$k = \pm\frac{\sqrt{2mE}}{\hbar}. \qquad [2.4.14]$$

So the general wave function for the free particle can be written as,

$$\Psi(x,t) = A\exp\left[i\left(kx - \frac{\hbar k^2}{2m}t\right)\right]. \qquad [2.4.15]$$

The next thing to look at is normalization. Looking back at the statistical interpretation brought to light by Max Born, the integral of $|\psi|^2$ must be equal to 1 - that is the probability's of the particle for each region of space add up to 1.

$$\int_{-\infty}^{\infty} |\Psi(x,t)|^2\, dx = 1 \qquad [2.4.16]$$

So Equation [2.4.16] must be true for solutions of the Schrodinger equation. So if $\psi(x,t)$ is a solution, $A\psi(x,t)$ is also a solution, where A is some complex constant. To normalize a wave function, A must be picked so that Equation [2.4.16] is satisfied.

$$\int_{-\infty}^{\infty} |A\Psi(x,t)|^2\, dx = 1 \qquad [2.4.17]$$

$$A = \sqrt{\frac{1}{\int_{-\infty}^{\infty} |\Psi(x,t)|^2 \, dx}} \qquad [2.4.18]$$

The function is now normalized for $t = 0$. Due to the nature of the Schrodinger equation it is also normalized for all time.

2.5 Quantum Harmonic Oscillator

The standard model for a classical quantum harmonic oscillator is a mass, m, attached to a spring with a given force constant, k. The motion is describe by Hooke's Law,

$$F = -kx = m\frac{d^2x}{dt^2} \qquad [2.5.1]$$

where friction is ignored, the solution is,

$$x(t) = A\sin(\omega t) + B\cos(\omega t), \qquad [2.5.2]$$

where,

$$\omega = \sqrt{\frac{k}{m}}, \qquad [2.5.3]$$

is the angular frequency of oscillation. The potential energy V is,

$$V(x) = \frac{1}{2}kx^2. \qquad [2.5.4]$$

This describes a perfect quantum harmonic oscillator, and if you were to infinitely stretch this spring it would break. Hooke's Law fails before the breaking point is reached. But any potential is approximately parabolic in the neighbourhood of a local minimum. A Taylor series expansion about the minimum yields,

$$V(x) = V(x_0) + V'(x_0)(x - x_0) + \frac{1}{2}V''(x_0)(x - x_0)^2 + ... \qquad [2.5.5]$$

$V(x_0)$ can be consumed by $V(x)$ as it is constant, and since x_0 is a minimum $V'(x_0) = 0$. The higher-order terms can be dropped as they are negligible given that $(x - x_0)$ is small, the potential can now be written as,

$$V(x) \cong \frac{1}{2}V''(x_0)(x - x_0)^2. \qquad [2.5.6]$$

This describes simple harmonic oscillation about the point x_0, with an effective spring constant $k = V''(x_0)$. To express this using quantum mechanics, the Schrodinger equation must be solved for the potential,

$$V(x) = \frac{1}{2}m\omega^2x^2. \qquad [2.5.7]$$

Given this potential, the time-independent Schrodinger equation for the quantum harmonic oscillator

is,

$$-\frac{\hbar^2}{2m}\frac{d^2\psi}{dx^2}+\frac{1}{2}m\omega^2x^2\psi=E\psi \qquad [2.5.8]$$

To solve this directly, it is necessary to simplify by using,

$$\eta=\sqrt{\frac{m\omega}{\hbar}}x \qquad [2.5.9]$$

The Schrodinger equation becomes,

$$\frac{d^2\psi}{d\eta^2}=(\eta^2-K)\psi, \qquad [2.5.10]$$

where K is the energy, in units of $(1/2)\hbar\omega$,

$$K=\frac{2E}{\hbar\omega} \qquad [2.5.11]$$

At very large η and therefore very large x, η^2 dominates over the constant K, so in this region,

$$\frac{d^2\psi}{d\eta^2}\approx\eta^2\psi, \qquad [2.5.12]$$

which has the approximate solution,

$$\psi\approx A\exp[-\eta^2/2]+B\exp[\eta^2/2]. \qquad [2.5.13]$$

The B term is not normalizable. The acceptable solutions have the asymptotic form,

$$\psi(\eta)\to A\exp[-\eta^2/2],\quad \text{at large } \eta. \qquad [2.5.14]$$

This suggests that removing the exponential part of,

$$\psi(\eta)=h(\eta)\exp[-\eta^2/2], \qquad [2.5.15]$$

to leave $h(\eta)$, (note that h is different from $\hbar$ previously stated) in the hope that it has a simpler functional form than $\psi(\eta)$. Differentiating,

$$\frac{d\psi}{d\eta}=\left(\frac{dh}{d\eta}-\eta h\right)\exp[-\eta^2/2], \qquad [2.5.16]$$

and,

$$\frac{d^2\psi}{d\eta^2}=\left(\frac{d^2h}{d\eta^2}-2\eta\frac{dh}{d\eta}+(\eta^2-1)h\right)\exp[-\eta^2/2], \qquad [2.5.17]$$

then substituting this into Equation [2.5.10], the Schrodinger equation becomes,

$$\frac{d^2h}{d\eta^2}-2\eta\frac{dh}{d\eta}+(K-1)h=0. \qquad [2.5.18]$$

Expressing h in the form of the power series of η,

$$h(\eta) = a_0 + a_1\eta + a_2\eta^2 + ... = \sum_{j=0}^{\infty} a_j\eta^j. \quad [2.5.19]$$

Differentiating the series,

$$\frac{dh}{d\eta} = a_1 + 2a_2\eta + 3a_3\eta^2 + ... = \sum_{j=0}^{\infty} ja_j\eta^{j-1}, \quad [2.5.20]$$

and,

$$\frac{d^2h}{d\eta^2} = 2a_2 + 2 \cdot 3a_3\eta + 3 \cdot 4a_4\eta^2 + ... = \sum_{j=0}^{\infty}(j+1)(j+2)a_j + 2\eta^j. \quad [2.5.21]$$

Substituting Equations [2.5.20] and [2.5.21] into Equation [2.5.18],

$$\sum_{j=0}^{\infty}[(j+1)(j+2)a_{j+2} - 2ja_j + (K-1)a_j]\eta^j = 0. \quad [2.5.22]$$

Due to the uniqueness of the power series expansion, the coefficient of each power of η must vanish,

$$(j+1)(j+2)a_{j+2} - 2ja_j + (K-1)a_j = 0. \quad [2.5.23]$$

Rearranging gives,

$$a_{j+2} = \frac{(2j+1-K)}{(j+1)(j+2)}a_j. \quad [2.5.24]$$

This recursion formula is equivalent to the Schrodinger equation. It generates all the even numbered coefficients:

$$a_2 = \frac{(1-K)}{2}a_0, \quad a_4 = \frac{(5-K)}{12}a_2 = \frac{(5-K)(1-K)}{24}a_0, \quad ... \quad [2.5.25]$$

and all the odd numbered coefficients:

$$a_3 = \frac{(3-K)}{6}a_1, \quad a_5 = \frac{(7-K)}{20}a_3 = \frac{(7-K)(3-K)}{120}a_1, \quad ... \quad [2.5.26]$$

The complete solution is,

$$h(\eta) = h_{\text{even}}(\eta) + h_{\text{odd}}(\eta), \quad [2.5.27]$$

where,

$$h_{\text{even}}(\eta) = a_0 + a_2\eta^2 + a_4\eta^4 + ..., \quad [2.5.28]$$

is an even function of η, built on a_0, and

$$h_{\text{odd}} = a_1\eta + a_3\eta^3 + a_5\eta^5 + ..., \quad [2.5.29]$$

is an odd function, built on a_1. Equation [2.5.19] defines $h(\eta)$ in terms of two constants a_0 and a_1, which is to be expected from a second-order differential equation. Not all of the solutions found in

this way are normalizable. At very large j, the recursion formula becomes,

$$a_{j+2} \approx \frac{2}{j} a_j, \qquad [2.5.30]$$

with the solution,

$$a_j \approx \frac{C}{(j/2)!}, \qquad [2.5.31]$$

for some constant C. This yields at large η

$$h(\eta) \approx C \sum \frac{1}{(j/2)!} \eta^j \approx C \sum \frac{1}{j!} \eta^{2j} \approx C \exp\left[\eta^2\right]. \qquad [2.5.32]$$

For normalizable solutions the power series must terminate. There will occur a value of j, where the recursion formula gives $a_{j+2} = 0$. This will truncate either the h_{even}, or h_{odd} series, the other one will be zero as: $a_0 = 0$, if j is even, $a_1 = 0$ if j is odd. For acceptable solutions, Equation [2.5.24] requires,

$$K = 2n + 1. \qquad [2.5.33]$$

For some non-negative integer n, when looking at Equation [4.1.4] the energy is,

$$E_n = \left(n + \frac{1}{2}\right) \hbar\omega, \quad \text{for } n = 0, 1, 2, ... \qquad [2.5.34]$$

Substituting the allowed values of k into the recursion formula gives,

$$a_{j+2} = \frac{-2(n-j)}{(j+1)(j+2)} a_j. \qquad [2.5.35]$$

If $n = 0$ there is only one term in the series:

$$h_0(\eta) = a_0 \qquad [2.5.36]$$

So

$$\psi(0) = a_0 \exp[-\eta^2/2]. \qquad [2.5.37]$$

For $n = 1$, where $j = 1$ give $a_3 = 0$:

$$h_1(\eta) = a_1 \eta. \qquad [2.5.38]$$

So

$$\psi_1(\eta) = a_1 \eta \exp[-\eta^2/2] \qquad [2.5.39]$$

For $n = 2$:

$$h_2(\eta) = a_0(1 - 2\eta^2) \qquad [2.5.40]$$

So

$$\psi_2 = a_0(1 - 2\eta^2) \exp[-\eta^2/2] \qquad [2.5.41]$$

In general, $h_n(\eta)$ will be a polynomial of degree n in η involving even powers only - if n is an

ever integer; odd powers only, if n is an odd integer. They are called Hermite polynomials, $H_n(\eta)$. The first few are listed in the table below.

$H_0 = 1,$
$H_1 = 2\eta,$
$H_2 = 4\eta^2 - 2,$
$H_3 = 8\eta^3 - 12\eta,$
$H_4 = 16\eta^4 - 48\eta^2 + 12,$
$H_5 = 32\eta^5 - 160\eta^3 + 120\eta.$

Table 2.1: The first few Hermite polynomials, $H_n(\eta)$.

An arbitrary multiplicative factor is chosen so that the coefficients of the highest power of η is 2^n. The normalized stationary states for the quantum harmonic oscillator are,

$$\psi_n(x) = \left(\frac{m\omega}{\pi\hbar}\right)^{1/4} \frac{1}{\sqrt{2^n n!}} H_n(\eta) \exp[-\eta^2/2] \qquad [2.5.42]$$

2.6 Orthonormality

So far this chapter has shown that given a time independent potential $V(x)$, and using the time independent Schrodinger equation, separable solutions $\psi(x)$ can been found. For each energy a different wave function $(\psi_1(x), \psi_2(x), \psi_3(x)...)$ is found. The general solution to the Schrodinger equation is a linear combination of separable solutions.

$$\Psi(x,t) = \sum_{n=1}^{\infty} c_n \psi_n(x) \exp[-iE_n t/\hbar], \qquad [2.6.1]$$

where the summation of $\psi_n(x)$ multiplied by a weighting factor c_n is the linear combination of solutions, with the time dependency ($\exp[-iE_n t/\hbar]$) as shown in Equation [2.4.10]. In the same sense at $t = 0$,

$$\Psi(x,0) = \sum_{n=1}^{\infty} c_n \psi_n(x). \qquad [2.6.2]$$

A linear combination of eigenfunctions can be used to express any other function, $f(x)$ - this is possible as $\psi_n(x)$ is complete.

$$f(x) = \sum_{n=1}^{\infty} c_n \psi_n \qquad [2.6.3]$$

This is the familiar Fourier series of $f(x)$ - any function can be expanded in this way. First lets show that eigenstates $(\psi_1(x), \psi_2(x), \psi_3(x)...)$ are complete.

$$\int \psi_m(x)^* \psi_n(x)\, dx = 0, \qquad [2.6.4]$$

whenever $m \neq n$. The solutions to the infinite square well,

$$\psi_n(x) = \sqrt{\frac{2}{a}} \sin\left(\frac{n\pi}{a}x\right). \qquad [2.6.5]$$

Solving Equation [2.6.4], using the infinite square well solutions.

$$\begin{aligned}\int \psi_m(x)^* \psi_n(x)\, dx &= \frac{2}{a}\int_0^a \sin\left(\frac{m\pi}{a}x\right)\sin\left(\frac{n\pi}{a}x\right) \\ &= \frac{1}{a}\int_0^a \left(\cos\left(\frac{m-n}{a}\pi x\right) - \cos\left(\frac{m+n}{a}\pi x\right)\right) dx \\ &= \left[\frac{1}{(m-n)\pi}\sin\left(\frac{m-n}{a}\pi x\right) - \frac{1}{(m+n)\pi}\sin\left(\frac{m+n}{a}\pi x\right)\right]_0^a \\ &= \frac{1}{\pi}\left(\frac{\sin((m-n)\pi)}{(m-n)} - \frac{\sin((m+n)\pi)}{(m+n)}\right) = 0\end{aligned} \qquad [2.6.6]$$

If $m = n$ then the integral is equal to 1, this can be substituted by a variable called the Kronecker delta (δ_{mn}) - that is 0 if $n \neq m$ and 1 if $n = m$. Now using Equation [2.6.3], and the knowledge that the states are orthogonal, multiply both sides of the equation by $\psi_m(x)^*$, and integrate.

$$\int \psi_m(x)^* f(x) = \sum_{n=1}^{\infty} c_n \int \psi_m(x)^* \psi_n(x)\, dx = \sum_{n=1}^{\infty} \delta_{mn} = c_m \qquad [2.6.7]$$

The Kronecker delta saves the c_n term when $n = m$. Rearranging for c_n,

$$c_n = \int \psi_n(x)^* f(x)\, dx. \qquad [2.6.8]$$

Thus c_n has been found, it is the weighting factor that dictates the amount $\psi_n(x)$ contributes to the overall function. This holds true for a large number of potentials, in this sense orthogonality and completeness are quite general.

It is the conventional view that a function constructed in this way will oscillate no faster than the fastest oscillation used in its construction. For cases when the constructed function oscillates faster than this the term superoscillation is used to describe the oscillation.

CHAPTER

THREE

SUPEROSCILLATIONS

"The pendulum of the mind oscillates between sense and nonsense,
not between right and wrong."
Carl Gustav Jung

The purpose of this Chapter is to gain a greater understanding of Superoscillations. To achieve this an integral representation of superoscillations is inspected using asymptotic analysis, namely the Saddle Point method. The method is shown to be a good approximation of the exact expression. This chapter has been produced by following Professor Sir Michael Berry's paper 'Faster Than Fourier' [1].

3.1 Model for Super Oscillations

As strange as it might sound, it is possible for functions to oscillate faster than any of their Fourier components, this is the basis of super-oscillatory behaviour. To explore this statement consider a function, $f(x)$, whose spectrum of frequencies, k, is band limited by $|k| \leq 1$ - meaning that the fastest frequency $f(x)$ contains is 1. Given this $f(x)$ is conventionally expected to oscillate no faster than $\cos(x)$, but for $f(x)$ to be considered super-oscillatory it must oscillate as $\cos(Kx)$, where K can be arbitrarily large. An example of this is,

$$f(x, A, \delta) = \frac{1}{\delta\sqrt{2\pi}} \int_{-\infty}^{\infty} du \exp[ixk(u)] \exp\left[-\frac{1}{2\delta^2}(u - iA)^2\right], \qquad [3.1.1]$$

where the wave-number function, $k(u)$, is even, with $k(0) = 1$ and $|k| \leq 1$ for real u. A is real and positive, and δ is small. Examples of the wave-number function are: (see Figure 3.2)

$$k_1(u) = \frac{1}{1 + \frac{1}{2}u^2}, \quad k_2(u) = \operatorname{sech} u, \quad k_3(u) = \exp\left[-\frac{1}{2}u^2\right], \quad k_4(u) = \cos u \qquad [3.1.2]$$

Careful inspection of Equation [3.1.1], with k_4 when δ is small, shows that the second exponential will act similar to a delta function with a complex argument and project the value of the first

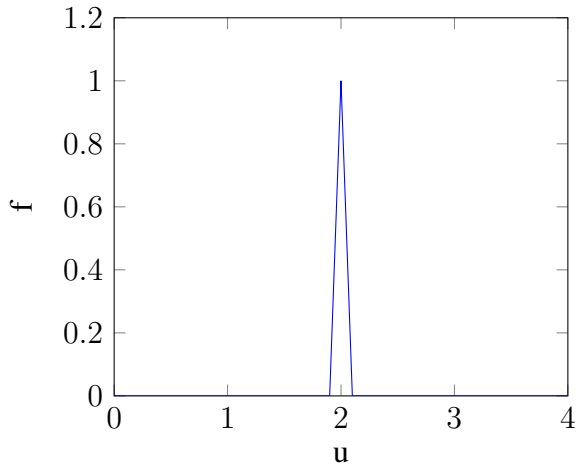

Figure 3.1: The second exponential of Equation [3.1.1], f, for small, δ and A=2 - acts like a complex delta function centred at iA.

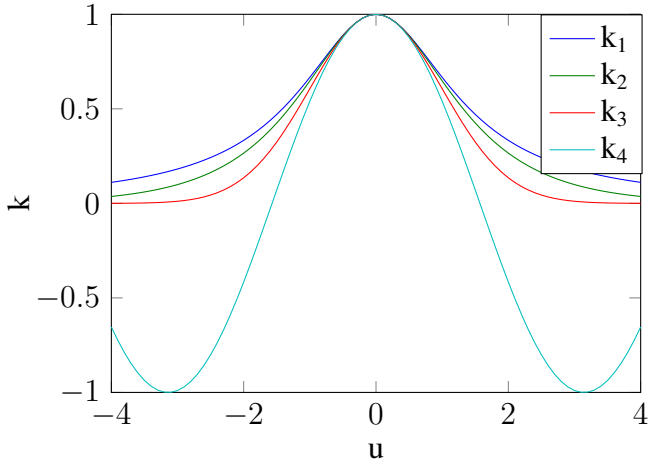

Figure 3.2: The wave-number functions k_1, k_2, k_3, k_4. Where k is band limited by $|k| \leq 1$.

exponential at $u = iA$ - Shown in Figure 3.1. Thus f will vary as,

$$f \approx \exp[iKx], \quad \text{where } K = k_n(iA). \tag{3.1.3}$$

Using k_4 from Equation [3.1.2], k increases from $u = 0$ along the imaginary axis, so that $K > 1$ - this can be seen in Figure 3.3. K can be arbitrarily large and so corresponds to superoscillations, for example if $K = 3$, then from Equation [3.1.3], $f = \exp[i3x]$, which when compared to the expected, $f = \exp[ix]$, oscillates faster showing superoscillations. The two oscillations are shown in Figure 3.4.

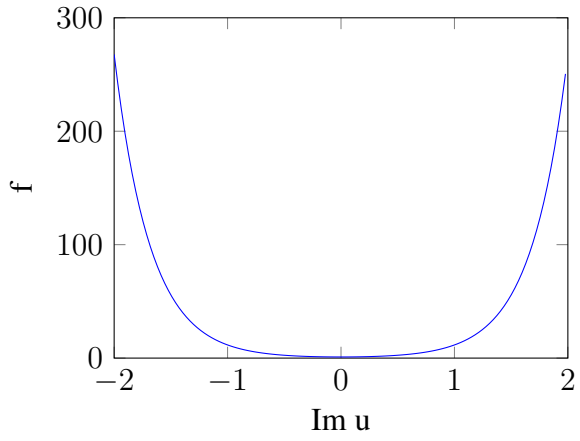

Figure 3.3: $f = \cos(u)$ as u moves along the imaginary axis. Where $u = iA$, so that $f > 1$.

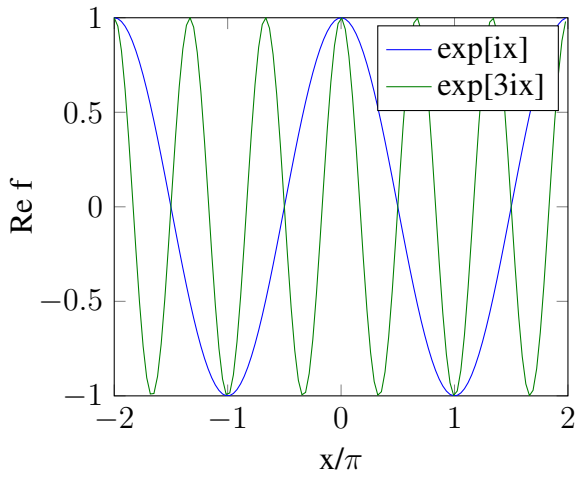

Figure 3.4: Conventionally expected $\exp[ix]$ compared to superoscillatory $\exp[3ix]$.

3.2 Asymptotics

The aim of this section is to get asymptotic approximations for the integral, Equation [3.1.1]. To begin, it is convenient to make the substitution,

$$\xi = x\delta^2, \tag{3.2.1}$$

so that Equation [3.1.1] can be written as,

$$I = \frac{1}{\delta\sqrt{2\pi}} \int_{-\infty}^{\infty} \exp\left[-\left(\frac{1}{2}(u - iA)^2 - i\xi k(u) \right) \frac{1}{\delta^2} \right] du. \tag{3.2.2}$$

For small δ, I can now be approximated by the saddle-point method. To achieve this I is re-arranged into the appropriate form,

$$\int \exp[v\omega(u)]\, \phi(u)\, dz \tag{3.2.3}$$

$$\text{where,} \quad v = -\frac{1}{\delta^2}, \qquad \omega(u) = \frac{1}{2}(u - iA)^2 - i\xi k(u), \qquad \phi(u) = \frac{1}{\delta\sqrt{2\pi}}. \tag{3.2.4}$$

The saddles, u_s, of the function, $\omega(u)$, have to be located so that the path of integration can be deformed through the saddle points.

$$\omega(u) = \frac{1}{2}u^2 - iAu - \frac{1}{2}A^2 - i\xi k(u) \qquad [3.2.5]$$

Now Differentiate to locate the saddles as zeros.

$$\omega'(u) = u - iA - i\xi k'(u) = u - i(\xi k'(u) + A), \qquad [3.2.6]$$

$$\text{for,} \quad \omega'(u) = 0, \qquad u = i(\xi k'(u) + A), \quad \therefore u_s = i(\xi k'(u_s) + A) \qquad [3.2.7]$$

Then replace $\omega(u)$ by its quadratic approximation near u_s, by using a Taylor series expansion of $\omega(u)$.

$$\omega(u) = \omega(u_s) + a_2(u - u_s)^2 + a_3(u - u_s)^3 + ... \qquad [3.2.8]$$

$$\text{Where,} \ a_1 = \omega'(u_s) = 0, \quad a_2 = \frac{1}{2}\omega''(u_s), \quad a_3 = \frac{1}{9}\omega'''(u_s) \qquad [3.2.9]$$

Using the first two terms of the expansion in Equation [3.2.8] gives sufficient accuracy, as a_3 is of the order $O(\omega^{-3})$. I can be written as,

$$I = \phi(u_s)\exp[v\omega(u_s)] \int \exp[va_2(u - u_s)^2]\, du \qquad [3.2.10]$$

Now $a_2 = \frac{1}{2}\omega''(u_s) < 0$ sets the path of integration through the saddle point and down into the valley below. If $a_2 = A\exp(ai)$, where $A > 0$ and $u = u_s + r\exp(i\theta)$, then $a_2(u-u_s)^2 = Ar^2\exp((a+2\theta)i)$ - which is real and negative when $\theta = \pm\frac{1}{2}\pi - \frac{1}{2}a$. This, as required, sets our path of integration down the direction of steepest descent, as $\exp((a + \pi - a)i) = -1$.

Now by making the Substitution $a_2(u - u_s)^2$, and changing variable to dr.

$$u = u_s = r\exp[i\theta], \qquad \frac{du}{dr} = \exp[i\theta], \qquad du = \exp[i\theta]\, dr, \qquad [3.2.11]$$

$$I = \phi(u_s)\exp[v\omega(u_s)] \int \exp\left[-Avr^2 + \frac{1}{2}i(\pi - a)\right] dr \qquad [3.2.12]$$

and the Substitution $Avr^2 = \mu^2$ from Equation [3.2.12].

$$I = \phi(u_s)\exp\left[v\omega(u_s) + \frac{1}{2}i(\pi - a)\right] \frac{1}{\sqrt{Av}} \int_{-\infty}^{\infty} \exp[-\mu^2]\, d\mu \qquad [3.2.13]$$

$$\text{Where,} \qquad dr = \frac{1}{\sqrt{Av}}d\mu, \qquad \exp\left[\frac{1}{2}\pi i\right] = i = \sqrt{-1} \qquad [3.2.14]$$

$$I = \phi(u_s)\exp[v\omega(u_s)]\left(\frac{-1}{Av\exp[ai]}\right)^{\frac{1}{2}}\int_{-\infty}^{\infty}\exp[-\mu^2]\,d\mu \qquad [3.2.15]$$

The integral on the right hand side can be identified as a Gaussian Integral, with the solution.

$$\int_{-\infty}^{\infty}\exp[-\mu^2]\,d\mu = \sqrt{\pi} \qquad [3.2.16]$$

Remembering that $a_2 = A\exp[ai] = \frac{1}{2}\omega''(u_s)$, I can be written as,

$$I = \phi(u_s)\ \exp[v\omega(u_s)]\left(\frac{-2\pi}{v\omega''(u_s)}\right)^{\frac{1}{2}} \qquad [3.2.17]$$

By substituting Equation [3.2.1], [3.2.4] and [3.2.7] back into Equation [3.2.17].

$$I = \frac{1}{\delta\sqrt{2\pi}}\left(\frac{2\pi\delta^2}{1-i\xi k''(u_s)}\right)^{\frac{1}{2}}\exp\left[ixk(u_s) + \frac{1}{2\delta^2}(u_s - iA)^2\right] \qquad [3.2.18]$$

$$\text{Where, } \omega''(u_s) = 1 - i\xi k''(u_s) \qquad [3.2.19]$$

$$I = \frac{exp[ixk(u_s) + \frac{1}{2\delta^2}(u_s - iA)^2]}{\sqrt{1 - ix\delta^2 k''(u_s)}} \qquad [3.2.20]$$

This is the asymptotic Saddle Point approximation to the original integral Equation [3.2.2]. The solution derived here is the same as the result exhibited in Berry's paper [1].

It is now revealing to understand the behaviour of the dominant saddle as ξ varies. Given the saddle,

$$u_s = i(\xi k'(u_s) + A) \qquad [3.2.21]$$

When $\xi << 1$, that is $x << \delta^{-2}$, $u_s \approx iA$ and Equation [3.2.20] reduces to Equation [3.1.3] - this is the realm of superoscillations. When $\xi >> 1$, that is $x >> \delta^{-2}$ saddles are the zeros of $k'(u)$, in the wave number functions, Equation [3.1.2], that when band limited has a single maximum is at $u = 0$. In this case Equation [3.2.20] reduces to,

$$f \approx \frac{1}{\delta\sqrt{x|k''(0)|}}\exp[ix - 1/4\pi]\exp\left[\frac{A^2}{2\delta^2}\right] \qquad [3.2.22]$$

This is the behaviour to be expected, f is of the order $\exp[A^2/2\delta^2]$, and so exponentially amplified relative to the superoscillatory range given that δ is small.

It is important now to observe the local wavenumber (the number of wavelengths per unit dis-

tance),

$$q(\xi) = -Im\,\frac{\delta\Phi(u_s(\xi),\xi,A)}{\delta\xi} = Re\,k(u_s(\xi)), \qquad [3.2.23]$$

illustrated in Figure 3.5. $q(\xi)$ decreases rapidly as ξ increases - this is true for all $k(u)$ exhibited in

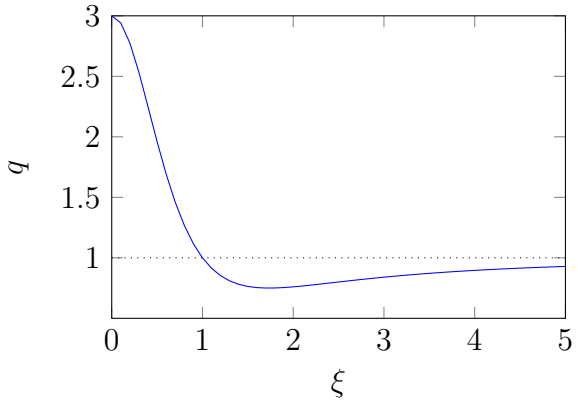

Figure 3.5: Local wavenumber $q(\xi)$, [3.2.23], for $k_5(u)$, $A = 2$

this chapter. The implication of this is that to observe superoscillations ξ must be smaller than 1. So if x is to be large in order to exhibit many super oscillations, δ must be correspondingly smaller. The exponential amplification of the conventional regime will be larger as governed by Equation [5.3.5]. Where,

$$k_5(u) = 1 - \frac{1}{2}u^2 \qquad [3.2.24]$$

In this case,

$$q(\xi) = 1 - \frac{1}{2}\left(\frac{A}{\xi - i}\right)^2 \qquad [3.2.25]$$

Now the initial integral Equation [3.1.1], can be solved in terms of special functions if k_5 is used. It is band limited so that $|k| < 1$ this is achieved by restricting the range of integration to $|u| \leq 2$. The resultant truncated integral is,

$$f(x,A,\delta) = \frac{1}{\delta\sqrt{2\pi}}\int_{-2}^{2} du \exp\left[ix\left(1 - \frac{u^2}{2}\right)\right]\exp\left[-\frac{1}{2\delta^2}(u - iA)^2\right] \qquad [3.2.26]$$

By expanding the powers of the exponentials and taking the terms of the exponential without u outside the integral. Then collecting terms of u^2 and manipulating signs.

$$f = \frac{1}{\delta\sqrt{2\pi}}\exp[x]\exp\left[\frac{A^2}{2\delta^2}\right]\int_{-2}^{2} du\ \exp -\left[\left(\frac{ix}{2} + \frac{1}{2\delta^2}\right)u^2 - i\frac{Au}{\delta^2}\right] \qquad [3.2.27]$$

Simplify the expression by making the substitutions,

$$K = \left(\frac{ix}{2} + \frac{1}{2\delta^2}\right)^{\frac{1}{2}}\ ,\ \ Q = \frac{iA}{2\delta^2\left(\frac{ix}{2} + \frac{1}{2\delta^2}\right)^{\frac{1}{2}}},\ \ 2KQ = \frac{iA}{\delta^2}$$

So that,

$$f = \frac{1}{\delta\sqrt{2\pi}}\exp[ix]\exp\left[\frac{A^2}{2\delta^2}\right]\int_{2}^{-2} du\exp -[K^2u^2 + 2KQu]. \qquad [3.2.28]$$

Now completing the square for the exponent of the right hand exponential,

$$f = \frac{1}{\delta\sqrt{2\pi}} \exp[ix] \exp\left[\frac{A^2}{2\delta^2}\right] \int_2^{-2} du \exp -[(Ku+Q)^2 - Q^2]. \quad [3.2.29]$$

Separating the powers of the exponential, and letting,

$$t = Ku + Q, \qquad u = \frac{1}{K}(t-Q), \qquad du = \frac{1}{K}dt, \quad [3.2.30]$$

So that the bounds of the integral become,

$$\begin{aligned} u = 2 &\longrightarrow t = Q + 2K, \\ u = -2 &\longrightarrow t = Q - 2K. \end{aligned} \quad [3.2.31]$$

and now,

$$f = \frac{1}{\delta\sqrt{2\pi}} \exp[ix] \exp\left[\frac{A^2}{2\delta^2}\right] \exp[Q^2] \int_{Q-2K}^{Q+2K} dt \frac{1}{K} \exp[-t^2]. \quad [3.2.32]$$

Multiplying by $\frac{2\sqrt{\pi}}{2\sqrt{\pi}}$, and cancelling like terms, then separating the integral into two intervals about zero and reversing the limits of integration.

$$f = \frac{1}{\delta K 2\sqrt{2}} \exp[ix] \exp\left[\frac{A^2}{2\delta^2}\right] \exp[Q^2] \left(-\frac{2}{\sqrt{\pi}} \int_0^{Q-2K} \exp[-t^2]\, dt + \frac{2}{\sqrt{\pi}} \int_0^{Q+2K} \exp[-t^2]\, dt \right) \quad [3.2.33]$$

As $\exp[-t^2]$ is an even function, $-f(-x) = f(x)$, so the negative integral can have its limits changed to absorb the minus.

$$f = \frac{1}{\delta K 2\sqrt{2}} \exp[ix] \exp\left[\frac{A^2}{2\delta^2}\right] \exp[Q^2] \left(\frac{2}{\sqrt{\pi}} \int_0^{2K-Q} \exp[-t^2]\, dt + \frac{2}{\sqrt{\pi}} \int_0^{Q+2K} \exp[-t^2]\, dt \right) \quad [3.2.34]$$

Now by making use of the error function [2],

$$\operatorname{erf}(x) = \frac{2}{\sqrt{\pi}} \int_0^x \exp[-t^2]\, dt \quad [3.2.35]$$

Equation [3.2.34] can be re-written as,

$$f = \frac{1}{\delta K 2\sqrt{2}} \exp[ix] \exp\left[\frac{A^2}{2\delta^2}\right] \exp[Q^2] \left\{ \operatorname{erf}(2K+Q) + \operatorname{erf}(2K-Q) \right\} \quad [3.2.36]$$

Arranging the substitutions for K and Q into the forms of the arguments of the error functions.

$$\begin{aligned} 2K + Q &= 2\left(\frac{ix}{2} + \frac{1}{2\delta^2}\right)^{\frac{1}{2}} + \frac{iA}{2\delta^2(\frac{ix}{2} + \frac{1}{2\delta^2})^{\frac{1}{2}}} \\ 2K + Q &= \frac{2ix\delta^2 + 2 + iA}{\delta(2ix\delta^2 + 2)^{\frac{1}{2}}} \end{aligned} \quad [3.2.37]$$

Similarly,

$$\begin{aligned} 2K - Q &= \frac{2ix\delta^2 + 2 - iA}{\delta(2ix\delta^2+2)^{\frac{1}{2}}} \\ Q^2 &= \frac{-A^2}{2\delta^2(ix\delta^2+1)} \\ \frac{1}{K} &= \frac{\sqrt{2}\delta}{(ix\delta^2+1)^{\frac{1}{2}}} \end{aligned} \qquad [3.2.38]$$

and putting Equations [3.2.37] and [3.2.38] back into Equation [3.2.33].

$$f = \frac{1}{2(ix\delta^2+1)^{\frac{1}{2}}} \exp\left[ix + \frac{A^2}{2\delta^2} - \frac{A^2}{2\delta^2(ix\delta^2+1)}\right]\left\{\text{erf}\left(\frac{2ix\delta^2+2+iA}{\delta(2ix\delta^2+2)^{\frac{1}{2}}}\right) + \text{erf}\left(\frac{2ix\delta^2+2-iA}{\delta(2ix\delta^2+2)^{\frac{1}{2}}}\right)\right\} \qquad [3.2.39]$$

Now manipulating the exponent,

$$\begin{aligned} ix + \frac{A^2}{2\delta^2} - \frac{A^2}{2\delta^2(ix\delta^2+1)} &= \frac{ix(ix\delta^2+1)2\delta^2}{2\delta^2(ix\delta^2+1)} + \frac{A^2(ix\delta^2+1)}{2\delta^2(ix\delta^2+1)} - \frac{A^2}{2\delta^2(ix\delta^2+1)} \\ &= \frac{ix(2ix\delta^2+2)\delta^2}{2\delta^2(ix\delta^2+1)} + \frac{A^2(ix\delta^2)}{2\delta^2(ix\delta^2+1)} \\ &= \frac{ix(2ix\delta^2+A^2+2)}{2(ix\delta^2+1)} \end{aligned} \qquad [3.2.40]$$

Putting this back into the expression for f, Equation [3.2.39].

$$f(x,A,\delta) = \frac{1}{2(ix\delta^2+1)^{\frac{1}{2}}} \exp\left[\frac{ix(2ix\delta^2+A^2+2)}{2(ix\delta^2+1)}\right]\left\{erf\left(\frac{2ix\delta^2+2+iA}{\delta(2ix\delta^2+2)^{\frac{1}{2}}}\right) + erf\left(\frac{2ix\delta^2+2-iA}{\delta(2ix\delta^2+2)^{\frac{1}{2}}}\right)\right\} \qquad [3.2.41]$$

Using k_5, Equation [3.2.24] the truncated integral, Equation [3.2.26], has been solved in terms of error functions, Equation [3.2.41]. The superoscillation wavenumber, Equation [3.1.3] is,

$$K = k_5(iA) = 1 + \frac{1}{2}A^2. \qquad [3.2.42]$$

Using k_5 and Equation [3.2.21], there is a single saddle at,

$$u_s(\xi) = \frac{A}{\xi - i}, \qquad [3.2.43]$$

and the local wavenumber is,

$$q(\xi) = 1 - \frac{1}{2}\left(\frac{A}{\xi - i}\right)^2 = 1 + \frac{A^2(1-\xi^2)}{2(1+\xi^2)^2}. \qquad [3.2.44]$$

For this case, the Saddle Point method, Equation [3.2.20] gives,

$$f(x,A,\delta) \approx \frac{1}{\sqrt{1+ix\delta^2}} \exp\left[ix\left(1 + \frac{A^2}{2(1+x^2\delta^4)}\right)\right] \exp\left[\frac{A^2\delta^2x^2}{2(1+x^2\delta^4)}\right]. \qquad [3.2.45]$$

3.3 Numerics

The aim of this section is to display superoscillations and compare the saddle point method, Equation [3.2.20], with the exact integral Equation [3.1.1]. In Figure 3.6, $A = 2$, $\delta = 0.2$ exhibiting $K = 3$ from, Equation [3.2.42] showing the fastest superoscillations for this set up. The computations shown are for k_5, Equation [3.2.24], although similar results are obtained from wave-number functions, Equation [3.1.2]. $Re\, f$ is displayed with $Im\, f$ being similar.

Figure 3.6 with parts (a), (b) and (c). In (a) superoscillations are seen for small x. For $x = 3$, $\xi = 0.12$, using Equation [3.2.44], the local wave-number $q(\xi) = 2.9$, so for the range of (a), $q(\xi) \approx 3$, using $q(\xi) = 2\pi/\lambda$, the wavelength is $\lambda = 2\pi/3$. The period is $2\pi/3$ showing $K = 3$, where the real part of $\exp[i3x]$ is $\cos(3x)$. Moving along x from 3 to 6 the difference in amplitude can already be seen. Next (b) shows a range of x where there are conventional oscillations. For $x = 40$, $\xi = 1.6$ (see Figure 3.4), the Local wave-number is over 3 times smaller - giving a period that points to the real part of $\exp[iKx]$ being $\cos(0.5x)$ that oscillates slower than the fastest contribution $\cos(x)$. In (a) and (b) the saddle point method agrees well with the exact expression, Equation [3.2.41]. In (c) the y-axis is logarithmic, this is needed to better show data over a larger range of x. The vertical lines (spikes) downwards are zeros of the oscillations. The transition from superoscillations to conventional oscillations can be seen below $x = 25$. As previously discussed superoscillations occur when $x\delta << 1$.

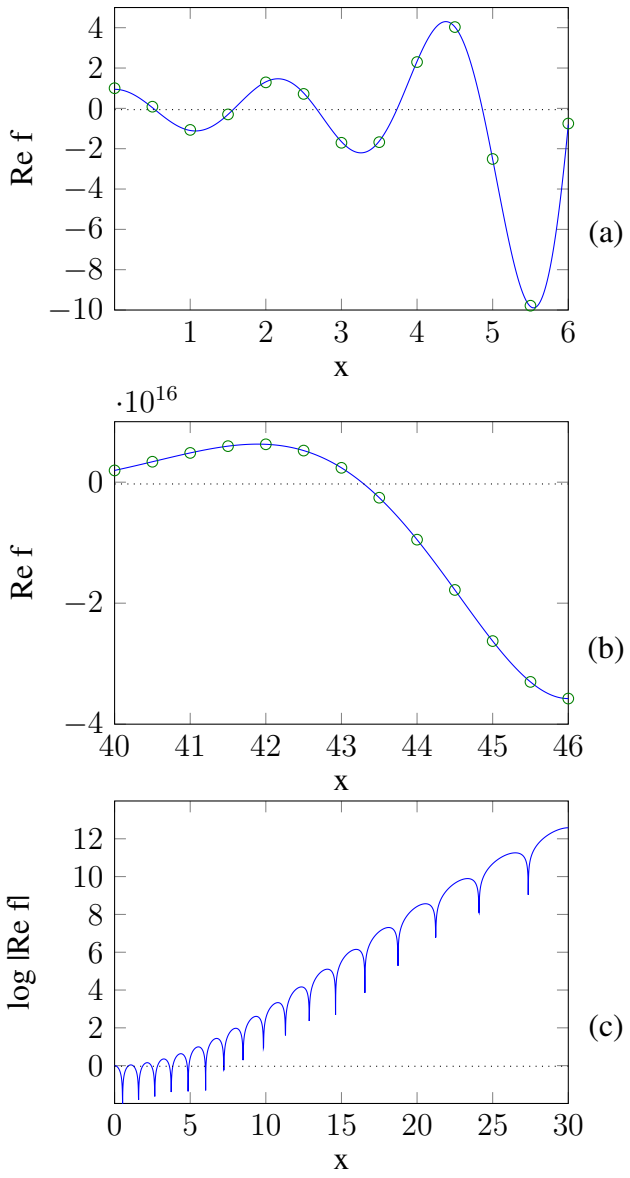

Figure 3.6: Computations of $f(x, 2, 0.2)$ for the truncated integral, Equation [3.2.26]. With (a) showing superoscillations and (b) conventional oscillations. Circles show the exact expression, Equation [3.2.41], and full lines show the saddle point method, Equation [3.2.45]. In (c) the logarithms are base 10.

CHAPTER

FOUR

TIME DEPENDENT SUPEROSCILLATIONS

"Nothing happens until somthing moves."

Albert Einstein

The purpose of this Chapter is to investigate the persistence of Superoscillations in time evolving in free space. This Chapter has been produced by following Professors Sir Michael Berry and Sandu Popescu's paper Evolution of quantum super oscillations and optical super resolution without evanescent waves [2].

In Chapter 3 the existence of band-limited functions that can oscillate faster than any of their Fourier components have been established as superoscillations. The purpose here is to explore the question: How long do superoscillations survive if $f(x)$ is the initial state of a quantum wavefunction $\psi(x,t)$ evolving in free space?

4.1 Initial Super Oscillatory State

For this study we define the function $f(x)$, a periodic super oscillatory wave.

$$f(x) = (\cos x + ia \sin x)^N \quad \text{where } a > 1 \text{ and } N >> 1 \qquad [4.1.1]$$

Figure 4.1, displays $f(x)$, using a representation that will be employed extensively in what follows. To show the oscillations, and to accommodate for the exponentially large variations in $|f|$ it is convenient to plot $\log|Re\, f|$, so that the oscillations are visible as downwards spikes at the zeros of $Re\, f$ (graphs of $Im\, f$ are very similar).

For general a, $f(x)$ has a period of π if N is even and 2π if N is odd. If $a = 1$, then $f(x) = \exp(iNx)$ which represents a plane wave travelling to the right. For $a > 1$ the result is far more interesting, the oscillation near $x = 0$ are faster. The reasoning being that close to zero,

$$\cos x \approx 1, \quad \sin x \approx x \qquad [4.1.2]$$

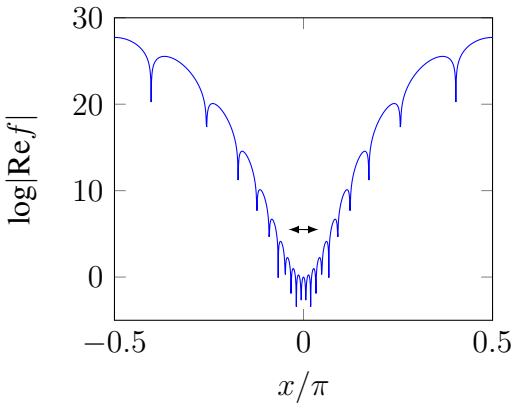

Figure 4.1: The superoscillatory function $f(x)$, plotted as log|Ref| for $a = 4, N = 20$. The double headed arrow marks the shortest period $\pi/N = \pi/20$ in the Fourier series; because $a = 4$, the fastest superoscillations (near $x = 0$) are four times smaller.

So Equation [4.1.1] can be written,

$$f(x) \approx (1 + iax)^N = \exp[\log(1 + iax)^N] \qquad [4.1.3]$$

A Taylor series expansion of the $\log$ at $x = 0$ simplifies this to,

$$f(x) \approx \exp[iaNx] \qquad [4.1.4]$$

It is intrinsic to investigate this and confirm superoscillations. The Fourier series for $f(x)$,

$$f(x) = \sum_{m=0}^{N} C_m \exp[iNk_m x], \quad \text{where, } k_m = 1 - \frac{2m}{N} \qquad [4.1.5]$$

where k_m contains only wavenumbers $|k_m| \leq 1$. So the most rapidly varying contribution from the Fourier series of $f(x)$ is,

$$\exp[iNx], \qquad \text{where, } k_m = 1. \qquad [4.1.6]$$

With this in mind consider Figure 4.2 with parts (a), (b), (c) and (d) displaying Equations [4.1.1], [4.1.4], [4.1.5] and [4.1.6] - where $a = 2$, $N = 20$. In (a) Equation [4.1.1], $f(x)$, and its Fourier series Equation [4.1.5] are shown to be in complete agreement. Next (b) builds upon (a) by also showing Equation [4.1.6] the highest frequency contribution from the Fourier series. It is easily seen that Equation [4.1.1], $f(x)$, is superoscillatory as it oscillates faster than its fastest Fourier component. In (c) Equation [4.1.4] is introduced this displays the fastest superoscillations of $f(x)$. Lastly (d) is a magnification showing, that the fastest superoscillation is twice the frequency of the, fastest contribution from the Fourier series - The degree of superoscillations is seen to be defined by a.

The Fourier series, Equation [4.1.5], is found in the following manner. Begin by writing, Equation [4.1.1] in exponential form.

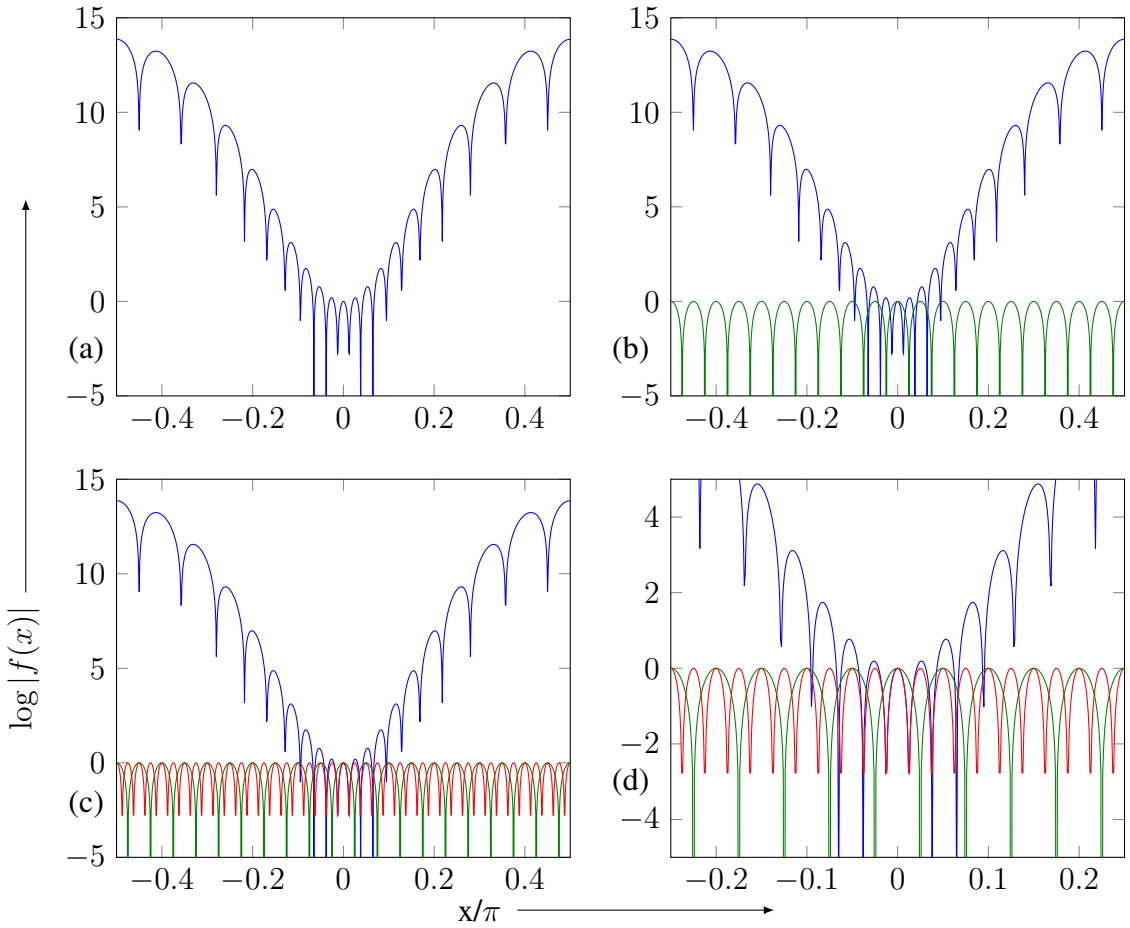

Figure 4.2: (a) Equation [4.1.1] and Equation [4.1.5] in complete alignment. (b) Exhibits Equation [4.1.6] the highest frequency contribution from the Fourier series in green. (c) Equation [4.1.4] for the fastest superoscillations of $f(x)$ is also shown in red. (d) Magnification of (c).

$$\begin{aligned} f(x) &= \left(\frac{1}{2}(\exp[ix] + \exp[-ix]) + ia\frac{1}{2i}(\exp[ix] - \exp[-ix])\right)^N \\ &= \frac{1}{2^N}((1+a)\exp[ix] + (1-a)\exp[-ix])^N \end{aligned} \tag{4.1.7}$$

Next expand for a set of N in an attempt to find a general expression that isn't bound by the power of N. For $N = 2$,

$$\begin{aligned} f(x) &= \frac{1}{2^2}((1+a)\exp[ix] + (1-a)\exp[-ix])((1+a)\exp[ix] + (1-a)\exp[-ix]) \\ &= \frac{1}{2^2}((1+a)^2\exp[2ix] + 2(1-a)(1+a) + (1-a)^2\exp[-2ix]) \end{aligned} \tag{4.1.8}$$

For $N = 3$,

$$\begin{aligned} f(x) &= \frac{1}{2^3}((1+a)\exp[ix] + (1-a)\exp[-ix])^3 \\ &= \frac{1}{2^3}((1+a)^3\exp[3ix] + 3(1+a)(1+a)(1-a)\exp[ix]... \\ &+ 3(1+a)(1-a)(1-a)\exp[-ix] + (1-a)^3\exp[-3ix]) \end{aligned} \tag{4.1.9}$$

In general,

$$\begin{aligned} f(x) &= \frac{1}{2^N}\sum_{m=0}^{N}(1-a)^{N-m}(1+a)^m \exp[-i(N-2m)x]\frac{N!}{(N-m)!m!} \\ &= \frac{1}{2^N}\sum_{m=0}^{N}(1-a)^{N-m}(1+a)^m \frac{N!}{(N-m)!m!}\exp[-iNk_m x] \end{aligned} \quad [4.1.10]$$

This result can also be found using the binomial theorem. Comparing Equation [4.1.10], with Equation [4.1.5], C_m can be shown as,

$$\begin{aligned} C_m &= \frac{1}{2^N}(1-a)^{N-m}(1+a)^m\frac{N!}{(N-m)!m!} \\ &= \frac{(-1)^m}{2^N}(a-1)^{N-m}(1+a)^m\frac{N!}{(N-m)!m!} \end{aligned} \quad [4.1.11]$$

Now arranging into the form outlined in paper [2].

$$\begin{aligned} (a-1)^{N-m}(1+a)^m &= (a-1)^{\frac{N}{2}}(a-1)^{\frac{N}{2}-m}(a+1)^{\frac{N}{2}}(a+1)^{m-\frac{N}{2}} \\ &= (a^2-1)^{\frac{N}{2}}\left(\frac{a-1}{a+1}\right)^{\frac{N}{2}(1-\frac{2m}{N})} \end{aligned} \quad [4.1.12]$$

and using k_m Equation [4.1.5],

$$\begin{aligned} \frac{N!}{(N-m)!m!} &= \frac{N!}{(N(1-\frac{m}{N}))!(N\frac{m}{N})!} \\ &= \frac{N!}{(N(2-\frac{2m}{N})/2)!(N(1-1+\frac{m}{N}))!} \\ &= \frac{N!}{(N(1-k_m)/2)!(N(1-1+2\frac{m}{N})/2)!} \\ &= \frac{N!}{(N(1+k_m)/2)!(N(1-k_m)/2)!} \end{aligned} \quad [4.1.13]$$

Now putting Equations [4.1.12] and [4.1.13] into Equation [4.1.11],

$$C_m = \frac{N!}{2^N}(-1)^m\frac{(a^2-1)^{N/2}((a-1)/(a+1))^{Nk_m/2}}{(N(1+k_m)/2)!(N(1-k_m)/2)!} \quad [4.1.14]$$

Thus C_m of Fourier series of $f(x)$ Equation [4.1.5] has been found.

At this point it is convenient to point out a limitation in the computation of $f(x)$ - specifically when using the Fourier series, Figure 4.3 with parts (a) and (b), displays $f(x)$ as full curves using Equations [4.1.1] and the Fourier series as dotted curves Equation [4.1.5]. In (a) $N = 20$, $a = 2$, complete agreement can be seen between the two constructions. In (b) $N = 20$, $a = 4$, in this case the Fourier series fails to represent $f(x)$ correctly - specifically ignoring the superoscillations and displaying the fastest Fourier component in its place. This will need further investigation that will not be done here, but a careful look at all the variables involved leads me to believe it might be due to the

very small numbers being computed.

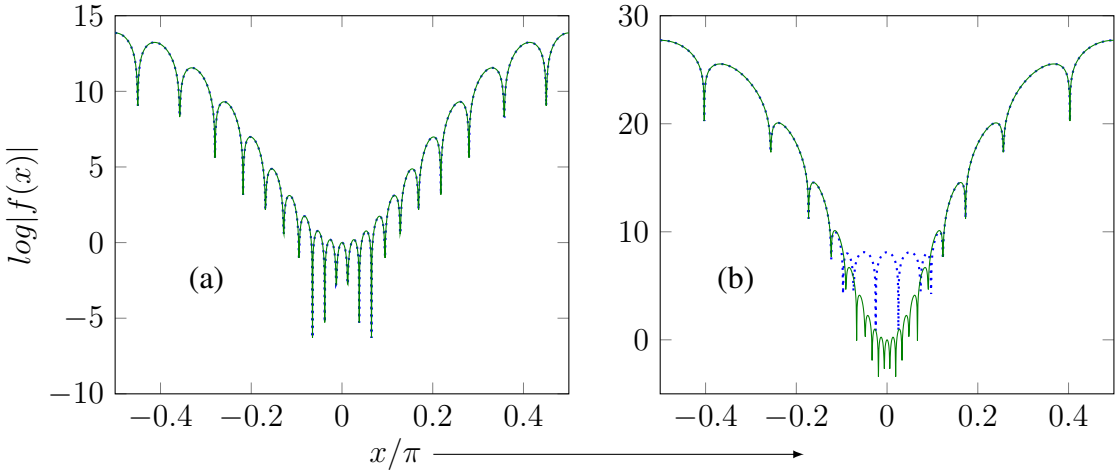

Figure 4.3: Full curves Equation [4.1.1]; dotted curves Fourier series Equation [4.1.5]. For (a) $N = 20$, $a = 2$; for (b) $N = 20$, $a = 4$.

To understand the essence of superoscillations it is instructive to look at Figures 4.4 and 4.5, displaying dotted curves representing all of the frequency components of the Fourier series Equation [4.1.5]; full curves $f(x)$ Equation [4.1.1] where $N = 20$, $a = 2$. At the centre all the components have zeros evenly spaced either side of $x/\pi = 0$. The full curve $f(x)$ has zeros that do not correspond to zeros of the components this is against what is conventionally expected. Keep in mind the superoscillations of the solid line they will not be evident in the next Figure. Figure 4.5, is Figure 4.4 represented on standard axis. Now the way in which the components interact can be seen; at the centre where the full curve is superoscillatory it is apparent that very subtle cancellation is taking place between the components . At either side the exponentially larger amplitudes can be seen as the sum of constructive interference between the components.

To gain a clearer understanding of the superoscillations, we write $f(x)$ in polar form, $r\exp(i\theta)$ - where,

$$r = |x + y| = (rr^*)^{\frac{1}{2}} = (f(x)f(x)^*)^{\frac{1}{2}} \quad \text{and,} \quad \theta = \tan^{-1}\frac{\text{Im}f(x)}{\text{Re}f(x)}. \tag{4.1.15}$$

In this case,

$$\begin{aligned} r &= (f(x)f(x)^*)^{\frac{1}{2}} = ((\cos x + ia\sin x)^N(\cos x - ia\sin x)^N)^{\frac{1}{2}} \\ &= (\cos^2 x + a^2\sin^2 x)^{\frac{N}{2}}. \end{aligned} \tag{4.1.16}$$

This can be simplified further if the function $(\cos x + ia\sin x) = f_1(x)$ is written as,

$$f_1(x) = r\exp[i\theta]. \tag{4.1.17}$$

Then,

$$f(x) = r^N\exp[iN\theta]. \tag{4.1.18}$$

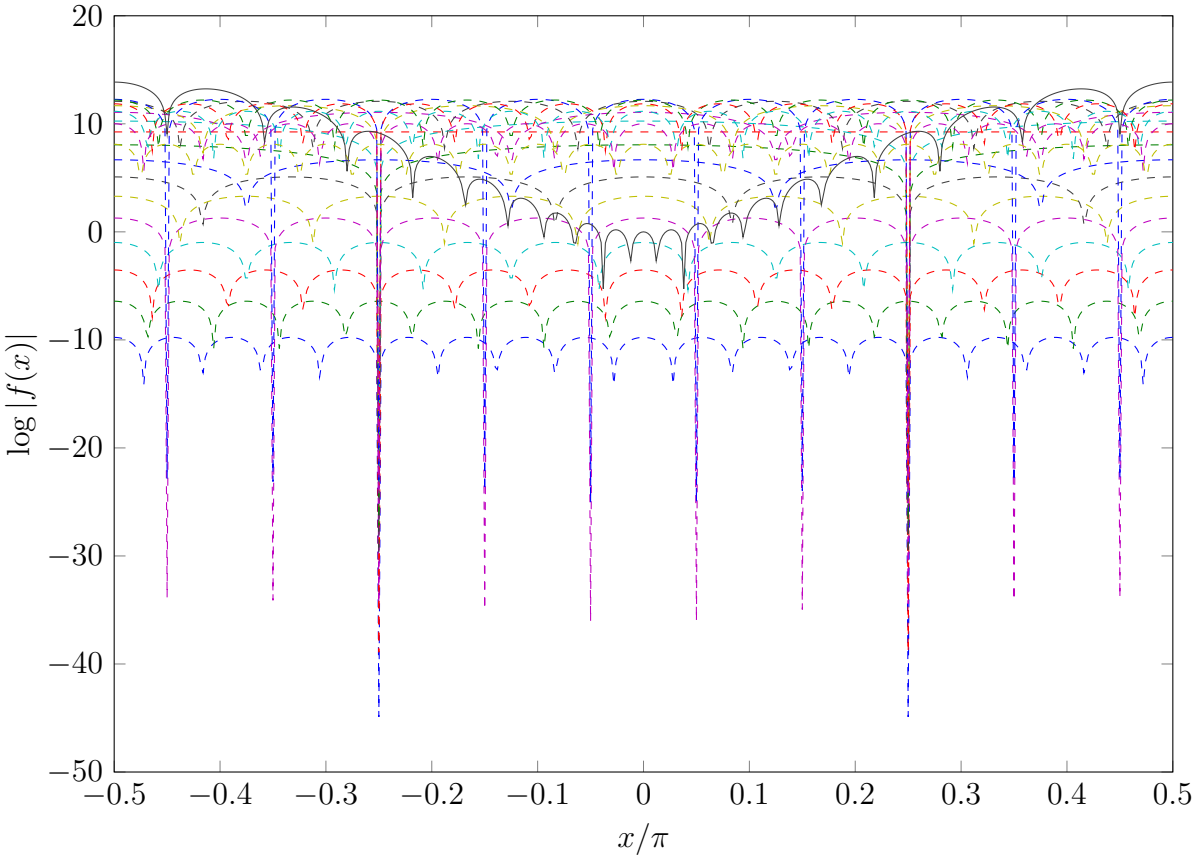

Figure 4.4: $\log|f(x)|$: Full curves Equation [4.1.1], dotted curves components of Equation [4.1.5]. Where $N = 20$, $a = 2$.

Where,

$$\theta = \arctan\frac{a\sin x}{\cos x} = \arctan a(\tan x). \qquad [4.1.19]$$

So in polar form,

$$f(x) = (\cos^2 x + a^2\sin^2 x)^{\frac{N}{2}}\exp[iN\arctan(a\tan x)]. \qquad [4.1.20]$$

To simplify this further consider

$$\begin{aligned} f(x) &= (\cos x + ia\sin x)^N \\ \log f(x) &= N\log(\cos x + ia\sin x) \\ \frac{d}{dx}\log f(x) &= N\frac{d}{dx}\log(\cos x + ia\sin x) \end{aligned} \qquad [4.1.21]$$

Make the substitution where,

$$\begin{aligned} y &= \cos x + ia\sin x \\ y' &= -\sin x + ia\cos x \end{aligned} \qquad [4.1.22]$$

So that,

$$\frac{d}{dx}\log y = \frac{dy}{dx}\frac{d\log y}{dy} = \frac{1}{y}\frac{dy}{dx} = \frac{-\sin x + ia\cos x}{\cos x + ia\sin x}. \qquad [4.1.23]$$

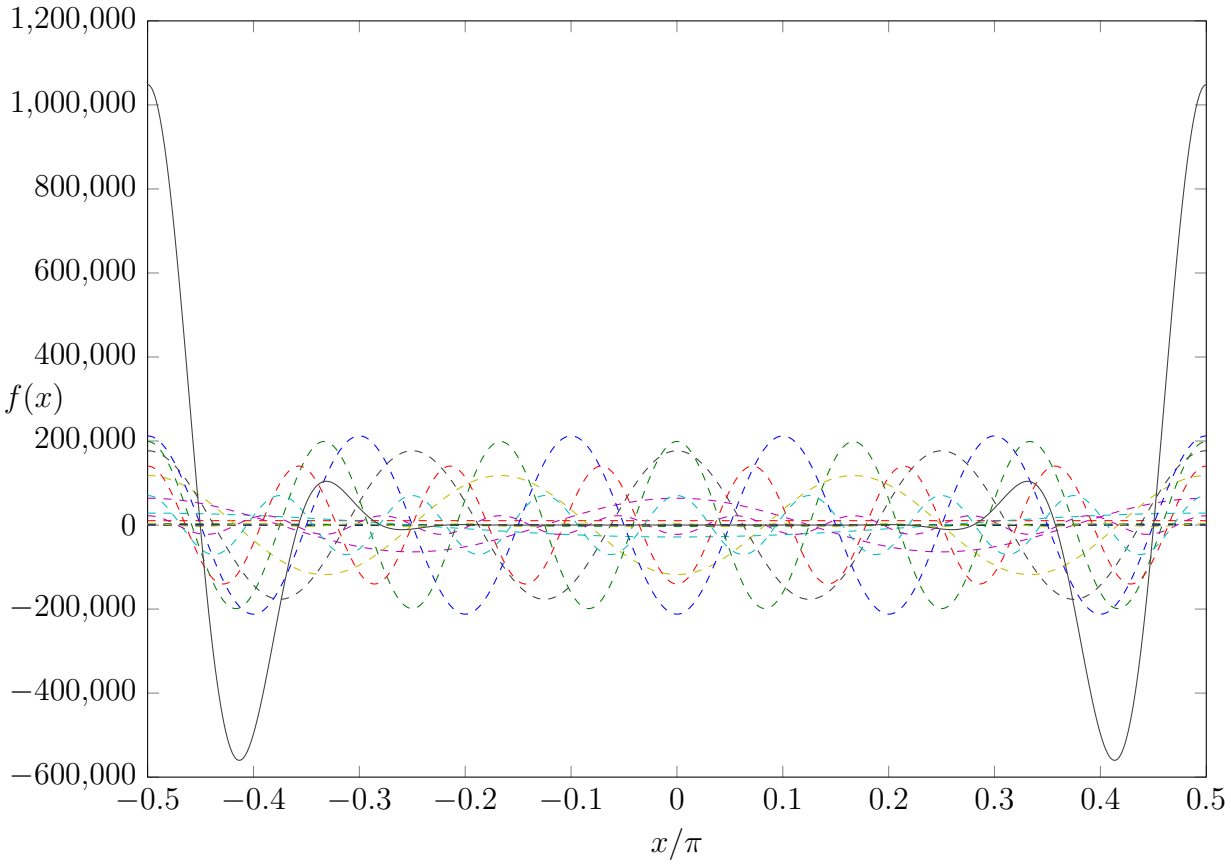

Figure 4.5: Full curves Equation [4.1.1], dotted curves components of Equation [4.1.5]. Where $N = 20$, $a = 2$.

Now,

$$\begin{aligned}\frac{d}{dx}\log f(x) &= N\frac{-\sin x + ia\cos x}{\cos x + ia\sin x} \\ &= N\frac{(a^2-1)\sin x\cos x + ia}{\cos^2 + a^2\sin^2 x}\end{aligned} \tag{4.1.24}$$

Where the,

$$\mathrm{Im}\frac{d}{dx}\log f(x) = \frac{Na}{\cos^2 + a^2\sin^2 x} \tag{4.1.25}$$

This can now be arranged into the form of the local wavenumber $k(x)$.

$$\frac{1}{N}\mathrm{Im}\frac{d}{dx}\log f(x) = \frac{a}{\cos^2 + a^2\sin^2 x} = k(x) \tag{4.1.26}$$

$$\therefore (\cos^2 x + a^2\sin^2 x)^{\frac{N}{2}} = \left(\frac{a}{k(x)}\right)^{\frac{N}{2}} \tag{4.1.27}$$

Now the polar form of $f(x)$, Equation [4.1.20] can be written as,

$$f(x) = \left(\frac{a}{k(x)}\right)^{\frac{N}{2}} \exp[iN\arctan(a\tan x)], \tag{4.1.28}$$

To fully emulate paper[2]'s arrangement of $f(x)$, consider the integral,

$$\begin{aligned} I &= \int_0^x k(x')dx' = \int_0^x \frac{a}{\cos^2 x' + a^2 \sin^2 x'} dx' \\ &= \int_0^x \frac{a}{1 + (a^2 - 1)\sin^2 x'} dx' \end{aligned} \tag{4.1.29}$$

Now $a > 1$ so $(a^2 - 1) > 0$. The following integral is 2.562.1 of Gradshteyn & Ryzhik [23].

$$\text{For } \frac{b}{a} > -1, \quad \int \frac{1}{a + b\sin^2 x} dx = \frac{1}{\sqrt{a(a+b)}} \arctan\left(\sqrt{\frac{a+b}{a}} \tan x\right) \tag{4.1.30}$$

In this case,

$$\begin{aligned} I &= a \int_0^x \frac{1}{1 - (a^2 - 1)\sin^2 x'} dx' \\ &= a \left[\frac{1}{\sqrt{1 + a^2 - 1}} \arctan\left(\sqrt{\frac{1 + a^2 - 1}{1}} \tan x'\right) \right]_0^x \\ &= a \left[\frac{1}{a} \arctan(a \tan x) \right] = \arctan(a \tan x) \end{aligned} \tag{4.1.31}$$

So Equation [4.1.28] can be written,

$$f(x) = \left(\frac{a}{k(x)}\right)^{\frac{N}{2}} \exp\left[iN \int_0^x k(x')\, dx'\right] \tag{4.1.32}$$

this is the same form of $f(x)$ displayed in paper [2]. Where the local wavenumber is,

$$k(x) = \frac{1}{N} \text{Im} \frac{d}{dx} \log f(x) = \frac{a}{\cos^2 x + a^2 \sin^2 x} \tag{4.1.33}$$

The equation $k(x)$ describes the state of oscillation, it varies from superoscillatory $k(0) = a$ to the slowest variation $k(\pi/2) = 1/a$. Superoscillations are observed within the region $|k(x)| > 1$,

$$\frac{a}{\cos^2 x + a^2 \sin^2 x} > 1. \tag{4.1.34}$$

So rearranging for x,

$$\begin{aligned} a &> \cos^2 x + \sin^2 + (a^2 - 1)\sin^2 x \\ a - 1 &> (a + 1)(a - 1)\sin^2 x \end{aligned} \tag{4.1.35}$$

In terms of $\sin$,

$$\frac{1}{a + 1} > \sin^2 x \tag{4.1.36}$$

In terms of cos,

$$\begin{aligned} \frac{1}{a+1} &> (1 - cos^2 x) \\ \cos^2 x &> \frac{a}{a+1} \end{aligned} \tag{4.1.37}$$

Taking the square root of Equations [4.1.36] and [4.1.37] together,

$$\frac{1}{\sqrt{a+1}} > \sin x \tag{4.1.38}$$

$$\sqrt{\frac{a}{a+1}} < \cos x \tag{4.1.39}$$

So now,

$$\frac{\cos x}{\sin x} > \frac{\sqrt{\frac{a}{a+1}}}{\sqrt{1/(a+1)}} \tag{4.1.40}$$

Rearranging and simplifying gives the superoscillatory region as,

$$|x| < \operatorname{arccot} \sqrt{a} \tag{4.1.41}$$

The number of oscillations in this region can be found using Equations [4.1.33] and [4.1.40],

$$\begin{aligned} n_{osc} &= \frac{N}{2\pi} \int_{-arccot\sqrt{a}}^{arccot\sqrt{a}} k(x)\, dx \\ &= \frac{N}{2\pi} \int_{-arccot\sqrt{a}}^{arccot\sqrt{a}} \frac{a}{\cos^2 + a^2 \sin^2 x}\, dx \\ &= \frac{Na}{2\pi} \frac{1}{a} \Big[\arctan a \tan x \Big]_{-\operatorname{arccot}\sqrt{a}}^{\operatorname{arccot}\sqrt{a}} \\ &= \frac{N}{2\pi} (\arctan a \tan(\operatorname{arccot}\sqrt{a}) - \arctan a \tan(-\operatorname{arccot}\sqrt{a})) \end{aligned} \tag{4.1.42}$$

As $\tan(-x) = -\tan(x)$,

$$n_{osc} = \frac{N}{\pi} (\arctan(a \tan(\operatorname{arccot}\sqrt{a}))) \tag{4.1.43}$$

Given that, $\operatorname{arccot}\sqrt{a} = \arctan(1/\sqrt{a})$ and $\tan(\arctan(1/\sqrt{a})) = \frac{1}{\sqrt{a}}$. The number of oscillations within the superoscillatory region is,

$$n_{osc} = \frac{N}{\pi} \arctan(a \frac{1}{\sqrt{a}}) = \frac{N}{\pi} \arctan \sqrt{a}, \tag{4.1.44}$$

This differs by a factor of 2 from paper[2]'s result. Computations have confirmed Equation [4.1.44] to be correct, paper[2]'s result is probably a typographical error. The number of oscillations is shown to depend strongly on N, with only a weak dependence on a.

Equation [4.1.32], shows that in the superoscillatory region, where $|k(x)| > 1$, $|f|$ is exponentially smaller, than in the conventional region where $|k(x)| < 1$. As N increases the exponential difference increase, therefore N is an asymptotic parameter; that describes both the number of oscillations in the superoscillatory region and the corresponding exponential smallness of $|f|$.

Equation [4.1.4], is a good approximation when the amplitude of the superoscillations is approximately constant lets call it the region of fast superoscillations - This region is smaller than [4.1.41]. To explore where Equation [4.1.4], is a good approximation, Equation [4.1.32] will be expanded near $x = 0$ to get a slightly better approximation.

$$f(x) = \left(\frac{a}{a/(\cos^2 x + a^2 \sin^2 x)}\right)^{\frac{N}{2}} \exp\left[iN \int_0^x k(x')\, dx'\right] \qquad [4.1.45]$$

Evaluate this for small x. First the pre-factor

$$\begin{aligned} p &= (\cos^2 x + a^2 \sin^2 x)^{\frac{N}{2}} \\ &= (1 + (a^2 - 1)\sin^2 x)^{\frac{N}{2}} \end{aligned} \qquad [4.1.46]$$

Making use of the Taylor series and $\exp[x] \sim (x + 1)$. If x is small $\sin x \approx x$,

$$\begin{aligned} p &= (1 + (a^2 - 1)x^2)^{\frac{N}{2}} \\ &\approx \left(1 + \frac{1}{2}(a^2 - 1)x^2\right)^N \\ &\approx \left(\exp\left[\frac{1}{2}(a^2 - 1)x^2\right]\right)^N \\ &= \exp\left[\frac{1}{2}N(a^2 - 1)x^2\right] \end{aligned} \qquad [4.1.47]$$

Now the integral,

$$\begin{aligned} \int_0^x k(x')\, dx &= \int_0^x \frac{a}{\cos^2 x' + a^2 \sin^2 x'}\, dx' \\ &\approx a \int_0^x \frac{1}{1 + (a^2 - 1)x'^2}\, dx' \\ &\approx a \int_0^x (1 - (a^2 - 1)x'^2)\, dx' \\ &= a\left[x' - \left(\frac{a^2 - 1}{3}\right) x'^3\right]_0^x \\ &\approx ax \end{aligned} \qquad [4.1.48]$$

where terms of the order x^3 and higher are ignored. Combining Equations [4.1.48], [4.1.47] and [4.1.45],

$$f(x) \approx \exp\left[\frac{1}{2}N(a^2 - 1)x^2\right] \exp[iNax]. \qquad [4.1.49]$$

This is a slightly better approximation than Equation [4.1.4], describing the fast superoscillations. The region of fast superoscillations is,

$$|x| < x_{fs} = \frac{1}{\sqrt{N(a^2-1)}}. \qquad [4.1.50]$$

In this region the coefficient of $\exp[iNax]$ varies from 1 to $\exp[\frac{1}{2}] \approx 1.6$. The number of oscillations in this region is given by the $\exp(iNax)$ part of Equation [4.1.49].

$$\begin{aligned} \exp[iNax] &= \exp\left[iNa\frac{2}{N(a^2-1)}\right] = \exp[2\pi i n_{fs}] \\ 2\pi n_{fs} &= \frac{2a\sqrt{N}}{\sqrt{a^2-1}} \end{aligned} \qquad [4.1.51]$$

The number of fast superoscillations is,

$$n_{fs} = \frac{\sqrt{N}}{\pi}\frac{a}{\sqrt{a^2-1}}. \qquad [4.1.52]$$

Superoscillations is a subtle phenomenon, associated with delicate interference between the Fourier components of $f(x)$. This can be seen as, there is no indication of superoscillations in the power spectrum,

$$P(k) = N\frac{c_m^2(m=(1-k)N/2)}{2\sum_0^N c_m^2} \underset{N\gg 1}{\approx} \frac{1}{\sigma\sqrt{2\pi}}\exp\left[-\frac{(k-\langle k\rangle)^2}{2\sigma^2}\right] \qquad [4.1.53]$$

where

$$\langle k\rangle = \frac{1}{2}, \qquad \sigma \equiv \sqrt{(k-\langle k\rangle)^2} = \sqrt{\frac{a^2-1}{2Na^2}}. \qquad [4.1.54]$$

Thus the asymptotic spectrum Figure 4.6, is a narrow Gaussian centred on the wavenumber $k = 1/a$, representing the exponentially dominant slow oscillations near $|x| = \pi$.

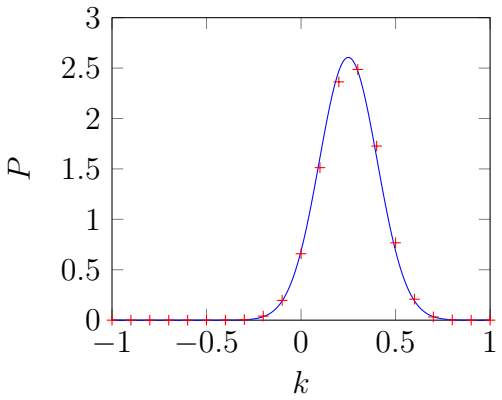

Figure 4.6: Spectrum of $f(x)$ for $a = 4, N = 20$. Crosses: the exact spectrum (middle member of [4.1.53]); smooth curve: Gaussian approximation (right-hand member of [4.1.53]).

4.2 Quantum Evolution

To look at the quantum evolution we write the equation as

$$iN\frac{\partial\psi(x,t)}{\partial t} = -\frac{1}{2}\frac{\partial^2\psi(x,t)}{\partial x^2} \quad \text{where,} \quad N = \frac{1}{\hbar}, \quad m = 1. \tag{4.2.1}$$

The initial state is

$$\psi(x,0) = f(x) = (\cos x + ia\sin x)^N \tag{4.2.2}$$

The state at a future time t, can be written as a integral over the propagator,

$$\psi(x,t) = \sqrt{\frac{N}{2\pi it}}\int_{-\infty}^{\infty} dx' f(x')\exp[iN(x-x')^2/2t] \tag{4.2.3}$$

or as a sum of Fourier components,

$$\psi(x,t) = \sum_{m=0}^{N} C_m \exp[iN(k_m x - k_m^2 t/2)] \tag{4.2.4}$$

Figure 4.7 and 4.8 show the disappearance of superoscillations as density plots of time and space, and graphs of $\psi(x,t)$ for several values of t. Figure 4.7 exhibits density plots with parts (a), (b), (c) and (d) - The lines are the zeros of the function. In (a) the vertical lines display superoscillations, these are shown to persist for a time. In (b) after longer times the oscillations become slower, seen as greater separation between the vertical lines. In (c) the oscillations are eventually as expected from the Fourier components Equation [4.1.5], with $|k| \leq 1$. The initial structure of exponentially weak superoscillations disappearing into a mass of confusion at the bottom of the graph. In (d) the periodic nature of t is observed, with the period of $N\pi/2$. The mass of superoscillations has been shifted in x by $\pi/2$. For the most part the oscillations are slower still reflecting the mean $\langle k\rangle = 1/a$ of the power spectrum, Equation [4.1.53].

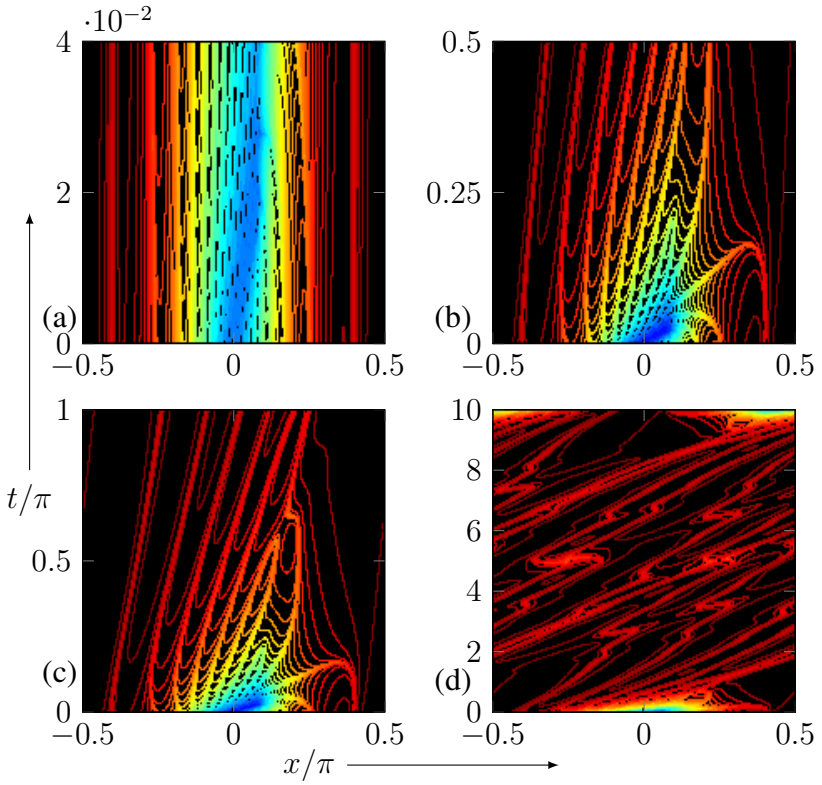

Figure 4.7: Density plots of $-\log|\mathrm{Re}\psi|$ of the evolution of the wavefunction Equation [4.2.4], for $a = 4, N = 20$. $(a)\ 0 \leq t \leq 0.04\pi$; $(b)\ 0 \leq t \leq \pi/2$; $(c)\ 0 \leq t \leq \pi$; $(d)\ 0 \leq t \leq 10\pi$. In this representation, the zeros of $Re\psi$ appear as thick lines.

Figure 4.8 with parts (a), (b), (c), (d), (e) and (f) illustrates the disappearance of superoscillations in more detail, for a series of values of t. In (a) $t = 0$ the structure of the superoscillations that is becoming familiar. In (b) $t = 0.015\pi$ the region of fast superoscillations is shifted in x, one of the superoscillations has disappeared. In (c) $t = 0.08\pi$ more of the superoscillations have disappeared. In (d) $t = 0.706\pi$ this is the time when, according to the theory of the next section the superoscillations have disappeared - this is confirmed in the graph. In (e) $t = 0.5\pi$ conventional oscillations are exhibited. In (f) $t = \pi$ conventional oscillations are shown.

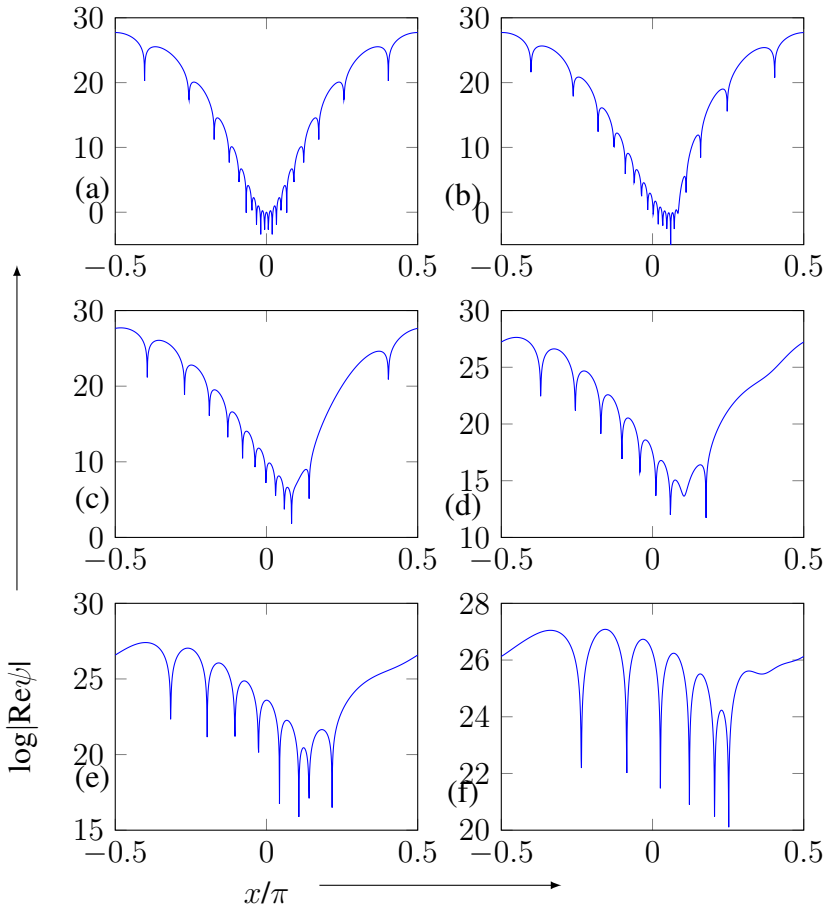

Figure 4.8: Superoscillations disappearing as t increases, for $a = 4, N = 20$. $(a)\ t = 0$; $(b)\ t = 0.015\pi$; $(c)\ t = 0.08\pi$; $(d)\ t = 0.706$; $(e)\ t = 0.5\pi$; $(f)\ t = \pi$.

4.3 Complex Momenta

To understand the disappearance of superoscillations, it is necessary to have a representation of ψ that is more transparent than the Fourier series Equation [4.1.5]. This can be derived by using asymptotics exploiting $N \gg 1$, which implies that the integrand in Equation [4.2.3] varies rapidly in both modulus and phase. To accommodate this, it is convenient to rewrite Equation [4.2.3] as,

$$\begin{aligned}\psi(x,t) &= \sqrt{\frac{N}{2\pi i t}} \int_{-\infty}^{\infty} dx' f(x') \exp[iN(x-x')^2/2t] \\ &= \sqrt{\frac{N}{2\pi i t}} \int_{-\infty}^{\infty} dx' \exp\left[iN\left(\int_0^{x'} dx'' q(x'') + (x-x')^2/2t\right)\right]\end{aligned} \qquad [4.3.1]$$

which means,

$$f(x') = \exp\left[iN \int_0^{x'} q(x'')\, dx''\right] \qquad [4.3.2]$$

So $q(x)$ is the complex momentum,

$$\begin{aligned} q(x) &= -\frac{i}{N}\frac{\delta}{\delta x}\log f(x) \\ &= -\frac{i}{N}\frac{\delta}{\delta x}\log(\cos x + ia\sin x)^N \\ &= \frac{a\cos x + i\sin x}{\cos x + ia\sin x}. \end{aligned} \tag{4.3.3}$$

This simply shows that $k(x)$ defined by Equation [4.1.33], is related to $q(x)$ via,

$$k(x) = \text{Re}\,(q(x)) \tag{4.3.4}$$

Now $\psi(x,t)$, Equation [4.3.1] can now be written,

$$\begin{aligned} \psi(x,t) &= \sqrt{\frac{N}{2\pi it}}\int_{-\infty}^{\infty} dx' \exp\left[iN\left(\int_0^{x'} \frac{a\cos x'' + i\sin x''}{\cos x'' + ia\sin x''}\,dx'' + (x-x')^2/2t\right)\right] \\ &= \sqrt{\frac{N}{2\pi it}}\int_{-\infty}^{\infty} dx' \exp\left[iN\Phi(x',x,t)\right] \end{aligned} \tag{4.3.5}$$

where the complex phase $N\Phi$ is,

$$\Phi(x',x,t) = \int_0^{x'} \frac{a\cos x'' + i\sin x''}{\cos x'' + ia\sin x''}\,dx'' + (x-x')^2/2t. \tag{4.3.6}$$

Now for $N \gg 1$, the integral can be approximated by the saddle-point method, detailed in Chapter 2. This will give $\psi(x,t)$ as one or more contributions from the saddles $x_j(x,t)$ satisfying,

$$\frac{\delta}{\delta x'}\Phi(x',x,t) = 0 \Rightarrow q(x') = \frac{x-x'}{t} \Rightarrow x' = x_j(x,t) \tag{4.3.7}$$

Physically, the saddles can be regarded as complex momenta determining ψ as a superposition of waves. In the present case the saddle point theory gives,

$$\phi(z_0) = 1 \tag{4.3.8}$$

$$\begin{aligned} \omega''(z_0) &= i\frac{\delta^2}{\delta x'^2}\left(\int_0^{x'} q(x'')\,dx'' + \frac{(x-x')^2}{2t}\right) \\ &= i\frac{\delta}{\delta x'}\left(q(x') - \frac{(x-x')}{t}\right) \\ &= i(q'(x') + 1/t) \end{aligned} \tag{4.3.9}$$

Using Equation [2.3.8], the saddle point solution becomes,

$$\begin{aligned}\psi(x,t) &= \sum_j \left(\frac{1}{q'(x')+1/t}\right)^{\frac{1}{2}} \sqrt{\frac{1}{2t}} \exp\left[iN\left(\int_0^{x_j} q(x'')\,dx'' + (x-x_j)^2/2t\right)\right] \\ &= \sum_j \left(\frac{1}{q'(x_j)t+1}\right)^{\frac{1}{2}} f(x_j)\exp[iN(x-x_j)^2/2t]\end{aligned} \tag{4.3.10}$$

The summation is for all saddles that contribute. For very small t, there is just one contributing saddle, which from Equation [4.3.7] is close to x; as t increases, other saddles appear. The saddle point method can be implemented numerically giving results that agree with Figures 4.7 and 4.8 computed from the Fourier series. To implement the procedure analytically a further simplification can be made, exploiting the fact that the phenomenon the disappearance of superoscillations - involves small x and t. $f(x)$ and $q(x)$ can be replaced by simpler functions and new scaled variables introduced.

$$f(\eta) = (1+i\eta)^N \tag{4.3.11}$$

Then

$$q(\eta) = -\frac{i}{N}\frac{\delta}{\delta\eta}\log f(\eta) = \frac{1}{1+i\eta} \tag{4.3.12}$$

Where

$$x = \eta/a, \qquad t = \tau/a^2, \qquad dx = \frac{1}{a}d\eta \tag{4.3.13}$$

Now take Equation [4.2.3], and change the variables according to this prescription. The scaling eliminates a from the definition of $\psi(\xi,\tau)$,

$$\begin{aligned}\psi(\eta,\tau) &= \sqrt{\frac{Na^2}{2\pi i\tau}}\int_{-\infty}^{\infty}\frac{1}{a}\,d\eta' f(\eta')\exp\left[iN\left(\frac{\eta}{a}-\frac{\eta'}{a}\right)^2/\frac{2\tau}{a^2}\right] \\ &= \sqrt{\frac{N}{2\pi i\tau}}\int_{-\infty}^{\infty} d\eta' f(\eta')\exp[iN(\eta-\eta')^2/2\tau] \\ &= \sqrt{\frac{N}{2\pi i\tau}}\int_{-\infty}^{\infty} d\eta'\exp\left[iN\left(\int_0^{\eta'} d\eta'' q(\eta'') + (\eta-\eta')^2/2\tau\right)\right] \\ &= \sqrt{\frac{N}{2\pi i\tau}}\int_{-\infty}^{\infty} d\eta'\exp\left[iN\Phi_{app}(\eta',\eta,\tau)\right]\end{aligned} \tag{4.3.14}$$

The integral can be evaluated in this form. To Begin simplify the exponent.

$$\begin{aligned}\int_0^{\eta'} d\eta'' q(\eta'') &= \int_0^{\eta'}\frac{1}{1+i\eta''}\,d\eta'' = -i\Big[\log(1+i\eta'')\Big]_0^{\eta'} \\ &= -i\log(1+i\eta')\end{aligned} \tag{4.3.15}$$

Substitute this back into the expression,

$$\begin{aligned}\psi(\eta,\tau) &= \sqrt{\frac{N}{2\pi i\tau}}\int_{-\infty}^{\infty} d\eta' \exp[iN(-i\log(1+i\eta')+(\eta-\eta')^2/2\tau)] \\ &= \sqrt{\frac{N}{2\pi i\tau}}\int_{-\infty}^{\infty} d\eta'(1+i\eta')^N \exp[iN(\eta-\eta')^2/2\tau].\end{aligned} \tag{4.3.16}$$

Now change the variables as follows,

$$\begin{aligned} &iN(\eta-\eta')^2/2\tau = -x^2, && ix = \sqrt{\frac{iN}{2\tau}}(\eta-\eta'), \\ &\eta-\eta' = \sqrt{\frac{w\tau}{iN}}ix = \sqrt{\frac{2i\tau}{N}}x, && \eta' = \eta - \sqrt{\frac{2i\tau}{N}}x, \\ &d\eta' = -\sqrt{\frac{2i\tau}{N}}\,dx, && \eta' = \pm\infty \to x = \mp\infty \end{aligned} \tag{4.3.17}$$

Substitute these back into Equation [4.3.16],

$$\begin{aligned}\psi(\eta,\tau) &= \sqrt{\frac{N}{2\pi i\tau}}\int_{+\infty}^{-\infty}\left(1+i\eta-i\sqrt{\frac{2i\tau}{N}}\,x\right)^N \exp(-x^2)\left(\left(\frac{2i\tau}{N}\right)^{\frac{1}{2}}\right)dx \\ &= (1+i\eta)^N\frac{1}{\sqrt{\pi}}\int_{-\infty}^{+\infty}\left(1-\frac{i}{1+i\eta}\sqrt{\frac{2i\tau}{N}}x\right)^N \exp(-x^2)\,dx\end{aligned} \tag{4.3.18}$$

Simplify this further by letting,

$$q = \frac{i}{1+\eta}\sqrt{\frac{2i\tau}{N}} \tag{4.3.19}$$

Now use the binomial theorem to expand,

$$\begin{aligned}(1-qx)^N &= 1 - Nqx + \frac{N(N-1)}{2!}q^2x^2 - \frac{N(N-1)(N-2)}{3!}q^3x^3 + ... + q^Nx^N \\ &= \sum_{m=0}^{N}\frac{(-1)^m}{m!}\frac{N!}{(N-m)!}q^mx^m\end{aligned} \tag{4.3.20}$$

Substitute this into Equation [4.3.18],

$$\psi(\eta,\tau) = N!(1+i\eta)^N\frac{1}{\sqrt{\pi}}\sum_{m=0}^{N}\frac{(-1)^m}{m!(N-m)!}\,q^m\int_{-\infty}^{\infty}x^m\exp(-x^2)\,dx \tag{4.3.21}$$

The integral on the right hand side is zero if m is odd, as the integrand is odd when m is odd. This means the maximum of the sum can be halved if m is replaced by $2m$. So now,

$$\psi(\eta,\tau) = N!(1+i\eta)^N\frac{1}{\sqrt{\pi}}\sum_{m=0}^{N/2}\frac{(-1)^{2m}}{(2m)!(N-2m)!}\,q^{2m}\int_{-\infty}^{\infty}x^{2m}\exp(-x^2)\,dx. \tag{4.3.22}$$

This integral has a standard solution,

$$\int_{-\infty}^{\infty} x^{2m} \exp(-x^2)\, dx = \frac{1.3.5...|2m-1|}{2^m}\sqrt{\pi} \qquad [4.3.23]$$

Substituting this result,

$$\psi(\eta,\tau) = N!(1+i\eta)^N \sum_{m=0}^{N/2} \frac{1}{(2m)!(N-2m)!} q^{2m} \frac{1.3.5...|2m-1|}{2^m} \qquad [4.3.24]$$

Now simplify as,

$$\begin{aligned} \frac{1.3.5...|2m-1|}{(2m)!} &= \frac{1.3.5...|2m-1|}{2m(2m-1)(2m-2)...5.4.3.2.1} \\ &= \frac{1}{2m(2m-2)...4.2} \\ &= \frac{1}{2^m\, m!} \end{aligned} \qquad [4.3.25]$$

So Equation [4.3.24], simplifies to

$$\psi(\eta,\tau) = N!(1+i\eta)^N \sum_{m=0}^{N/2} \frac{1}{2^m\, m!(N-2m!)} q^{2m} \frac{1}{2^m} \qquad [4.3.26]$$

Replacing q with its original form Equation [4.3.19],

$$\psi(\eta,\tau) = N!(1+i\eta)^N \sum_{m=0}^{N/2} \frac{1}{m!(N-2m!)} \left(-\frac{1}{(1+i\eta)^2}\frac{i\tau}{2N}\right)^m \qquad [4.3.27]$$

This is equivalent to ψ (22) in paper [2] with a small difference of a factor of 2 in the denominator, having checked this computationally it must just be a small typo in the paper. Computations show that this simplification preserves the essential structure of the wave $\psi(x,t)$ and the agreement persists for times over which the super-oscillations disappear.

Equation [4.3.14], can now be evaluated using the saddle point method. First locate the saddle points by setting,

$$\frac{\delta\Phi(\eta',\eta,\tau)}{\delta\eta'} = 0 \qquad [4.3.28]$$

Where,

$$\Phi(\eta',\eta,\tau) = -i\log(1+i\eta') + (\eta-\eta')^2/2\tau \qquad [4.3.29]$$

So,

$$\begin{aligned}\frac{\delta(\eta',\eta,\tau)}{\delta\eta'} &= \frac{1}{1+i\eta'} - \frac{\eta-\eta'}{\tau} = 0 \\ \tau - (1+i\eta')(\eta-\eta') &= 0 \\ \eta'^2 - (i+\eta)\eta' + i(\eta-\tau) &= 0\end{aligned} \quad [4.3.30]$$

This is a simple quadratic for η' that can be solved in the usual way,

$$\eta' = \frac{1}{2}\left(i+\eta \pm \sqrt{+(i+\eta)^2 - 4i(\eta-\tau)}\right) \quad [4.3.31]$$

For small τ, there are two saddles η_+ and η_- given by the square root.

$$\eta' = \eta_\pm = \frac{1}{2}\left(i+\eta \pm \sqrt{1-\eta^2 + 2i(\eta-2\tau)}\right) \quad [4.3.32]$$

Now making use of the saddle point theory in Chapter 2 - for,

$$\psi(\eta,\tau) = \sqrt{\frac{N}{2\pi i\tau}}\int_{-\infty}^{\infty} d\eta' \exp[iN(-i\log(1+i\eta') + (\eta-\eta')^2/2\tau)] \quad [4.3.33]$$

The saddle point components in this case are,

$$\phi(\eta') = 1 \quad [4.3.34]$$

$$\omega(\eta') = \log(1+i\eta') + (\eta-\eta')^2/2\tau \quad [4.3.35]$$

$$\frac{d\omega(\eta')}{d\eta'} = iq(\eta') - i\frac{\eta-\eta'}{\tau} \quad [4.3.36]$$

$$\frac{d^2\omega(\eta')}{d\eta'^2} = iq'(\eta') + i/\tau \quad [4.3.37]$$

Combining the contributions from both saddles,

$$\psi(\eta,\tau) = \sum_{\eta_\pm} a_\pm \exp[iN\Phi_\pm(\eta,\tau)]\left(\frac{1}{1+\tau q'(\eta_\pm(\eta,\tau))}\right)^{1/2} \quad [4.3.38]$$

Where $a_\pm$ is 1 if the saddle $\pm$ contributes and zero if i does not. What follows will try to explain this. The behaviour of the saddles divides the η, τ plane into regions, according to two criteria. At particular points the contributions $\exp[iN\Phi_\pm(\eta,\tau)]$ differ exponentially in absolute value; there are regions where the $+$ saddle dominates the $-$ one, and vice versa. These regions are separated by 'anti-Stokes lines', where the absolute values of the exponentials are equal. Also important are 'Stokes lines', where the absolute values are maximally different; the importance of these lines of extreme dominance is that across them the sub-dominant (small) exponential can appear or disappear whilst 'hidden' behind the dominant one. In addition the square root in Equation [4.3.32], introduces a branch cut, across which the $+$ and $-$ contributions interchange. These three lines are determined

by,

$$\begin{aligned} \text{anti-Stokes line: } & Im[\Phi_+(\eta,\tau) - \Phi_-(\eta,\tau)] = 0 \\ \text{Stokes line: } & Re[\Phi_+(\eta,\tau) - \Phi_-(\eta,\tau)] = 0 \\ \text{branch cut: } & \text{argument of } \sqrt{} \text{ in [4.3.32] negative real} \\ & \Rightarrow \tau > 0.5, \quad \eta = 2\tau. \end{aligned} \qquad [4.3.39]$$

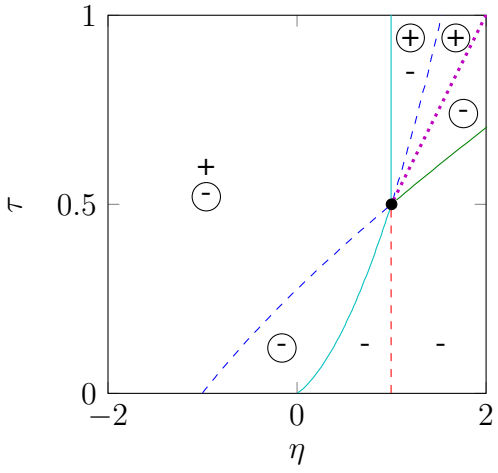

Figure 4.9: Structure of the η, τ plane according to the saddle-point approximation. Full curves: anti-Stokes lines; dashed curves: Stokes lines; dotted line: branch cut; black dot: saddle coalescence; + and -: contributing saddles, with the dominant saddle encircled. The Stokes and anti-Stokes lines were computed numerically using Equation [4.3.39]

Figure 4.9 shows the structure of these lines on the (η, τ) plane. At a glance the dominant point where all the line converge can bee seen at $\eta = 1$, $\tau = 1/2$, here the two saddles coalesce, merging together. The structure that the lines make across this plane is significant, and will now be explained. By moving in a clockwise motion starting from the bottom right corner of the graph each section made by the lines will be visited and examined. In the bottom right corner the only saddle to make a contribution is the negative one, note that it is sub-dominant but there is no accompanying positive exponential it is hidden by a discontinuity. In fact the negative exponential contributes all along the small τ part of the plane, this has been seen computationally by using the saddle point solution. Now by moving left a Stokes Line is encountered. Here the absolute values of the exponentials are maximally different. Having crossed the stokes line the new region still only has a negative contribution as the dominant positive saddle is still absent. Continuing to the left an anti-stokes line is met. Here the absolute values of the exponentials are equal and crossing the line yields the first change of dominance. The negative saddle is dominant here and is circled to show this, in terms of the plane the saddle that represents the negative exponential is now higher that the hidden positive exponential. The sub-dominant positive saddle as is the case for all small τ is absent. Now by moving further left and crossing the second Stokes line reaching the region that boarders the entire left side of the

figure, here the positive exponential finally appears all be it sub-dominantly contributing along with the negative exponential. This situation continues to persists as τ increase, until the next anti-stokes line is encountered, at $\tau > 1/2$, $\eta = 1$. This is the most important event in the circuit as the wave numbers change magnitude here, this is significant as knowledge of this can be used to investigate the disappearance of superoscillations further. By moving to the right and crossing the anti-stokes line, the positive saddle becomes dominant as is encircled to show this. The next set of lines are all relatively close compared to those below the coalescence point. Continuing on the next line encountered is a Stokes line, by crossing it and entering the next region the negative saddle disappears solely leaving the dominant positive saddle. The next event is crossing the dotted branch cut line here due to the nature of the square root the saddle switch and the positive one becomes the negative one. The negative saddle is now the dominant, by crossing the last anti-stokes line the path taken around the coalescence point has gone full circle ending back in the initial region.

Figure 4.10, illustrates the accuracy of the saddle-point approximation. It is astonishing to see how well the approximation compares to Equation [4.3.27] even inevitable failure when $\tau = 1/2$, through the saddle coalescence at $\eta = 1$ where the approximation diverges because of the vanishing of the denominator in Equation [4.3.38], is barely visible in 4.10 (b) and the magnification in (c).

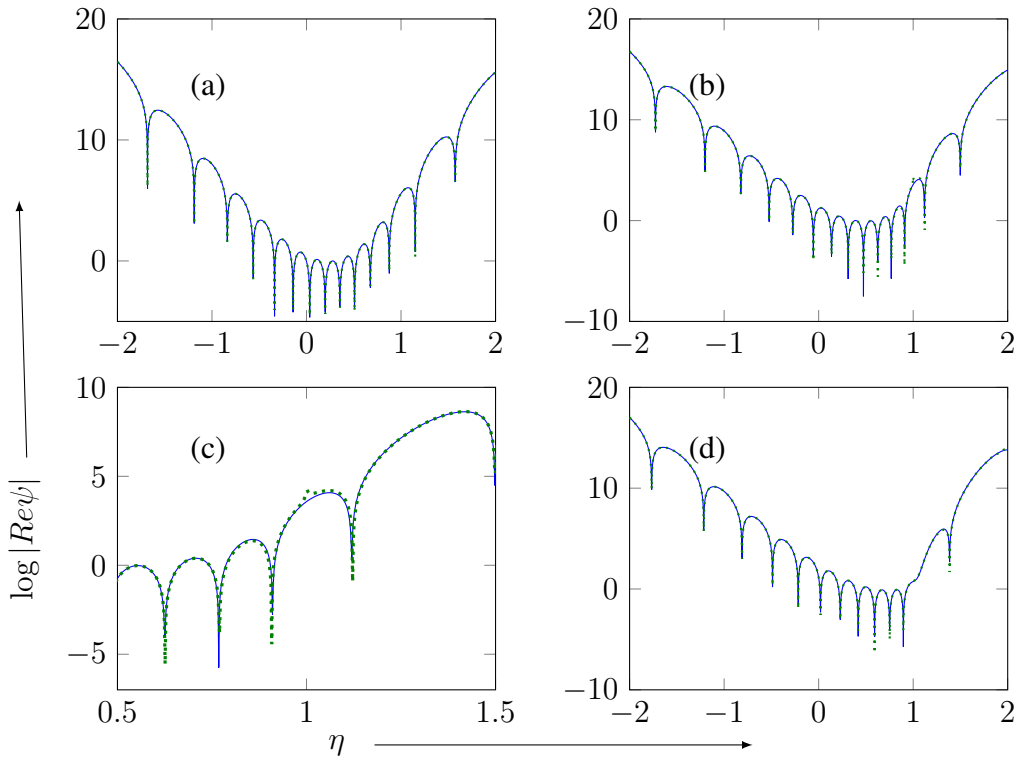

Figure 4.10: Full curves: Equation [4.3.27]; dashed curves: saddle-point approximation Equation [4.3.38], for (a) $\tau = 0.25$; (b) $\tau = 0.5$; (c) magnification of (b); (d) $\tau = 0.75$.

To understand the wall phenomena and the disappearance of superoscillations, the key thing is the crossing of the anti-Stokes line at $\eta = 1$, $\tau > 1/2$ where the dominance of the saddles changes from η_- to η_+. The wavenumber changes magnitude here,

$$\begin{aligned} k_{\pm} &= Re\, q_{\pm}(\eta_{\pm}(1,\tau),1,\tau) = Re\frac{1}{1+i\eta_{\pm}(1,\tau)} \\ &= Re\frac{1-i\eta^{*}_{\pm}(1,\tau)}{(1+i\eta_{\pm}(1,\tau))(1-i\eta^{*}_{\pm}(1,\tau))} \end{aligned} \quad [4.3.40]$$

Now the saddles Equation [4.3.32], with $\sqrt{i} = \frac{1+i}{\sqrt{2}}$ can be written as,

$$\eta_{\pm} = \frac{1}{2}(1+i)(1 \pm \sqrt{2\tau-1}) \quad [4.3.41]$$

$$\eta^{*}_{\pm} = \frac{1}{2}(1-i)(1 \pm \sqrt{2\tau-1}^{*}) \quad [4.3.42]$$

There are four separate regimes where evaluating Equation [4.3.40] will provide insight. They are, (i) Saddle point $+$, $\tau > 1/2$ (ii) Saddle point $-$, $\tau > 1/2$ (iii) Saddle point $+$, $\tau < 1/2$ (iv) Saddle point $-$, $\tau < 1/2$. Remembering that when the wavenumber is greater than 1 superoscillations are being exhibited, the following investigates the regions where the wavenumber decays from showing superoscillations to conventional ones.

(i) Saddle point $+$, $\tau > 1/2$

$$1 + i\eta_{+} = 1 + \frac{1}{2}(i-1)(1+\sqrt{2\tau-1}) \quad [4.3.43]$$

$$1 - i\eta^{*}_{+} = 1 - \frac{1}{2}(i+1)(1+\sqrt{2\tau-1}) \quad [4.3.44]$$

$$(1+i\eta_{+})(1-i\eta^{*}_{-}) = \frac{1}{4}((1-\sqrt{2\tau-1})^2 + (1+\sqrt{2\tau-1})^2) = \tau \quad [4.3.45]$$

$$\begin{aligned} k_{+} &= Re\,\frac{1-1/2(1+i)(1+\sqrt{2\tau-1})}{\tau} \\ &= \frac{1-\sqrt{2\tau-1}}{2\tau} \end{aligned} \quad [4.3.46]$$

(ii) Saddle point $-$, $\tau > 1/2$

Using the same method as for (i)

$$k_{-} = \frac{1+\sqrt{2\tau-1}}{2\tau} \quad [4.3.47]$$

$$k_{\pm} = \frac{1 \mp \sqrt{2\tau-1}}{2\tau} \quad [4.3.48]$$

(iii) Saddle point $+$, $\tau < 1/2$

The difference here is that $\sqrt{2\tau-1}$, is imaginary so

$$\sqrt{2\tau-1} = i\sqrt{1-2\tau} \quad \text{So} \quad \sqrt{2\tau-1}^{*} = -i\sqrt{1-2\tau} \quad [4.3.49]$$

$$1 + i\eta_{+} = 1 + \frac{1}{2}(i-1)(1+i\sqrt{1-2\tau}) \quad [4.3.50]$$

$$1 - i\eta_+^* = 1 - \frac{1}{2}(i+1)(1 - i\sqrt{1-2\tau}) \tag{4.3.51}$$

$$(1 + i\eta_+)(1 - i\eta_+^*) = \frac{1}{4}(1 - \sqrt{1-2\tau})(1+i)(1-i) = \frac{1}{2}(1 - \sqrt{1-2\tau}) \tag{4.3.52}$$

$$\begin{aligned} k_+ &= Re\, \frac{1 - 1/2(1+i)(1-\sqrt{1-2\tau})}{1/2(1-\sqrt{1-2\tau})} \\ &= \frac{2}{1-\sqrt{1-2\tau}}(1/2(1-\sqrt{1-2\tau})) = 1 \end{aligned} \tag{4.3.53}$$

(iv) Saddle point $-$, $\tau < 1/2$ Using the same method as (iii)

$$k_- = 1 \tag{4.3.54}$$

At $\tau = 1/2$ Equation [4.3.48] is equal to 1 which fits perfectly. So the wave-vector k for $\tau > 1/2$ is,

$$k_\pm = \frac{1 \mp \sqrt{2\tau - 1}}{2\tau} \tag{4.3.55}$$

The wall phenomena starts at $\tau = 1/2$ here, $k_+ = k_- = 1$. As τ increases, both wave-numbers decrease, with k_+ decreasing faster than k_-.

Using Equation [4.3.55] the value of τ when superoscillations disappear can be found - called τ_d. This will occur when k_- decreases to below the maximum value of k in the Fourier series Equation [4.1.5]. In Equation [4.1.5] this maxima is $k = 1$, but that is in (x, t) space. In (η, τ) space Equation [4.3.11] shows,

$$\exp[iNk_m x] = \exp[iNk_m \eta/a] \tag{4.3.56}$$

So the scaling shows that this corresponds to $k_\pm = 1/a$ in (η, τ)

$$\frac{1}{a} = \frac{1 + \sqrt{2\tau - 1}}{2\tau} \tag{4.3.57}$$

$$\tau^2 - (a + a^2/2)\tau + a^2/2 = 0 \tag{4.3.58}$$

This is a simple quadratic so,

$$\tau_d = \frac{a + a^2/2 \pm \sqrt{(a + a^2/2)^2 - 4a^2/2}}{2} \tag{4.3.59}$$

That can be rearranged into the form,

$$\tau = \frac{a^2}{4}\left(1 + \frac{2}{a} + \sqrt{1 + \frac{4}{a} - \frac{4}{a^2}}\right) \tag{4.3.60}$$

As $a >> 1$, $\tau_d \approx a^2/2$. In the original units $\tau = a^2 t$,

$$t_d = \frac{1}{4}\left(1 + \frac{2}{a} + \sqrt{1 + \frac{4}{a} - \frac{4}{a^2}}\right) \xrightarrow{a\to\infty} \frac{1}{2} \qquad [4.3.61]$$

So t_d depends only on a and the dependence is weak - t_d is independent of N. In the case of Figure 4.8 where $a = 4$, $N = 20$ the disappearance of superoscillations happens at $t = 0.706$.

The time for the disappearance of superoscillations has been found by making small angle approximations. It is now instructive to interpret this result by using the original Fourier series Equation [4.2.4]. Figure 4.11 with parts (a), (b), (c) and (d) illustrates superoscillations at different times, t for $a = 4$, $N = 20$ where the shortest wavelength contribution from the Fourier series is 0.1π with the half wavelengths being 0.05π. In (a) $t = 0.600$ the shortest wavelength is 0.0539π, displaying superoscillations with the positive part of the waveform having a length of 0.01π and the negative part of the waveform having a length of 0.0439π, both halves of the waveform are shorter than the shortest contributing wavelength. In (b) $t = 0.622$ the shortest wavelength is 0.0974π, here the positive part of the waveform is 0.0462π and the negative part of the waveform having a length of 0.0512π. The overall wavelength is shorter than the shortest contributing one, so would suggest superoscillations but here the negative half of the waveform is larger than the shortest half wavelength contribution. The complete oscillations is now not superoscillatory. The time $t = 0.622$ is the first time where this is the case and stated as the time of disappearance of superoscillations for the free particle given the parameters $a = 4$, $N = 20$. In (c) $t = 0.706$ the shortest wavelength is 0.1009π the positive part of the waveform having a length of 0.0481π and the negative part of the waveform having a length of 0.0528π. Here the overarching wavelength is not superoscillatory and with the positive half being shorter that the contribution and the negative half being longer. No superoscillation is present here. In (d) t=1.700 the shortest wavelength is 0.0996π, here the positive part of the waveform is 0.0207π and the negative part having a length of 0.0789π. This is an interesting case as by observation and calculation superoscillations have ceased but the overall wavelength and the positive half are shorter than the shortest contribution. The negative part of the waveform here is longer than the contribution so given the definition defined in part (b) superoscillations do not exist here. The effect being displayed is the squeezing out of oscillations as time increases due to the shifting of the subtle interference between contributions that creates superoscillations. At a first glance these could be mistaken to be superoscillations but are in fact not.

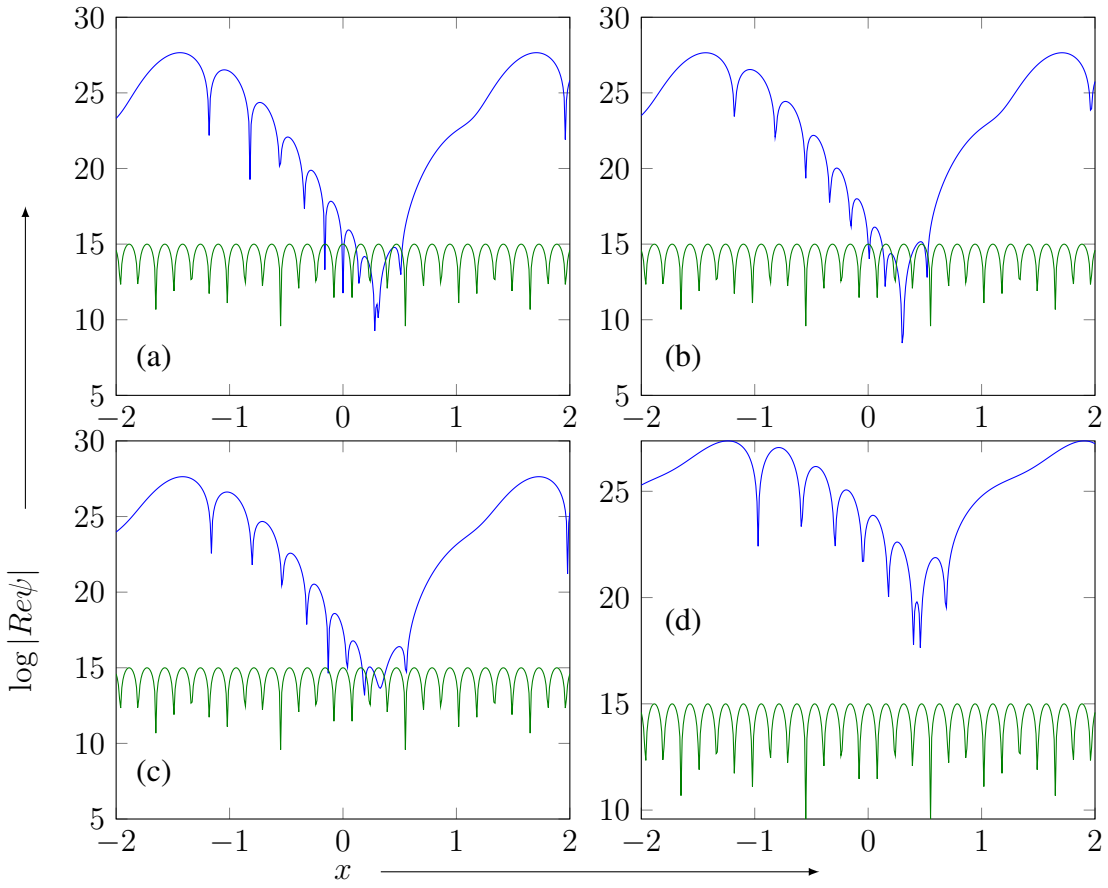

Figure 4.11: Superoscillations disappearing as time increases, for a=4, N=20 at times, (a) t=0.650, (b) t=0.690, (c) t=0.706 and (d) t=1.700. Compared to the fastest frequency of the Fourier series 4.2.4.

CHAPTER

FIVE

TIME DEPENDENT SUPEROSCILLATIONS IN THE QUANTUM HARMONIC OSCILLATOR

"The aim of art is to represent not the outward appearance of things,
but their inward significance."
Aristotle

The purpose of this Chapter is to investigate the persistence of Superoscillations in time evolving in the Quantum Harmonic Oscillator. Four different mathematical representations of the initial super oscillatory wavepacket are scrutinized. The findings are discussed in chapter six "Interpretation". The following has been achieved by building on the physics of the previous chapters.

5.1 Initial Superoscillatory State

To examine how superoscillations evolve in the quantum harmonic oscillator it is convenient to define a superoscillatory wavepacket, the function $\psi(x)$.

$$\psi(x,0) = \frac{1}{\sqrt{G}}(\cos px + ia \sin px)^N \qquad [5.1.1]$$

where the constant p=1, is an arbitrary wavevector defined nonetheless to help keep track of units throughout the following manipulations. The equation is valid in the region $-\pi/p < x < \pi/p$ and zero elsewhere at time = 0. It is set up this way by writing,

$$\psi(x,0) = \sum_{n=0}^{\infty} C_n \phi_n \qquad [5.1.2]$$

where C_n are coefficients to be determined and ψ_n are eigenfunctions of the harmonic oscillator. The wave must now be normalized and by doing so G will be found.

$$|\psi(x,0)|^2 = \psi(x,0)\psi^*(x,0) = \left(\frac{1}{\sqrt{G}}\right)^2 (1 + (a^2 - 1)\sin^2 px)^N \qquad [5.1.3]$$

$$I = \frac{\left(\frac{1}{\sqrt{G}}\right)^2}{p} \int_{-\pi/p}^{\pi/p} \left(\frac{1}{\sqrt{G}}\right)^2 (1 + (a^2 - 1)\sin^2 y)^N \, dy \qquad [5.1.4]$$

The binomial theorem is used to expand Equation [5.1.4].

$$I = \frac{\left(\frac{1}{\sqrt{G}}\right)^2}{p} \sum_{m=0}^{N} (a^2-1)^m \frac{N!}{m!(N-m)!} \int_{-\pi}^{\pi} \sin^{2m} y \, dy \qquad [5.1.5]$$

Now the standard integral below is used to complete the normalization.

$$\int_{-\pi}^{\pi} \sin^{2m} y \, dy = \frac{2\sqrt{\pi}\Gamma(m+1/2)}{\Gamma(m+1)} \qquad [5.1.6]$$

where the Gamma function is, $\Gamma(m) = (m-1)!$, in this case $\Gamma(m+\frac{1}{2}) = (\frac{2(m+0.5)!}{2m+1})$, $\Gamma(m+1) = m!$. So that,

$$\begin{aligned} I &= \frac{\left(\frac{1}{\sqrt{G}}\right)^2}{p} \sum_{m=0}^{N} (a^2-1)^m \frac{N!}{m!(N-m)!} \frac{2\sqrt{\pi}\Gamma(m+1/2)}{\Gamma(m+1)} \\ &= \frac{2\sqrt{\pi}\left(\frac{1}{\sqrt{G}}\right)^2}{p} \Gamma(N+1) \sum_{m=0}^{N} (a^2-1)^m \frac{\Gamma(m+1/2)}{\Gamma^2(m+1)\Gamma(N-m+1)} \end{aligned} \qquad [5.1.7]$$

By rearranging for G,

$$G = \frac{2\sqrt{\pi}}{p} \Gamma(N+1) \sum_{m=0}^{N} (a^2-1)^m \frac{\Gamma(m+1/2)}{\Gamma^2(m+1)\Gamma(N-m+1)} \qquad [5.1.8]$$

Now the normalized initial wave $\psi(x)$ can be written,

$$\psi(x,0) = \frac{1}{\sqrt{G}} (\cos px + ia \sin px)^N \qquad [5.1.9]$$

The wavepacket will now be examined in four distinct ways.

5.2 Expansion in Terms of Eigenfunctions

The next step is to define our normalized initial wave $\psi(x)$ as a sum of harmonic eigenfunctions.

$$\frac{1}{\sqrt{G}} (\cos px + ia \sin px)^N = \sum_{n=0}^{\infty} C_n \phi_n \qquad [5.2.1]$$

$$= \sum_{n=0}^{\infty} C_n \frac{1}{\sqrt{2^n n!}} \left(\frac{m\omega}{\pi\hbar}\right)^{1/4} \exp[-m\omega x^2/2\hbar] \, H_n\left(\sqrt{\frac{m\omega}{\hbar}} x\right) \qquad [5.2.2]$$

Where C_n are coefficients to be determined and $H_n(x)$ are the usual Hermite Polynomials. This expansion in terms of eigenstates rather than plane waves is appropriate for a particle evolving according to a quantum mechanical quantum harmonic oscillator Hamiltonian. This mean that the previously stated definition for superoscillations is no longer suitable. A superoscillating function should be de-

fined as one that oscillates faster that the most rapidly varying eigenfunction that is included in the eigenfunction sum Equation [5.2.2]. It is now convenient to write the Schroedinger equation and use the asymptotic parameter N to collect some variables,

$$\begin{aligned} i\hbar\frac{\delta\psi}{\delta t} &= -\frac{\hbar^2}{2m}\frac{\delta^2\psi}{\delta x^2} + \frac{1}{2}m\omega^2x^2\psi \\ iN\frac{\delta\psi}{\delta t} &= -\frac{1}{2}\frac{\delta^2\psi}{\delta x^2} + \frac{1}{2}N^2\omega^2x^2\psi \end{aligned} \qquad [5.2.3]$$

where $N = m/\hbar$ and is to be taken as large. As before with p a new variable $s = 1$ is introduced to the left hand side (LHS) to identify the units of N that is analogous to $\hbar/m$ with the units $L^{-2}T$. So now ψ can be written,

$$\frac{1}{\sqrt{G}}(\cos px + ia\sin px)^{sN} = \sum_{n=0}^{\infty} C_n \frac{1}{\sqrt{2^n n!}}\left(\frac{N\omega}{\pi}\right)^{1/4} \exp[-N\omega x^2/2]\, H_n\left(\sqrt{N\omega}x\right) \qquad [5.2.4]$$

as a linear combination of separable solutions. Now the weighting factor C_n must be found. Orthogonality of the eigenfunctions gives,

$$C_n = \frac{1}{\sqrt{2^n n!}}\left(\frac{N\omega}{\pi}\right)^{1/4}\frac{1}{\sqrt{G}}\int_{-\infty}^{\infty}\exp[-N\omega x^2/2]\, H_n\left(\sqrt{N\omega}x\right)(\cos px + ia\sin px)^{sN}\, dx \qquad [5.2.5]$$

Now incorporating the time dependence, the evolving state of ψ can now be written as,

$$\psi = \sum_{n=0}^{\infty} C_n \frac{1}{\sqrt{2^n n!}}\left(\frac{N\omega}{\pi}\right)^{1/4} \exp[-N\omega x^2/2]\, H_n\left(\sqrt{N\omega}x\right)\exp(-i(n+1/2)\omega t) \qquad [5.2.6]$$

This can and has been evaluated numerically by computation and can be seen in Figure 6.1. The accuracy is limited by the fact that as n becomes large it is increasingly difficult to calculate the Hermite polynomials accurately, this is seen as the wavy lines that distort the structure of the superoscillations in small t. The non-zero part of the wave function is bounded at zero time, but as time evolves the it spreads out but is kept localized by the harmonic oscillator potential. Note that p is always taken as 1 and is used to make a direct comparison with Berry's papers. This is because x has units of distance and as the argument of sin or cos must be dimensionless p has to have units of inverse distance. The code created within Matlab can be found in Appendix A part (a).

5.3 Evolution in terms of the Propagator

An alternative method for evolving a wavefunction over time is to use the propagator. The propagator for the quantum harmonic oscillator [24] is,

$$K(x,x',t) = \left(\frac{N\omega}{2\pi i\sin\omega t}\right)^{1/2}\exp\left[\frac{iN\omega((x^2+x'^2)\cos\omega t - 2xx')}{2\sin\omega t}\right] \qquad [5.3.1]$$

Where as before $N = m/\hbar$. Now the evolving state $\psi(x,t)$ can be written as an integral over its propagator,

$$\psi(x,t) = \int_{-\infty}^{\infty} K(x,x',t)\psi(x',0)dx' \qquad [5.3.2]$$

As $f(x)$ is a localized function between $-\pi$ & π the integral must be done in this region as well. So,

$$\psi(x,t) = \frac{1}{\sqrt{G}}\left(\frac{N\omega}{2\pi i \sin\omega t}\right)^{1/2}\int_{-\pi}^{\pi}\exp\left[iN\left(\frac{\omega((x^2+x'^2)\cos\omega t - 2xx')}{2\sin\omega t}\right)\right](\cos px' + ia\sin px')^{sN}\,dx' \qquad [5.3.3]$$

which can be written as,

$$\psi(x,t) = \frac{1}{\sqrt{G}}\left(\frac{N\omega}{2\pi i \sin\omega t}\right)^{1/2}\int_{-\pi}^{\pi}\exp\left[iN\left(\int_0^{x'} q(x'')\,dx'' + \frac{\omega((x^2+x'^2)\cos\omega t - 2xx')}{2\sin\omega t}\right)\right]dx'. \qquad [5.3.4]$$

Where,

$$f(x') = (\cos px' + ia\sin px')^{sN} = \exp\left[iN\int_0^{x'} q(x'')dx''\right] \qquad [5.3.5]$$

Rearranging this for $q(x')$ gives,

$$q(x') = ps\frac{i\sin px' + a\cos px'}{\cos px' + ia\sin px'} \qquad [5.3.6]$$

Now Equation [5.3.4] can be written as,

$$\psi(x,t) = \frac{1}{\sqrt{G}}\left(\frac{N\omega}{2\pi i \sin\omega t}\right)^{1/2}\int_{-\pi}^{\pi}\exp[iN\Phi(x,x',t)]\,dx'. \qquad [5.3.7]$$

Where the complex phase,

$$\Phi(x,x',t) = \int_0^{x''} ps\frac{i\sin px'' + a\cos px''}{\cos px'' + ia\sin px''}\,dx'' + \frac{\omega((x^2+x'^2)\cos\omega t - 2xx')}{2\sin\omega t} \qquad [5.3.8]$$

Now Equation [5.3.7] is in the asymptotic form. As $N >> 1$ it can be used as an asymptotic parameter and the integral can be approximated using the saddle point method, Chapter 2. The saddle point method will give $\psi(x,t)$, Equation [5.3.4] as a number of contributions from the saddles $x_j(x,t)$ within the complex plane. The saddles are located by using,

$$\frac{\delta}{\delta x'}\Phi(x,x',t) = 0 \qquad [5.3.9]$$

$$q(x') = \frac{\omega}{\sin\omega t}(x - x'\cos\omega t) \Rightarrow x' = x_j(x,t) \qquad [5.3.10]$$

Using Equations [2.3.1] and [2.3.8],

$$I = \int \exp[Nf(x')]\phi(x')\,dx' = \sum_j \phi(x_j)\exp[Nf(x_j)]\left(\frac{-2\pi}{Nf''(x_j)}\right)^{1/2} \quad [5.3.11]$$

In this case,

$$\phi(x_j) = 1 \quad [5.3.12]$$

The most convenient form of $f(x)$ can be taken from Equation [5.3.4],

$$f(x') = i\left(\int_0^{x'} q(x'')\,dx'' + \frac{\omega((x^2+x'^2)\cos\omega t - 2xx')}{2\sin\omega t}\right) \quad [5.3.13]$$

Double differentiation gives,

$$f'(x') = iq(x') + \frac{i\omega}{\sin\omega t}(x'\cos\omega t - x) \quad [5.3.14]$$

$$f''(x') = iq'(x') + i\omega\frac{\cos\omega t}{\sin\omega t} \quad [5.3.15]$$

Now lets find $q'(x')$. Starting from,

$$q(x') = ps\frac{i\sin px' + a\cos px'}{\cos px' + ia\sin px'} \quad [5.3.16]$$

By making use of the quotient rule,

$$q'(x') = p^2 s\frac{i(1-a^2)}{(\cos px' + ia\sin px')^2}. \quad [5.3.17]$$

Assembling these into the form of the saddle point theory,

$$\psi(x,t) = \frac{1}{\sqrt{G}}\sum_j\left(\frac{\omega}{(q'(x_j)\sin\omega t + \omega\cos\omega t)}\right)^{1/2} f(x_j)\exp\left[iN\frac{\omega((x^2+x_j)\cos\omega t - 2xx_j)}{2\sin\omega t}\right] \quad [5.3.18]$$

where the sum is over all the saddles that contribute. There are actually only a maximum of two saddles that contribute to this integral. An important thing to notice here is that when we take the low ω limit that is $w \to 0$,

$$\cos\omega t \to 1, \qquad \sin\omega t \to \omega t \quad [5.3.19]$$

and the solution for the simple quantum harmonic oscillator collapses down to the exact solution for the free particle Equation [4.3.10].

$$\psi(x,t) = \frac{1}{\sqrt{G}}\sum_j\left(\frac{1}{1+q'(x_j)t}\right)^{1/2} f(x_j)\exp[iN(x-x_j)^2/2t] \quad [5.3.20]$$

The propagator method does have one substantial advantage over the eigenfunction expansion, the limitation imposed by the Hermite polynomials H_n is not felt here. Equation [5.3.18] has been sampled numerically by computation and can be seen in Figure 6.2. The code created within Matlab can be found in Appendix A part (b).

5.4 Small angle approximation: Exact solution

Superoscillations occur for small x and t, so now the integral will be done making use of small angle approximations. $f(x)$ and $q(x)$ can be replaced by simpler functions and new scaled variables introduced.

$$f(\eta') = (1 + i\eta')^{Ns} \tag{5.4.1}$$

Then,

$$q(\eta) = -\frac{i}{N}\frac{d}{d\eta}\log f(\eta) = \frac{s}{1+i\eta} \tag{5.4.2}$$

Also the following substitutions make things considerably simpler,

$$\eta' = apx', \qquad \tau = a^2p^2t, \qquad \Omega = \omega/a^2p^2 \tag{5.4.3}$$

Now take Equation [5.3.3], and change the variables according to this prescription.

$$\psi(\eta,\tau) = \frac{1}{\sqrt{G}}\int_{-\pi/ap}^{\pi/ap}\left(\frac{N\Omega}{2\pi i\sin\Omega\tau}\right)^{1/2}\exp\left[iN\frac{\Omega((\eta^2+\eta'^2)\cos\Omega\tau - 2\eta\eta')}{2\sin\Omega\tau}\right](1+i\eta')^{Ns}\,d\eta' \tag{5.4.4}$$

Now the integral can be evaluated exactly.

$$\psi(\eta,\tau) = \left(\frac{N\Omega}{2\pi i\sin\Omega\tau}\right)^{1/2}\exp[iN\Omega\eta^2\cot\Omega\tau/2]\int_{-\pi/ap}^{\pi/ap}(1+i\eta')^N\exp\left[iN\frac{\Omega(\eta'^2\cos\Omega\tau - 2\eta\eta')}{2\sin\Omega\tau}\right]d\eta' \tag{5.4.5}$$

Completing the square for the LHS exponent,

$$\begin{aligned}\left(\sqrt{\cos\Omega\tau}\eta' - \frac{\eta}{\sqrt{\cos\Omega\tau}}\right)^2 &= \eta'^2\cos\Omega\tau - 2\eta\eta' + \frac{\eta^2}{\cos\Omega\tau}\\ \therefore \eta'^2\cos\Omega\tau - 2\eta\eta' &= \left(\eta'\sqrt{\cos\Omega\tau} - \frac{\eta}{\sqrt{\cos\Omega\tau}}\right)^2 - \frac{\eta^2}{\cos\Omega\tau}\end{aligned} \tag{5.4.6}$$

with the simplified exponent η terms can be taken outside of the integral once more,

$$\begin{aligned}\psi(\eta,\tau) = \left(\frac{N\Omega}{2\pi i\sin\Omega\tau}\right)^{1/2}&\exp[iN\Omega\eta^2\cot\Omega\tau/2]\exp[-iN\Omega\eta^2/2\sin\Omega\tau\cos\Omega\tau]...\\ &\int_{-\pi/ap}^{\pi/ap}(1+i\eta')^N\exp\left[iN\Omega\frac{(\eta'\sqrt{\cos\Omega\tau} - \eta/\cos\Omega\tau)^2}{2\sin\Omega\tau}\right]d\eta'\end{aligned} \tag{5.4.7}$$

The exponentials outside of the integral can now be simplified,

$$\exp\left[iN\Omega\eta^2\frac{\cos\Omega\tau}{2\sin\Omega\tau}-iN\Omega\eta^2\frac{1}{2\sin\Omega\tau\cos\Omega\tau}\right]=\exp[-iN\Omega\eta^2\tan\theta/2] \quad [5.4.8]$$

The simplified integral takes the form,

$$\psi(\eta,\tau)=\left(\frac{N\Omega}{2\pi i\sin\Omega\tau}\right)^{1/2}\exp[-iN\Omega\eta^2\tan\theta/2]\int_{-\pi/ap}^{\pi/ap}(1+i\eta')^N\exp\left[iN\Omega\frac{(\eta'\sqrt{\cos\Omega\tau-\eta/\cos\Omega\tau})^2}{2\sin\Omega\tau}\right]d\eta' \quad [5.4.9]$$

Next a change of variable is made from η' to ξ.

$$iN\Omega\frac{(\eta'\sqrt{\cos\Omega\tau}-\eta\sqrt{\cos\Omega\tau})^2}{2\sin\Omega\tau}=-\xi \quad [5.4.10]$$

$$\eta'=-\sqrt{\frac{2i\sin\Omega\tau}{N\Omega\cos\Omega\tau}}\xi+\frac{\eta}{\cos\Omega\tau} \quad [5.4.11]$$

$$d\eta'=-\sqrt{\frac{2i\sin\Omega\tau}{N\Omega\cos\Omega\tau}}\,d\xi \quad [5.4.12]$$

During the change of variable the limits of the integral are changed as well. They are defined as,

$$\eta=\pm\infty\rightarrow\xi=\mp\infty \quad [5.4.13]$$

This can be seen by the reasoning below,

$$\xi=\sqrt{\frac{-iN\Omega}{\sin 2\Omega\tau}}(\eta'\cos\Omega\tau-\eta). \quad [5.4.14]$$

So when ξ is large (ξ_l),

$$\xi_l=\sqrt{\frac{-iN\Omega}{\sin 2\Omega\tau}}(\frac{\pi}{ap}\cos\Omega\tau-\eta) \quad [5.4.15]$$

and when ξ is small (ξ_s),

$$\xi_s=\sqrt{\frac{-iN\Omega}{\sin 2\Omega\tau}}(\frac{-\pi}{ap}\cos\Omega\tau-\eta) \quad [5.4.16]$$

In general, with these limits the integral can only be done numerically. However for small τ or when $\Omega\tau<<1,\ \sin\Omega\tau\rightarrow\Omega\tau$ and,

$$\sqrt{\frac{iN\Omega}{\sin 2\Omega\tau}}\quad\rightarrow\sqrt{\frac{iN}{\tau}}\quad\rightarrow\infty\quad\text{as}\quad\tau\rightarrow 0 \quad [5.4.17]$$

So for small times τ we can put the limits in as $\mp\infty$. Now putting Equations [5.4.10], [5.4.11] and [5.4.12] into Equation [5.4.9],

$$\psi(\eta,\tau) = -\left(\frac{1}{\pi\cos\Omega\tau}\right)^{1/2}\exp[-iN\Omega\eta^2\tan\Omega\tau/2]\left(1+\frac{i\eta}{\cos\Omega\tau}\right)^N ... \\ \int_{\infty}^{-\infty}\left(1-\frac{i}{1+i\frac{\eta}{\cos\Omega\tau}}\sqrt{\frac{2i\sin\Omega\tau}{N\Omega\cos\Omega\tau}}\xi\right)^N\exp[-\xi^2]\,d\xi \qquad [5.4.18]$$

Now make the substitution below, and reverse the limits of integration.

$$q = \frac{i\cos\Omega\tau}{\cos\Omega\tau+i\eta}\sqrt{\frac{2i\sin\Omega\tau}{N\Omega\cos\Omega\tau}} \qquad [5.4.19]$$

$$\psi(\eta,\tau) = \left(\frac{1}{\pi\cos\Omega\tau}\right)^{1/2}\exp[-iN\Omega\eta^2\tan\Omega\tau/2]\left(1+\frac{i\eta}{\cos\Omega\tau}\right)^N\int_{-\infty}^{\infty}(1-q\xi)^N\exp[-\xi^2]\,d\xi \qquad [5.4.20]$$

Equation [5.4.20] collapses down into Equation [4.3.18] as $\Omega\to 0$, which is as expected. The binomial theorem gives,

$$(1-q\xi)^N = \sum_{m=0}^{N}\frac{(-1)^m}{m!}\frac{N!}{(N-m)!}q^m\xi^m \qquad [5.4.21]$$

Using the expansion with Equation [5.4.20] yields,

$$\psi(\eta,\tau) = \left(\frac{1}{\pi\cos\Omega\tau}\right)^{1/2}\exp[-iN\Omega\eta^2\tan\Omega\tau/2]\left(1+\frac{i\eta}{\cos\Omega\tau}\right)^N\sum_{m=0}^{N}\frac{(-1)^m}{m!}\frac{N!}{(N-m)!}q^m ... \\ \int_{-\infty}^{\infty}\xi^m\exp[-\xi^2]\,d\xi \qquad [5.4.22]$$

For odd m the integral is zero, so the sum can be reduced to $N/2$ and m is replaced by $2m$.

$$\psi(\eta,\tau) = \left(\frac{1}{\pi\cos\Omega\tau}\right)^{1/2}\exp[-iN\Omega\eta^2\tan\Omega\tau/2]\left(1+\frac{i\eta}{\cos\Omega\tau}\right)^N\sum_{m=0}^{N/2}\frac{(-1)^{2m}}{2m!}\frac{N!}{(N-2m)!}q^{2m} ... \\ \int_{-\infty}^{\infty}\xi^{2m}\exp[-\xi^2]\,d\xi \qquad [5.4.23]$$

Given that $(-1)^{2m}=1$ and the standard integral Equation [4.3.23], ψ can be written,

$$\psi(\eta,\tau) = \left(\frac{1}{\cos\Omega\tau}\right)^{1/2}\exp[-iN\Omega\eta^2\tan\Omega\tau/2]\left(1+\frac{i\eta}{\cos\Omega\tau}\right)^N\sum_{m=0}^{N/2}\frac{N!}{m!(N-2m)!}\left(\frac{q}{2}\right)^{2m} \qquad [5.4.24]$$

Substituting q Equation [5.4.19], back in gives,

$$\psi(\eta,\tau)=\left(\frac{1}{\cos\Omega\tau}\right)^{1/2}\exp[-iN\Omega\eta^2\tan\Omega\tau/2]\sum_{m=0}^{N/2}\frac{N!}{m!(N-2m)!}\left(\frac{\cos\Omega\tau+i\eta}{\cos\Omega\tau}\right)^{N-2m}\left(\frac{-i\sin\Omega\tau}{2N\Omega\cos\Omega\tau}\right)^{m} \quad [5.4.25]$$

For this solution approximations have been made meaning that the expression is only valid for small x and t, but after that the integral has been evaluated exactly. This method helps provide a check for the next saddle point evaluation of the integral. Equation [5.4.25] has been sampled numerically by computation and can be seen in Figure 6.4. The code created within Matlab can be found in Appendix A part (c).

5.5 Small angle Saddle Point method

The small angle integral Equation [5.4.4] can also be solved using the saddle point method employed previously. The advantage here is that the saddles will be found as analytic expressions. The wavefunction can now be written,

$$\psi(\eta,\tau)=\left(\frac{N\Omega}{2\pi i\sin\Omega\tau}\right)^{1/2}\int_{-\pi/ap}^{\pi/ap}\exp\left[iN\left(-ik\log(1+i\eta')+\frac{\Omega((\eta^2+\eta'^2)\cos\Omega\tau-2\eta\eta')}{2\sin\Omega\tau}\right)\right]d\eta' \quad [5.5.1]$$

The phase is,

$$\Phi(\eta,\eta',\tau)=-is\log(1+i\eta')+\frac{\Omega((\eta^2+\eta'^2)\cos\Omega\tau-2\eta\eta')}{2\sin\Omega\tau} \quad [5.5.2]$$

The saddle points occur when,

$$\frac{\delta\Phi(\eta,\eta',\tau)}{\delta}=0 \quad [5.5.3]$$

$$\frac{s}{1+i\eta'}+\frac{\Omega(\eta'\cos\Omega\tau-\eta)}{\sin\Omega\tau}=0 \quad [5.5.4]$$

This is a quadratic for η',

$$\eta'^2-(i+\frac{\eta}{\cos\Omega\tau})\eta'+i\left(\frac{\eta}{\cos\Omega\tau}-\frac{s\sin\Omega\tau}{\Omega\cos\Omega\tau}\right)=0 \quad [5.5.5]$$

The saddle points are the values that satisfy η'. They are found in the usual way using the quadratic formula.

$$\eta'=\eta_j=\frac{1}{2}\left(i+\frac{\eta}{\cos\Omega\tau}\pm\sqrt{\left(i+\frac{\eta}{\cos\Omega\tau}\right)^2-4i\left(\frac{\eta}{\cos\Omega\tau}-\frac{s\sin\Omega\tau}{\Omega\cos\Omega\tau}\right)}\right) \quad [5.5.6]$$

The saddle points are,

$$\eta_{\pm j}(\eta,\tau)=\frac{1}{2}\left(i+\frac{\eta}{\cos\Omega\tau}\pm i\sqrt{1-\frac{\eta^2}{\cos^2\Omega\tau}+\frac{2i}{\cos\Omega\tau}\left(\eta-\frac{2s\sin\Omega\tau}{\Omega}\right)}\right) \quad [5.5.7]$$

As $\Omega \to 0$ then $cos\Omega\tau \to 1$ and $\sin\Omega\tau \to \Omega\tau$ and the saddles collapse down to the free space saddles Equation [4.3.32]. These saddle points can be used in the Saddle Point solution equation from Chapter 2.

$$I = \int \phi(\eta') \exp[Nf(\eta')]\, d\eta' = \sum_j \phi(\eta_j) \exp[Nf(\eta_j)] \left(-\frac{2\pi}{Nf''(\eta_j)}\right)^{1/2} \quad [5.5.8]$$

For this case,

$$f(\eta') = s\log(1+i\eta') + \frac{i\Omega(\eta^2+\eta'^2)\cos\Omega\tau - 2\eta\eta'}{2\sin\Omega\tau} \quad [5.5.9]$$

$$f'(\eta') = iq(\eta') + \frac{i\Omega(\eta'\cos\Omega\tau - \eta)}{\sin\Omega\tau} \quad [5.5.10]$$

$$f''(\eta') = i(q'(\eta') + \Omega\cot\Omega\tau) \quad [5.5.11]$$

and

$$\phi(\eta') = 1 \quad [5.5.12]$$

Arranging these parts the Saddle point method gives the solution to the integral as,

$$\psi(\eta,\tau) = \sum_j \left(\frac{\Omega}{q'(\eta_j)\sin\Omega\tau + \Omega\cos\Omega\tau}\right)^{1/2} \exp\left[iN\left(-is\log(1+i\eta) + \frac{\Omega(\eta^2+\eta_j^2)\cos\Omega\tau + 2\eta\eta_j}{2\sin\Omega\tau}\right)\right] \quad [5.5.13]$$

Where,

$$\begin{aligned} q(\eta_j) &= \frac{s}{1+i\eta_j} \\ q'(\eta_j) &= \frac{-is}{(1+i\eta_j)^2} \end{aligned} \quad [5.5.14]$$

Equation [5.5.13] has been sampled numerically by computation and can be seen in Figure 6.5. It has been checked that the approximations made maintain the essential structures being studied. The code created within Matlab can be found in Appendix A part (d).

CHAPTER

SIX

INTERPRETATION

"Research is what I'm doing when I don't know what I'm doing."

Wernher von Braun

The purpose of this Chapter is to check the derivations of the previous one by analysing their graphical form and to interpret the behaviour of the saddles from the saddle point method. The aim is to exhibit the different methods for displaying superoscillations and check that the simplifications preserve the essential structure of the wave ψ, that is being studied.

Next with the confirmation that the different approximations used are in agreement with each other, a discussion of how the (η, τ) plane is divided up by the behaviour of the contribution from the saddle points. This leads into the time of disappearance t_d for superoscillations in the quantum harmonic oscillator being found. This is seen to have a dependence ω that appears from the added complexity of the quantum harmonic oscillator and is shown to collapse down to the free particle case when is taken as very small. The critical frequency for superoscillations is then found and is shown to act as an upper limit where higher frequencies no longer exhibit superoscillations. This suggest that the free particle is somehow maximally superoscillating. Finally by inspecting a density plot along with the Stoke and anti-Stoke line structure of the contributing saddles it is seen that superoscillations only occur in the periodic regions in which only the negative saddle is contributing.

6.1 Accuracy of Techniques

The following figures are density plots of $-\log|Re\,\psi(x,t)|$, in this representation the zeros of Re ψ appear as thick lines. To gain some insight into the new system of superoscillations that are being studied, first compare the density plots of superoscillations evolving in free space Figure 4.7 with Figure 6.1, that pictures Equation [5.2.4] - presenting the superoscillations in the quantum harmonic oscillator as a sum of eigenfunctions given by Hermite polynomials. Figure 6.1 exhibits parts (a), (b), (c) and (d) where $a = 2$, $N = 14$ - In (a) the initial superoscillations are clearly visible as the lines that are very close together around $x = 0$. In (b) the superoscillations are visible as the weakly resolved intricate yellow lines around $x = 0$, after longer time the oscillations become slower, seen as greater separation between the lines. The superoscillations have clearly disappeared by $t = 0.20\pi$ - faster

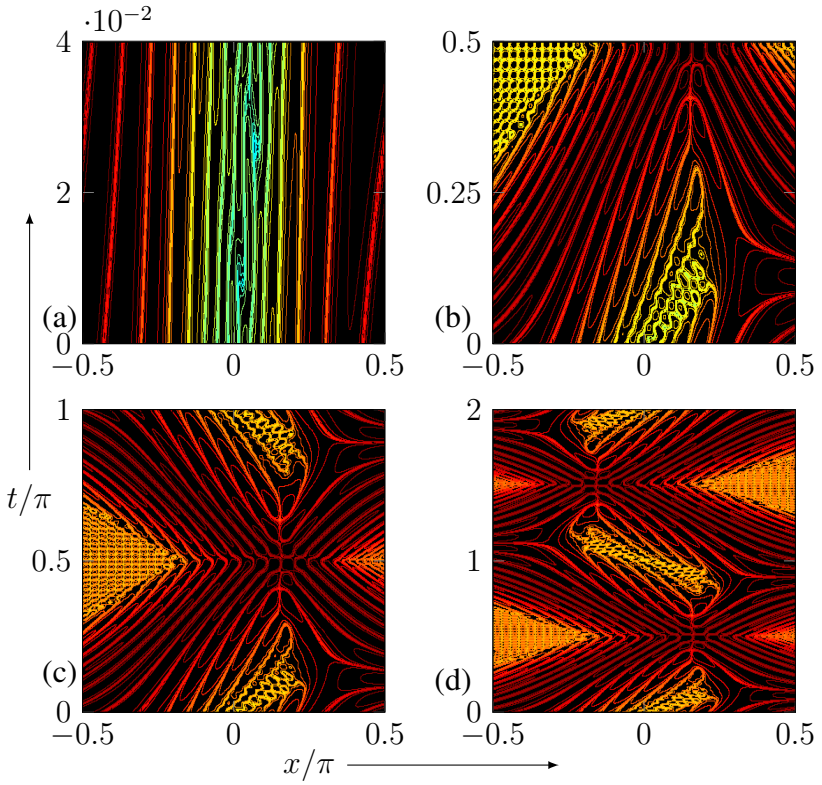

Figure 6.1: Density plot of $-\log|Re\psi(x,t)|$ defined as a sum of harmonic Eigenfunctions Equation [5.2.6] for $N = 14$, $a = 2, \omega = 1$. $(a) 0 \leq t \leq 0.04\pi$; $(b) 0 \leq t \leq \pi/2$; $(c) 0 \leq t \leq \pi$; $(d) 0 \leq t \leq 2\pi$.

than the equivalent section (b) in Figure 4.7. The main area of interest the region of superoscillations lacks detail but can see be clearly identified. The beginning of an undefined areas appear in the top left and right this is when the denominator $\cos(\omega t)$ blows up at $t = \pi/2$. In (c) the main difference between the two set-ups can be seen, strikingly the superoscillations re-form at $t = \pi$ identical to the initial wave at $t = 0$ but with a phase shift of 90 degrees. In (d) the superoscillations over time are seen to disappear, reappear, disappear again and then finally reappear completing the cycle at $t = 2\pi$ where the initial wave from $t = 0$ is seen again. The keen reader will notice that different N and a are displayed in both these graphs - this is due to a numerical failure in calculating using a sum of eigenfunctions, similar to the failure shown in Chapter 4, for the Fourier series representation. While the expansion in terms of eigenfunctions is illustrative, it offers no insight into the interesting phenomena shown in these figures. To investigate this further a more physically transparent way of describing the evolution of the wavepacket must now be used. Next the evolving state can be written as an integral over the propagator using the saddle point method to solve this integral superoscillations can be shown with the values $N = 20$, $a = 4$.

Figure 6.2 with parts (a), (b), (c) and (d) where $N = 14$, $a = 2$, pictures Equation [5.3.18] - giving $\psi(x,t)$ as a sum of contributing saddles. It is necessary to check that this method displays the same essential structure as shown in Figure 6.1. The graph indicates that it does and that the agreement persists for all time. This is remarkable given that there are approximations in both methods and the phenomenon being represented is exponentially small. The superoscillating regions are displayed with higher detail, this is an improvement on the previous method. Now that the two methods have

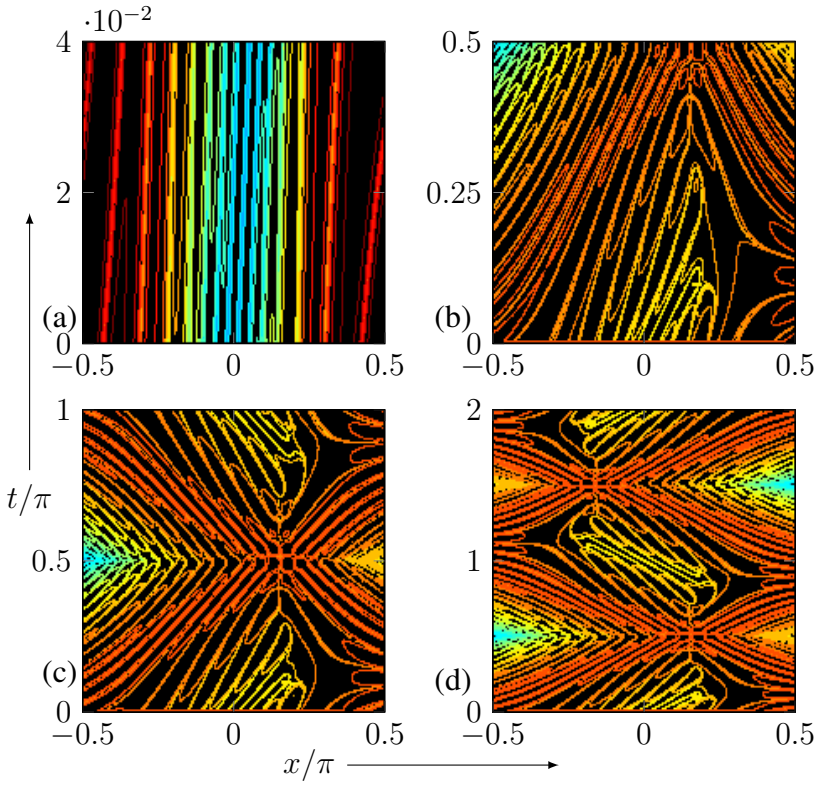

Figure 6.2: Density plot of $-\log|Re\psi(x,t)|$ defined as a sum of contributing saddles from the Saddle point solution Equation [5.3.18], for $N = 14$, $a = 2$. $(a)\ 0 \leq t \leq 0.04\pi$; $(b)\ 0 \leq t \leq \pi/2$; $(c)\ 0 \leq t \leq \pi$; $(d)\ 0 \leq t \leq 2\pi$.

been shown to agree the variables can be changed to $N = 20$, $a = 4$ as to better act as an extension of the work for the free particle.

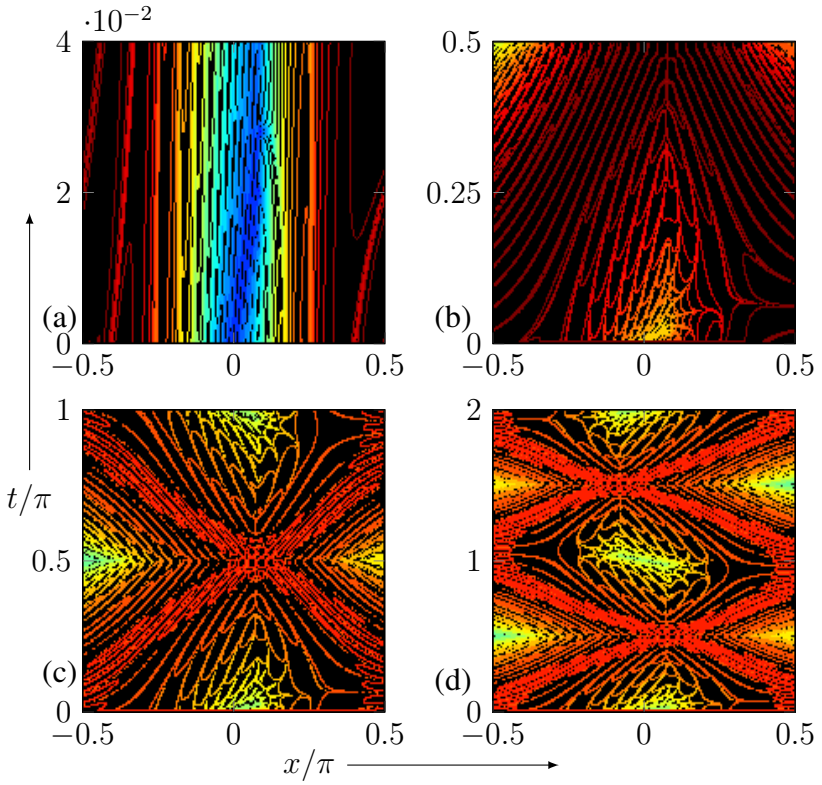

Figure 6.3: Density plot of $-\log|Re\psi(x,t)|$ defined as a sum of contributing saddles from the saddle point solution Equation [5.3.18], for $N = 20$, $a = 4$. $(a)\ 0 \leq t \leq 0.04\pi$; $(b)\ 0 \leq t \leq \pi/2$; $(c)\ 0 \leq t \leq \pi$; $(d)\ 0 \leq t \leq 2\pi$. Exhibiting a greater number of oscillations compared to Figure 6.2 due to N being larger.

Figure 6.3 with parts (a), (b), (c) and (d) where $N = 20$, $a = 4$, pictures Equation [5.3.18] - $\psi(x,t)$ as a sum of contributing saddles. When comparing with Figure 6.2 there is a greater number of oscillations as expected due to N being increased. The superoscillatory behaviour is much clear with these values. The repeating structure happens within the same interval of 2π. Comparing with Figure 4.7 the superoscillations are seen to disappear faster.

Figure 6.4 with parts (a), (b), (c) and (d) with $N = 20$, $a = 4$, pictures Equation [5.4.25] - where small angle approximations have been made to replace $f(x)$ and $q(x)$ with much simpler functions of scaled variables. This has been done as superoscillations persist for short times and are located within a small region of x. Comparing with Figure 6.3 the same periodic pattern of disappearance and reappearance can be seen. The superoscillations are located in the same regions and retain there essential structure. The undefined areas are observed for the same times but the effect of small time approximation can be seen around them, luckily these are not specific regions of interest and the simplification is seen to maintain the essential structures of study.

Figure 6.5 with parts (a), (b), (c) and (d) with $N = 20$, $a = 4$, pictures Equation [5.5.13] - where the integral of the simplified functions has been solved using the saddle point method and $\psi(\eta,\tau)$ is a sum of contributing saddles. The essential structures are again preserved and persist over all time. The advantage of this method is that an analytic expressions for the saddle points is found and can be

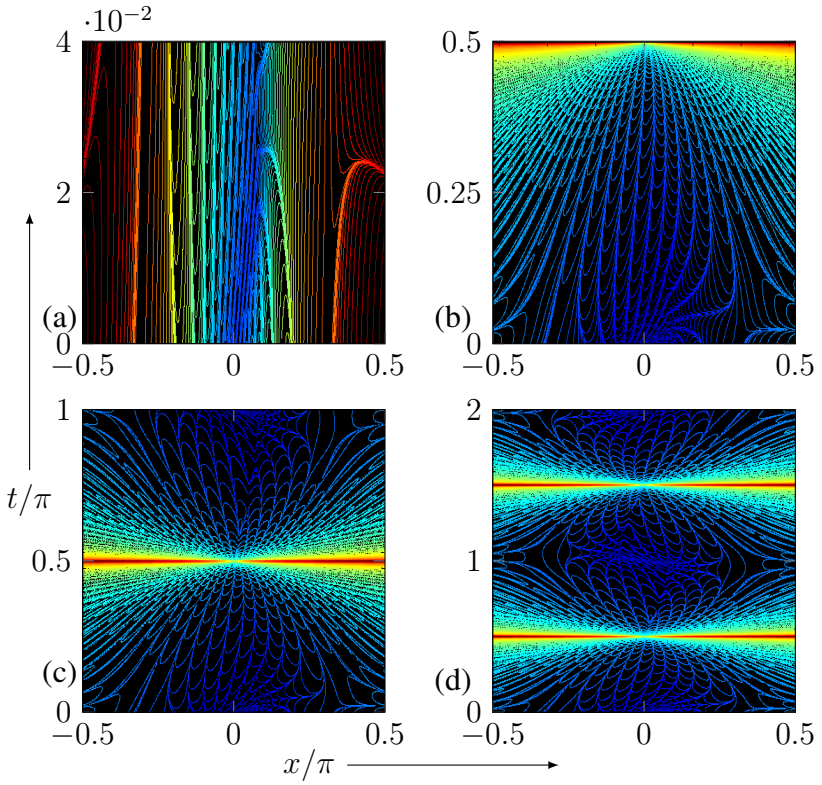

Figure 6.4: Density plot of $-\log|Re\psi(\eta,\tau)|$ defined by Equation [5.4.25], the small angle approximation - for $N = 20$, $a = 4$. $(a)\ 0 \le \tau \le 0.04\pi$; $(b)\ 0 \le \tau \le \pi/2$; $(c)\ 0 \le \tau \le \pi$; $(d)\ 0 \le \tau \le 2\pi$.

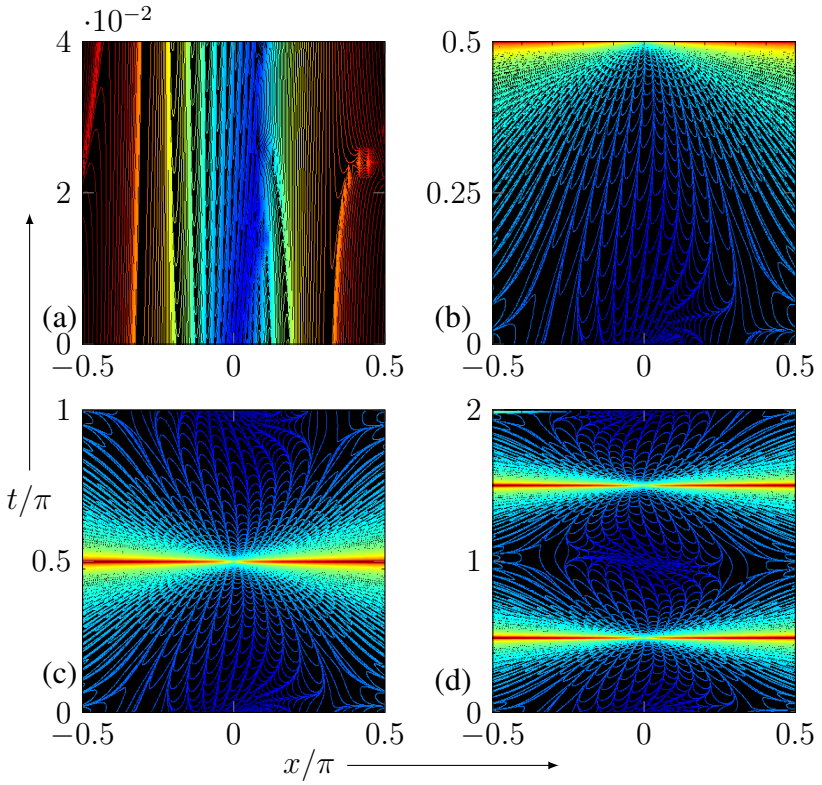

Figure 6.5: Density plot of $-\log|Re\psi(x,t)|$ defined as a sum of contributing saddles from the small angle saddle point solution Equation [5.5.13], for $N = 20$, $a = 4$. $(a)\ 0 \le t \le 0.04\pi$; $(b)\ 0 \le t \le \pi/2$; $(c)\ 0 \le t \le \pi$; $(d)\ 0 \le t \le 2\pi$. Small angle Saddle

used to investigate the periodic disappearance and reappearance of superoscillations.

The methods and simplifications of the previous chapter all maintain superoscillations and are used to investigate when they disappear and when they reappear in.

6.2 Deportment of saddles

The behaviour of the saddles splits the (η, τ) plane into different regions, separated by 'Stokes lines' and 'anti-Stokes lines. At given points the contribution from saddles to the wave function Equation [5.5.13], differs exponentially in absolute value; there are regions where $+$ dominates $-$, and vice versa. The dashed blue Stokes lines note the point in which these values are maximally different and full black anti-Stokes lines mark where the absolute values are equal. These lines represent the borders between one or the other saddle dominating if they both exist. These lines are key to an understanding of the asymptotics of the system [6]. Also shown on the plane as a green dotted line is a branch cut where the saddles interchange. This occurs because of the square root in Equation [5.5.13].

Figure 6.6 shows how the (η, τ) plane is structured by these lines. It shows the Stokes lines (blue dashed lines), the anti-Stokes lines (black full lines) and the branch cut (green dotted lines), the saddles are indicated by $+$ and $-$ signs with the dominant one being encircled. For small Ω the diagram represents the free particle example Figure 6 of paper [2]. For $\Omega = 1$, at $\eta = 1$ a curve is observed. The curved is observed to follow the line $\eta = \cos\Omega\tau$. There are two striking features, the point where the saddles coalesce $\eta = 0.8$, $\tau = 0.5$ and the dotted lines where the propagator defined by Equation [5.3.1] is undefined. As the line represents an infinity the influence of the saddles cannot be felt here. The overall structure is seen to reappear as an inverse of itself at $\tau = \pi/2$ and then repeat at $\tau = \pi$. Given this is will suffice to discuss the region $0 \leqslant \tau \leqslant \pi/2$. To begin start at the bottom right of this region and follow clockwise in a circuit around the region, moving through each section. In the bottom right only the $-$ saddle contributes, now move left and cross a Stokes lines here the $-$ saddle persists. Continue and cross an anti-Stokes line the $-$ saddle is still the only contribution here, next move along and cross the next Stokes line. Finally the $+$ saddle appears and contributes along with the $-$ saddle that remains the dominant one. Now moving right along the top of the prescribed region bordered by the dotted line, an anti-Stokes line is crossed here both saddle contribute with neither dominating the other. Continue and cross the next Stokes line in this area both saddles again contribute. Next crossing the branch cut line this region isn't well defined by the simplification used, but the saddles swap sign and are shown to both contribute.

The following figures display the analysis used to create the Figure 6.6. Figure 6.7, pictures the 3D complex plane of the phase Equation [5.5.2]. The surface exhibits two saddle points one in the light yellow area and the second in the slightly darker orange area. The purpose of this graph is to familiarize the reader with the look of the saddles on this surface to better interpret the following graphs 6.8 and 6.9 that display these complex planes in 2D.

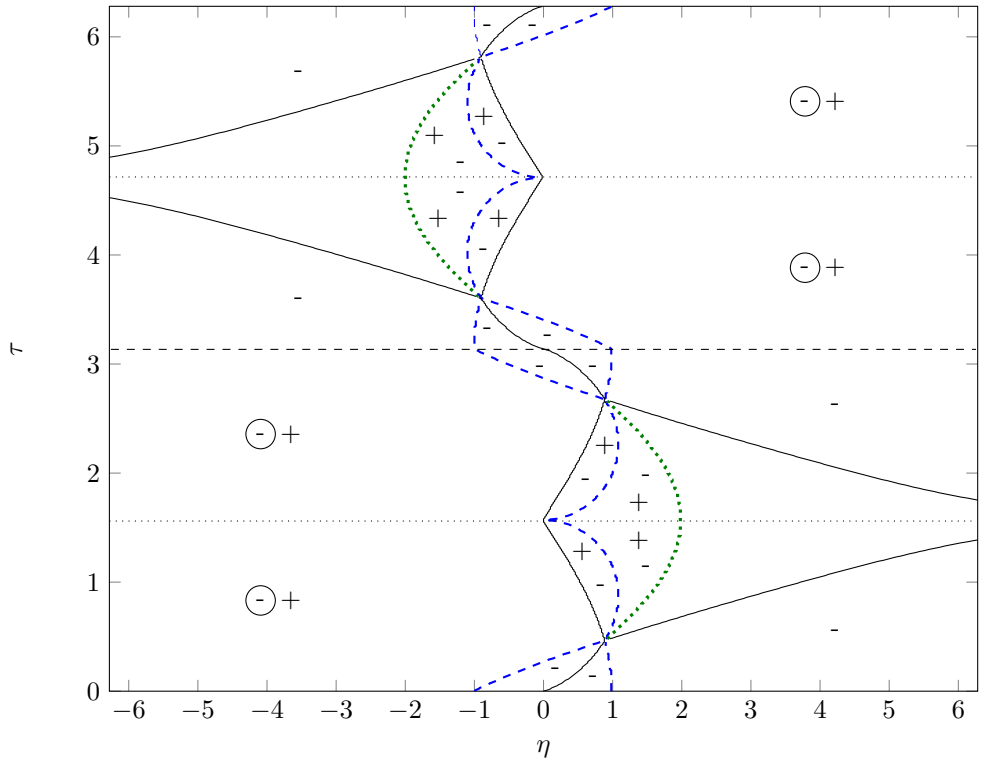

Figure 6.6: Structure of the (η, τ) plane according to the saddle-point approximation Equation [5.5.13]. It shows the Stokes lines (blue dashed lines), the anti-Stokes lines (black full lines) and the branch cut (green dotted lines). The $\pm$ detail the saddles with the dominant saddle encircled. Where $\Omega = 1$.

Figure 6.8, With parts (a) - (f) examines as slice of Figure 6.6 at time, $t = 0.05\pi$ - before the first saddle coalescence point. Part (a) pictures Superoscillations Equation [5.3.18] The blue line the overall wave form, the green and red lines the 2 contributing saddles. Part (b) is a magnification of (a), the numbered dashed lines (1) - (4) are the specific positions of the complex phase surfaces Equation [5.5.2], displayed in parts (c) - (f). In parts (a) and (b), (1) - (4) has been chosen so that is investigates the different sections defined by the Stokes structures of Figure 6.6. Parts (c) - (f) exhibit only one saddle marked by a black arrow. The missing saddle is taken by the discontinuity - refer to the 3D graph for a different example that displays the discontinuity Figure 6.7.

Figure 6.9, With parts (a) - (f) examines as slice of Figure 6.6 at time, $t = 0.3\pi$ - after the first saddle coalescence point. Part (a) pictures Superoscillations Equation [5.3.18] The blue line the overall wave form, the green and red lines the 2 contributing saddles. Part (b) is a magnification of (a), the numbered dashed lines (1) - (4) are the specific positions of the complex phase surfaces Equation [5.5.2], displayed in parts (c) - (f). In parts (a) and (b), (1) - (4) has been chosen so that is investigates the different sections defined by the Stokes structures of Figure 6.6. Part (c) displays two saddles, ones contribution is dominating the other. Parts (d) - (f) also exhibit two saddles where the contributions are close enough to both be relevant.

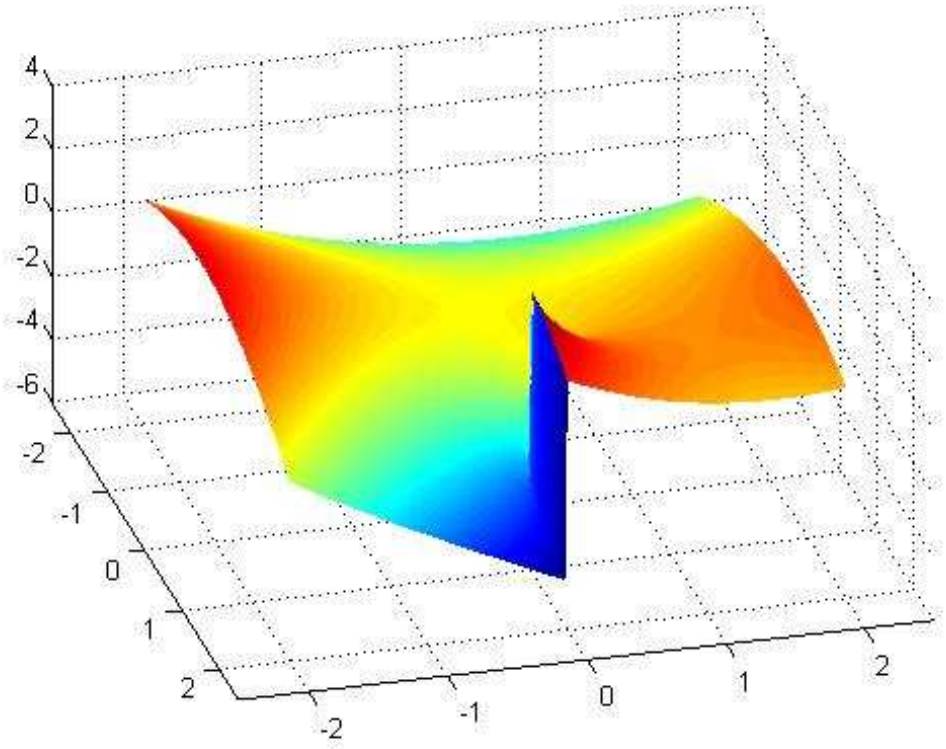

Figure 6.7: 3D plot of the complex plane given by the phase Equation [5.5.2]. Exhibiting saddle points that will be later displayed as 2D plots.

6.3 Time of Disappearance

To understand the disappearance of superoscillations, the key point is the exchange of dominance when crossing the line which is an Stokes line below the coalescence point and an anti-stokes line above it, this line starts at $\eta = 1$ when $\tau = 0$. For the free particle case this line is vertical, but for the Harmonic Oscillator it is,

$$\eta = \cos \Omega\tau \qquad [6.3.1]$$

The saddle points are,

$$\eta'_{\pm}(\eta, \tau) = \frac{1}{2}\left(i + \frac{\eta}{\cos \Omega\tau} \pm i\sqrt{1 - \frac{\eta^2}{\cos^2 \Omega\tau} + \frac{2i}{\cos \Omega\tau}\left(\eta - \frac{2s \sin \Omega\tau}{\Omega}\right)}\right) \qquad [6.3.2]$$

Choosing the point $\eta = \cos \Omega\tau$, the saddles are simplified considerably to,

$$\eta'_{\pm}(\cos \Omega\tau, \tau) = \frac{1}{2}\left(i + 1 \pm \sqrt{2i\left(\frac{2s}{\Omega} \tan \Omega\tau - 1\right)}\right) \qquad [6.3.3]$$

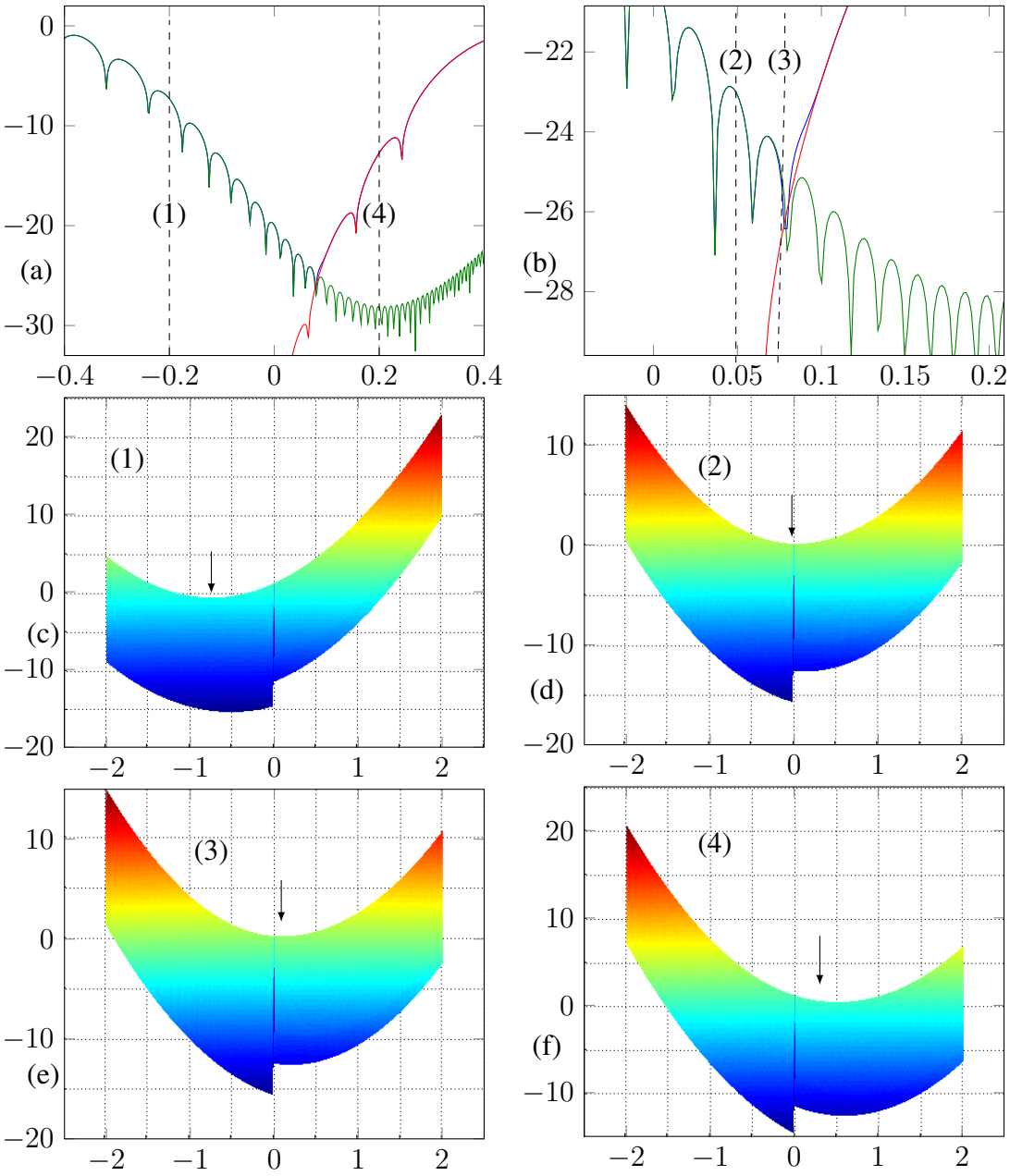

Figure 6.8: For the time, $t = 0.05\pi$. Parts (a) Superoscillations Equation [5.3.18] The blue line the overall wave form, the green and red lines the 2 contributing saddles. (b) A Magnification of (a). Also (c), (d), (e) and (f) showing the saddles in the complex plane Equation [5.5.2], for positions (1) -0.2, (2) 0.06, (3) 0.08 and (4) 0.2; where arrows mark saddle points and the height represents the contribution.

Using $\sqrt{i} = \frac{1+i}{\sqrt{2}}$ a further simplification can be made so that the complex conjugate can be taken with ease,

$$\eta'_{\pm}(\cos\Omega\tau, \tau) = \frac{1}{2}(i+1)\left(1 \pm \sqrt{\frac{2k}{\Omega}\tan\Omega\tau - 1}\right) \qquad [6.3.4]$$

The wavenumber $k_{\pm}$ now needs to be to evaluated,

$$k_{\pm} = Re\frac{1 - i\eta^*_{\pm}(\cos\Omega\tau, \tau)}{(1 - i\eta^*_{\pm}(\cos\Omega\tau, \tau))(1 + i\eta_{\pm}(\cos\Omega\tau, \tau))} \qquad [6.3.5]$$

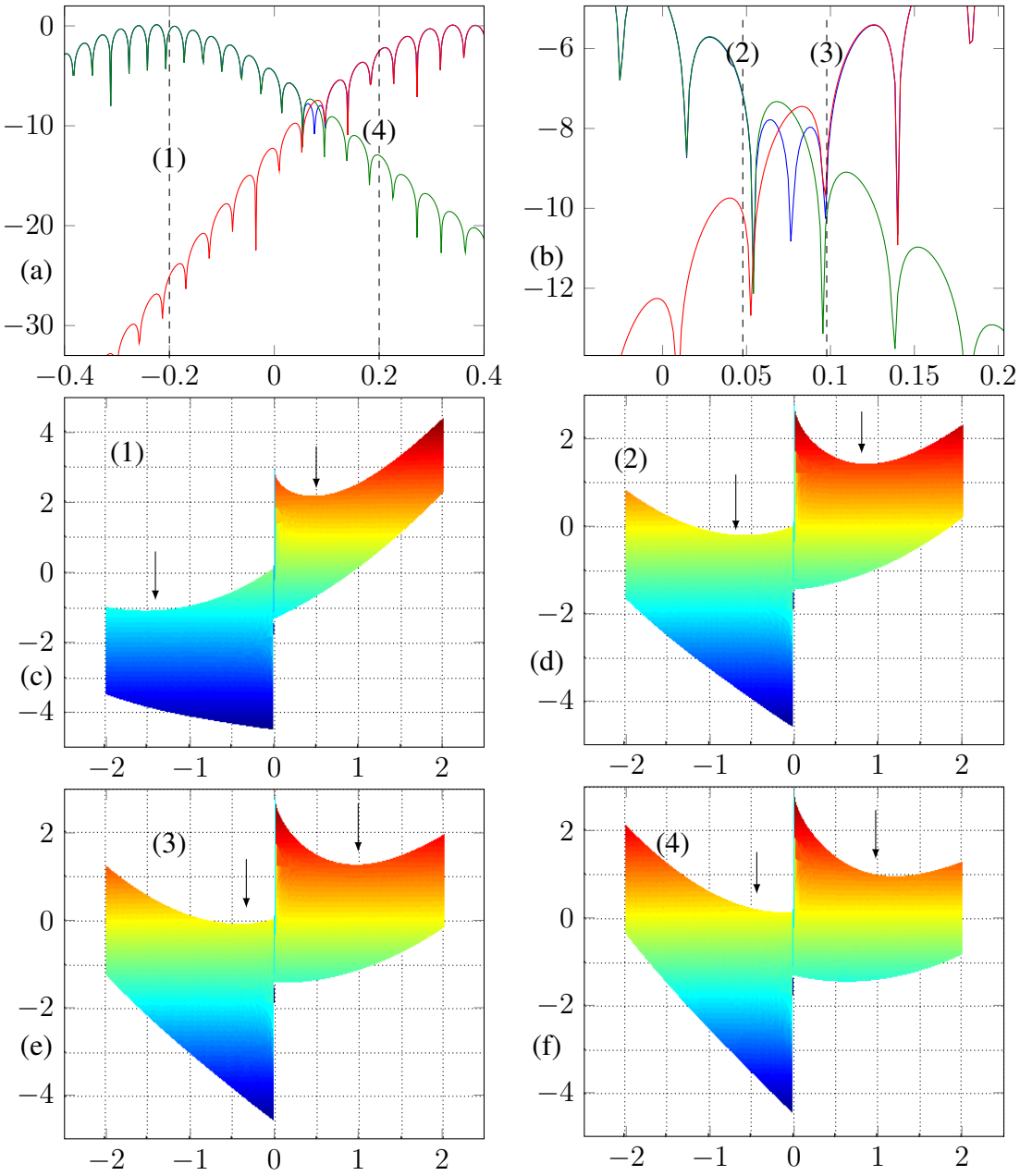

Figure 6.9: For the time, $t = 0.3\pi$. Parts (a) Superoscillations Equation [5.3.18] The blue line the overall wave form, the green and red lines the 2 contributing saddles. (b) A Magnification of (a). Also (c), (d), (e) and (f) showing the saddles in the complex plane Equation [5.5.2], for positions (1) -0.2, (2) 0.05, (3) 0.1 and (4) 0.2; where arrows mark saddle points and the height represents the contribution.

There are four separate regimes where evaluating $k_{\pm}$ will provide insight. They are, (i) Saddle point +, $\frac{2k}{\Omega}\tan\Omega\tau - 1 > 0$ (ii) Saddle point +, $\frac{2s}{\Omega}\tan\Omega\tau - 1 < 0$ (iii) Saddle point -, $\frac{2s}{\Omega}\tan\Omega\tau - 1 > 0$ (iv) Saddle point -, $\frac{2s}{\Omega}\tan\Omega\tau - 1 < 0$.

To begin the solution for k_+, using η_+,

$$\eta_+ = \frac{1}{2}\left(1 + \sqrt{\frac{2s}{\Omega}\tan\Omega\tau - 1}\right) + \frac{i}{2}\left(1 + \sqrt{\frac{2s}{\Omega}\tan\Omega\tau - 1}\right) \qquad [6.3.6]$$

Where the complex conjugate is,

$$\eta_+^* = \frac{1}{2}\left(1+\sqrt{\frac{2s}{\Omega}\tan\Omega\tau-1}^*\right) - \frac{i}{2}\left(1+\sqrt{\frac{2s}{\Omega}\tan\Omega\tau-1}^*\right) \quad [6.3.7]$$

Completing the form of the components for k,

$$1+i\eta_+ = \frac{1}{2}\left(1-\sqrt{\frac{2s}{\Omega}\tan\Omega\tau-1}\right) + \frac{i}{2}\left(1+\sqrt{\frac{2s}{\Omega}\tan\Omega\tau-1}\right) \quad [6.3.8]$$

and

$$1-i\eta_+^* = \frac{1}{2}\left(1-\sqrt{\frac{2s}{\Omega}\tan\Omega\tau-1}^*\right) - \frac{i}{2}\left(1+\sqrt{\frac{2s}{\Omega}\tan\Omega\tau-1}^*\right). \quad [6.3.9]$$

The following notation is to large so the substitution SRA has been made to shorten it.

$$SRA = \frac{2s}{\Omega}\tan\Omega\tau - 1 \quad [6.3.10]$$

Using Equations [6.3.8] and [6.3.9], to evaluate Equation [6.3.5].

$$k_\pm = 2\,Re\frac{\left(1-\sqrt{SRA}^*\right) - i\left(1+\sqrt{SRA}^*\right)}{\left(\left(1-\sqrt{SRA}^*\right) - i\left(1+\sqrt{SRA}^*\right)\right)\left(\left(1-\sqrt{SRA}\right) + i\left(1+\sqrt{SRA}\right)\right)} \quad [6.3.11]$$

Now there are two different cases, that must be looked at separately.

(i) The first is when $\frac{2s}{\Omega}\tan\Omega\tau - 1 > 0$ here the square root is real and the wavenumber is,

$$k_\pm = 2\,Re\frac{\left(1-\sqrt{\frac{2s}{\Omega}\tan\Omega\tau-1}^*\right) - i\left(1+\sqrt{\frac{2s}{\Omega}\tan\Omega\tau-1}^*\right)}{\left(1-\sqrt{\frac{2s}{\Omega}\tan\Omega\tau-1}\right)^2 + \left(1+\sqrt{\frac{2s}{\Omega}\tan\Omega\tau-1}\right)^2} \quad [6.3.12]$$

The denominator can be simplified to,

$$\left(1-\sqrt{\frac{2s}{\Omega}\tan\Omega\tau-1}\right)^2 + \left(1+\sqrt{\frac{2s}{\Omega}\tan\Omega\tau-1}\right)^2 = \frac{4s}{\Omega}\tan\Omega\tau \quad [6.3.13]$$

So now Equation [6.3.12] is,

$$k_+ = \frac{1-\sqrt{\frac{2s}{\Omega}\tan\Omega\tau-1}}{\frac{2s}{\Omega}\tan\Omega\tau} \quad [6.3.14]$$

Which collapses down to the free space Equation [4.3.42], when Ω is small.

(ii) The second case is when $\frac{2s}{\Omega}\tan\Omega\tau\tan -1 < 0$, here the square root is imaginary giving,

$$\sqrt{\frac{2s}{\Omega}\tan\Omega\tau - 1} = i\sqrt{1 - \frac{2s}{\Omega}\tan\Omega\tau} \tag{6.3.15}$$

and,

$$\sqrt{\frac{2s}{\Omega}\tan\Omega\tau - 1}^{*} = -i\sqrt{1 - \frac{2s}{\Omega}\tan\Omega\tau}. \tag{6.3.16}$$

Again a substitution has to be made to shorten the notation.

$$SRA2 = 1 - \frac{2s}{\Omega}\tan\Omega\tau \tag{6.3.17}$$

$$k_{\pm} = 2\,Re\frac{\left(1 + i\sqrt{SRA2}\right) - i\left(1 - i\sqrt{SRA2}\right)}{\left(\left(1 + i\sqrt{SRA2}\right) - i\left(1 - i\sqrt{SRA2}\right)\right)\left(\left(1 - i\sqrt{SRA2}\right) + i\left(1 + i\sqrt{SRA2}\right)\right)} \tag{6.3.18}$$

Taking the real part and cancelling,

$$k_{+} = \frac{1}{1 - \sqrt{1 - \frac{2s}{\Omega}\tan\Omega\tau}} \tag{6.3.19}$$

Equations [6.3.14] and [6.3.19] are equal to 1 when,

$$\tau = \frac{1}{\Omega}\arctan\frac{\Omega}{2s} \tag{6.3.20}$$

this is as expected given they were found by splitting into the two cases. Exactly the same results are found for the negative saddle η_{-} (iii) and (iv). Combining the two, for $\frac{2s}{\Omega}\tan\Omega\tau - 1 > 0$,

$$k_{\pm} = \frac{1 \mp \sqrt{\frac{2s}{\Omega}\tan\Omega\tau - 1}}{\frac{2s}{\Omega}\tan\Omega\tau} \tag{6.3.21}$$

and $\frac{2s}{\Omega}\tan\Omega\tau - 1 < 0$,

$$k_{\pm} = \frac{1}{1 \mp \sqrt{1 - \frac{2s}{\Omega}\tan\Omega\tau}} \tag{6.3.22}$$

Now the focus is on Equation [6.3.21] where $\tau > \Omega^{-1}\arctan(\frac{\Omega}{2s})$ as is later seen this is where superoscillations disappear. Now from the sum of eigenfunctions Equation [5.2.4] in normal space (x, t) the wavevector with the highest eigenvector contribution can be found from the asymptotic behaviour of the hermite polynomials [22] (22.15.3 & 22.15.4). The wavevector with the highest contribution eigenfunction is,

$$k_{max} = \sqrt{2N\omega n_{max}} \tag{6.3.23}$$

This has been verified numerically. For the units Ω, η, τ it becomes,

$$k_{max} = a\sqrt{2N\Omega n_{max}} \tag{6.3.24}$$

k_{max} when divided by Na relates to $k_{\pm}$,

$$\frac{\sqrt{2N\Omega n_{max}}}{N} = \frac{1+\sqrt{\frac{2s}{\Omega}\tan\Omega\tau - 1}}{\frac{2s}{\Omega}\tan\Omega\tau} \tag{6.3.25}$$

Now the time of disappearance τ can be found by rearranging,

$$\left(\frac{2\sqrt{2N\Omega n_{max}}}{N\Omega}\tan\Omega\tau - 1\right)^2 = \frac{2}{\Omega}\tan\Omega\tau - 1 \tag{6.3.26}$$

This is a quadratic for $\tan\Omega\tau$,

$$\frac{4\Omega n_{max}}{N\Omega^2}\tan^2\Omega\tau - \frac{2\sqrt{2N\Omega n_{max}}/N+1}{\Omega}\tan\Omega\tau + 1 = 0 \tag{6.3.27}$$

Using the quadratic formula to solve for $\tan\Omega\tau$,

$$\tan\Omega\tau = \frac{\frac{2\sqrt{2N\Omega n_{max}}}{\Omega}/N+1 \pm \sqrt{\frac{4\sqrt{2N\Omega n_{max}}}{N\Omega^2} - \frac{8\Omega n_{max}}{N\Omega^2} + \frac{1}{\Omega}}}{8\Omega n_{max}/(N\Omega^2)} \tag{6.3.28}$$

In the scaled (η, τ) space, the superoscillation disappearance time τ is,

$$\tau_d = \frac{1}{\Omega}\arctan\left(\frac{\frac{2\sqrt{2N\Omega n_{max}}}{\Omega}/N+1 \pm \sqrt{\frac{4\sqrt{2N\Omega n_{max}}}{N\Omega^2} - \frac{8n_{max}}{N\Omega} + \frac{1}{\Omega}}}{8n_{max}/(N\Omega)}\right) \tag{6.3.29}$$

In the original variable t, this corresponds to the superoscillations disappearance time,

$$t_d = \frac{1}{\omega}\arctan\left(\frac{\frac{2\sqrt{2N\omega n_{max}/a^2}}{\omega/a^2}/N+1 \pm \sqrt{\frac{4\sqrt{2N\omega n_{max}/a^2}}{N\omega^2/a^4} - \frac{8n_{max}}{N\omega/a^2} + \frac{1}{\omega/a^2}}}{8n_{max}/(N\omega/a^2)}\right) \tag{6.3.30}$$

Note that t_d depends on a, ω, N and n_{max}. This differs from the free particle case where the only dependence was on a. The dependence on ω appears from the added complexity of the quantum harmonic oscillator and is shown to collapse down to the free particle case when taken as very small. The dependence on N and n_{max} shows up due to how the wavevector with the highest contribution eigenfunction is defined.

6.4 The Critical Frequency

It is now important to look at the frequency of the superoscillations, as the inclusion of the frequency term is what separates the quantum harmonic oscillator from the free particle case. To understand the frequency of the quantum harmonic oscillator, the key point to investigate is the conditions that are necessary for superoscillations to occur. The following has been done numerically by finding relations over a set of data.

Now the wavenumber k_{max},

$$k_{max} = \frac{2\pi}{\lambda} = \sqrt{2N\omega n_{max}} \qquad [6.4.1]$$

in (x, t) space.

$$k_{max} = \frac{2\pi}{a\lambda} = \frac{2\pi}{\Lambda} = \sqrt{2N\Omega n_{max}} \qquad [6.4.2]$$

in (η, τ) space. Using Equation [5.2.6], several examples for when superoscillations are just occurring at $t = 0$ have been calculated - results shown in Table 6.1.

N	a	n_{max}	ω	Ω	λ	$a\lambda = \Lambda$
7	2	24	0.47	0.12	0.492	0.984
10	2	54	0.34	0.085	0.328	0.656
10	2	68	0.27	0.0675	0.327	0.654
12	2	52	0.42	0.105	0.272	0.544
12	2	42	0.53	0.1325	0.270	0.540
14	2	56	0.48	0.12	0.228	0.456
14	2.5	54	0.75	0.12	0.185	0.462
10	2.5	56	0.50	0.08	0.264	0.660
10	2.5	46	0.61	0.098	0.265	0.662

Table 6.1: Examples at which superoscillations just occur at $t = 0$ for the Harmonic Oscillator. Displaying variables N, a, n_{max}, ω, Ω, λ, Λ.

Using the data in Table 6.1 a function containing Ω has been found to be constant.

$$\frac{N}{n_{max}\Omega} = \text{constant} = 2.174 \quad \text{(This is an average)} \qquad [6.4.3]$$

Rearranging for Ω,

$$\Omega = \frac{N}{2.174\, n_{max}} \qquad [6.4.4]$$

Using the data in Table 6.1 a function containing Λ has been found to be constant,

$$\Lambda N = \text{constant} = 6.52 = 3 \times 2.174 \qquad [6.4.5]$$

this can be retailed to Equation [6.4.3] by a factor of 3.

$$\Lambda\Omega = \frac{3}{n_{max}} \qquad [6.4.6]$$

Using Equation [6.4],

$$\Lambda = \frac{2\pi}{\sqrt{2N\Omega n_{max}}} \qquad [6.4.7]$$

Substituting Equation [6.4.7] into [6.4.6] gives,

$$\frac{2\pi\Omega}{\sqrt{2N\Omega n_{max}}} = \frac{3}{n_{max}} \qquad [6.4.8]$$

Rearrange for the critical frequency Ω_c,

$$\Omega_c = \frac{9N}{2\pi^2 n_{max}} \qquad [6.4.9]$$

The critical frequency Ω_c acts as a limit. For frequencies higher than this superoscillations do not occur. For lower frequencies superoscillations occur and persist for longer periods of time as Ω decreases. As Ω decreases further so that it is very small, the quantum harmonic oscillator construct becomes more and more like the free particle case. This suggest the free particle is somehow maximally superoscillating. Table 6.2, displays a verification of the critical frequency for the values used to find it.

N	a	n_{max}	Ω	Ω_c
7	2	24	0.12	0.133
10	2	54	0.085	0.084
10	2	68	0.0675	0.067
10	2.5	56	0.08	0.081
10	2.5	46	0.098	0.099
12	2	52	0.105	.081
12	2	42	0.1325	0.099
14	2	56	0.12	0.114
14	2.5	54	0.12	0.118

Table 6.2: Verification of Ω_c

6.5 Final notes

Figure 6.10, is a combination of two types plots that have already been examined. A density plot for Equation [5.3.18] with the set-up $N = 20$, $a = 4$, $\omega = 1$ and Figure 6.6 displaying only the Stokes and anti-Stokes line structure in white. Using Equation [6.3.30], the time of disappearance t_d is found to be below the coalescence point. Visual inspection of the density plot is in agreement with as the superoscillation cease below the coalescence point - the oscillations are more sparse after this time. Superoscillations can be seen to periodically occur in the areas where only the negative saddle is present and are gone when both saddles are present.

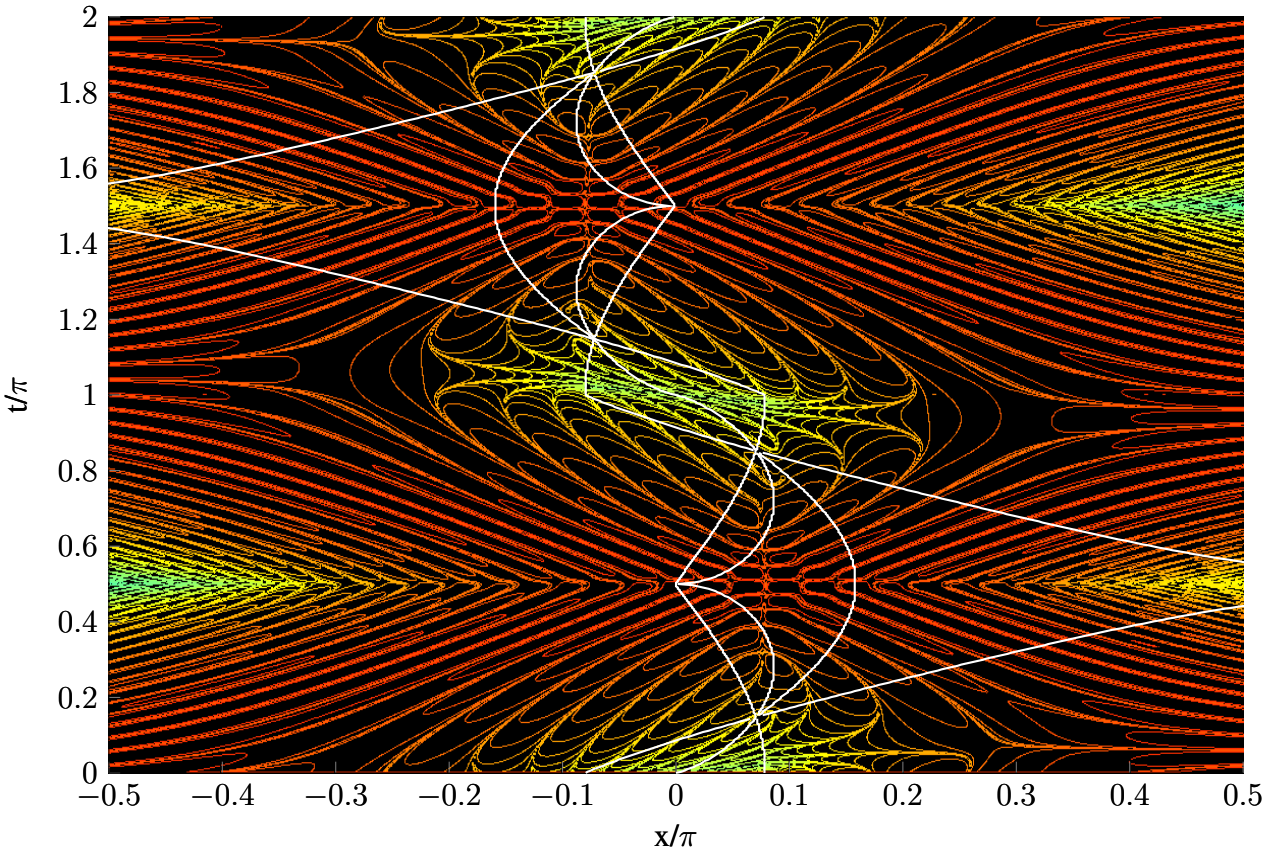

Figure 6.10: Density plot of $-\log|Re\psi(x,t)|$ defined as a sum of contributing saddles from the saddle point solution Equation [5.3.18], for $N = 20$, $a = 4$, $\omega = 1$. With an over lay (white lines) of the Stokes and anti-Stokes line structure.

CHAPTER

SEVEN

CONCLUSION

"Life grants nothing to us mortals without hard work."

Horace

This thesis set out to provide an introduction to superoscillations, and to further the research of Professors Sir Michael Berry and Sandu Popescu [2]. The aim was to apply their previous work on the persistence of superoscillations in free space to the quantum harmonic oscillator, with the main objective being to calculate a function for the disappearance time , t_d, of this phenomena. Due to the periodic nature of the harmonic oscillator it was expected that superoscillations would display a heightened periodic structure that is familiar to the periodic revival seen for free space - the secondary aim for this thesis was therefore to examine the effect this periodicity had upon the superoscillations.

To achieve the aims set-out by this thesis an understanding of the mathematical tools necessary to apply the practical integral approximation - the Saddle Point Method was needed. By studying books[15,16,17,18] this was achieved. Also much of the underlying physics needed for the research carried out in this thesis is presented in papers [1,2] and by recreating these papers a good understanding of the topic was achieved. This also offered a chance to practise the newly learnt Saddle Point method.

To investigate how the initial wave [5.1.1] evolves over time a different approach was needed to the one shown in paper [2] (evolving the initial state as a Fourier series of plane waves). This was achieved by defining the wave as a sum of harmonic eigenfunctions and combining with the time dependence Equation [5.2.6], which was then coded and evaluated numerically within Matlab. Next the propagator for the harmonic oscillator was used to create an integral representation of the wavefunction Equation [5.3.7], with which the Saddle Point method could be applied, to approximate the integral as a number of contributions from saddles of the complex plane, from the phase of the integral. The resulting time dependant wave function Equation [5.3.18], was then coded and evaluated numerically within Matlab and shown to display results comparable to that of the sum of harmonic oscillator eigenfunctions. The superoscillations had been seen to occur for small position, x, and time, t, so by switching to scaled variables and making use of small angle approximations, the eigenfunction integral Equation [5.2.6], could be solved exactly by direct mathematical manipulation - resulting in Equation [5.4.25], that through computation was shown to maintain the essential structures being

studied that include the periodic re-emergence of superoscillations and the superoscillating area.

Continuing the pursuit for disappearance time, t_d, for superoscillations in the harmonic oscillator the scaled variables small angle approximation of the summation of harmonic oscillator eigenfunctions integral Equation [5.4.4], was then solved using the Saddle Point method resulting in Equation [5.5.13]. Coding this result into Matlab and comparing with the graphs of the previous methods (Figures 6.1 - 6.5), it was verified that the essential structures had again been preserved in the simplification. The important point to note here is that this method offers a prescription for the saddles Equation [6.3.2], this meant that as the saddle points could now be calculated analytically and where as before they had to be found numerically. They could now be directly used to evaluate the wavenumber, k, Equation [6.3.5]. This was done for two regions that were separated by the exchange of dominance of the saddles located by crossing an anti-Stokes line. This exchange of dominance was found by investigating how the deportment of saddles divides the (η, τ) plane into regions that are separated by Stokes and anti-Stokes lines (See Figure 6.6). Once found, k, could be related to the wavevector with the highest contributing eigenfunction, k_{max} , Equation [6.3.25]. Given that the definition for superoscillations is a function $f(x)$, that oscillates faster than the highest contributing eigenfunction - when the wavenumber equates to the wavevector of the highest contributing eigenfunction, then superoscillations will have ceased. From here it was a simple re-arrangement for time to obtain the initial goal of defining, t_d, for superoscillations within the harmonic oscillator, Equation [6.3.30].

During much of this research it has been necessary to make use of the computational program Matlab - by sampling equations, all of the figures and data tables have been produced.

The new results, obtained by this thesis are two features that are distinctive for the harmonic oscillator: (i) The frequency, ω, is an extra control parameter which dictates the strength and duration of the superoscillations - the critical frequency, Ω_c Equation [6.4.9], acts as a limit for superoscillations frequencies higher than this do not correspond to superoscillatory systems; (ii) The periodic nature of the harmonic oscillator results in superoscillations constantly dissipating and reforming. This happens faster than the periodic revival seen for the free particle [2]. Similar to the works of Berry and Sandu for free space, the time, t_d, when superoscillations disappear was found for the harmonic oscillator, Equation [6.3.30]. This thesis also adds to the definition of superoscillations initially proposed by Berry & Sandu, by stating that superoscillations are not only functions that oscillate faster than their fastest Fourier component, but can be defined as a function, $f(x)$, that oscillates faster than the highest contributing eigenfunction.

The main problem that was encountered originated from the use of quantum‘ harmonic oscillator eigenfunctions as opposed to a Fourier series of plane waves demonstrated in Berry and Sandu [2] when defining the initial states of $\psi(x)$ as a sum of separable solutions. The limitation that this imposed was due to having to calculate the Hermite polynomials, H_n, for values higher than $n = 150$ the computational methods used broke down and gave unusable results, this meant that specific values

of the superoscillatory parameters N and a had to be chosen so that n stayed in a calculable range and the function could be correctly constructed. This obstacle meant that for the values $N = 20$, $a = 4$, that were used throughout the preceding paper [2], initial equivalent Figures could not be produced and compared - only after the employment of the Saddle point method and the result of the two methods be shown to agree could then the values $N = 20$, $a = 4$ be used to produced density plots for superoscillations in the harmonic oscillator that could be compared to the ones pictured for free space.

If this research was to be furthered, it should look into what is general and what is special for superoscillations in free space and the harmonic oscillator. What is the main contribution to the time of disappearance for the two cases? Also it could be broaden to the relativistic case, where the wave packet is expanded in terms of the eigenfunctions of the Dirac or Klein-Gordon equations.

Undertaking this research has been an enjoyable experience. Getting a chance to spend time working on topics that experts in there fields are actively pursuing has been pleasurable and enlightening. Superoscillations are a new and interesting phenomena with that pose exciting applications such as Super Resolution, it is safe to say that this is a topic that deserves further research.

BIBLIOGRAPHY

[1] M. V. Berry, *Faster than Fourier* in Quantum Coherence and Reality; in celebration of the 60th Birthday of Yakir Aharonov (J S Anandan and J L Safko, eds.) World Scientific, Singapore, pp 55-65, (1994).

[2] M. V. Berry & S. Popescu, *Evolution of quantum superoscillations, and optical superresolution without evanescent waves*, J.Phys. A. Math. Gen. **39** 6965-6977, (2006).

[3] P. J. S. G. Ferreira & A. Kempf, *The energy expense of superoscillations, in Signal Processing*, XI-Theories vol. II, pp. 347-350 (2002).

[4] A. Kempf & P. J. S. G. Ferreira, *Unusual properties of superoscillating particles*, J. Phys. A: Math. Gen. **37** 12067-12076, (2004).

[5] M. S. Calder & A. Kempf, *Analysis of superoscillatory wave functions*, Journal of Mathematical Physics 46, 012101 (2005).

[6] P. J. S. G. Ferreira & A. Kempf, *Superoscillations: Faster Than the Nyquist Rate*, VOL. 54, NO. 10, (2006).

[7] P. J. S. G. Ferreira1, A. Kempf & M. J. C. S. Reis, *Construction of Aharonov Berry superoscillations*, J. Phys. A: Math. Theor. **40** 5141, (2007).

[8] M. R. Dennis, A. C. Hamilton & J. Courtial, Optics Letters, Vol. 33, p. 2976 - 2978, (2008).

[9] M. V. Berry & M. R. Dennis, *Natural superoscillations in monochromatic waves in D dimensions*, J.Phys. A. Math. Gen. **42** 022003, (2009).

[10] M. V. Berry & P. Shukla, *Pointer supershifts and superoscillations in weak measurements*, J. Phys. A: Math. Theor. **45** 015301 (14pp), (2012).

[11] M. V. Berry, *Exact nonparaxial transmission of subwavelength detail using superoscillations*, J. Phys. A: Math. Theor. **46** 205203 (15pp), (2013).

[12] M.V. Berry, *Superoscillations, Endfire and Supergain*, Quantum Theory: A Two-Time Success Story, (2014).

[13] M. V. Berry & N. Moiseyev, *Superoscillations and supershifts in phase space: Wigner and Husimi function interpretations*, J. Phys. A: Math. Theor **47** 315203 (14pp), (2014).

[14] N. I. Zheludev *What diffraction limit?*, Nature, Vol. 7, (2008).

[15] A. Erdelyi, Asymptotic expansions, New York: Dover Publications, (1956).

[16] H. Jeffreys & B. Jeffreys, Methods of mathematical physics, Cambridge: C.U.P, (1956).

[17] E. T. Copson, Asymptotics Expansions, Cambridge University Press, (2005).

[18] N. G. de Bruijn, Asymptotic Methods in Analysis, New York, Dover, (1981).

[19] D. Griffiths, Quantum Mechanics, Pearson Prentice Hall, (2005).

[20] L. E. Ballentine, Quantum Mechanics, Prentice-Hall, (1990).

[21] R. Eisberg & R. Resnick, Quantum Physics of Atoms, Molecules, Solids, Nuclei and Particles, John Wiley & Sons, (1985).

[22] M. Abramowitz & I. Stegun, Handbook of Mathematical Functions, New York: Dover Publications, (1965).

[23] I. S. Gradshteyn & I. M. Ryzhik, Table of Integrals, Series and Products, 7th ed, San Diego: Academic Press, (2007).

[24] See K. Hira, Eur. J. Phys. **34**, 777, (2013). for example.

APPENDIX

A

MATLAB CODES

This appendix contains MATLAB codes created to computationally exhibit superoscillations as figures in the preceding chapters. The codes included are as follows:

a. Fits $f(x) = (cos(x) + iasin(x))^N$ with a linear combination of harmonic oscillator eigenfunctions. For a series of times displayed as a density map.

b. Calculates the wavepacket $f(x) = (cos(x)+iasin(x))^N$ using the propagator for the Harmonic oscillator. For a series of times displayed as a density map.

c. Calculates the wavefunction for the harmonic oscillator according to Equation [5.4.25]. These equations are valid in the small x and small t limit only. For a series of times displayed as a density map.

d. Calculates $\psi(x,t)$ using Equation [5.5.13]. It reads in x, t, ω and calculates η, τ and Ω. Then it works out the wavefunction. For a series of times displayed as a density map.

```
%%%%%%%%%%%%%%%%%%%%%%%%%%%%%%%%%%%%%%%%%%%%%%%%%%%%%%%%%%%%%%%%%%%%%%%%%%%%
% Fits f(x)=(cos(x)+1ia sin(x))^N with a linear combination of harmonic %
% oscillator eigenfunctions.                                             %
% The parameters needed for convergence are                              %
% N=10, a=2.0, nmax=42.                                                  %
% N=14, a=1.5, nmax=65.                                                  %
% N=14, a=1.6, nmax=63.                                                  %
% N=14, a=1.7, nmax=61.                                                  %
% N=14, a=1.8, nmax=61.                                                  %
% N=14, a=1.9, nmax=57.                                                  %
% N=14, a=2.0, nmax=59.                                                  %
% N=14, a=2.5  nmax=56.                                                  %
% N=14, a=3.0  Not stable.                                               %
% N=16, a=1.5, nmax=56.                                                  %
% N=14, a,1.5, nmax=99, om=0.1.                                          %
% The hermite polynomials cannot be calculated beyonds n=170.            %
% It does this for a series of times and Plots a density map.            %
%%%%%%%%%%%%%%%%%%%%%%%%%%%%%%%%%%%%%%%%%%%%%%%%%%%%%%%%%%%%%%%%%%%%%%%%%%%%
clear
N = 14;
a = 2;
om = 1.0;
p = 1;
k = 1;
tmin = 0.000*pi;
tmax = 0.50*pi;
dt = 0.002*pi;
t = tmin:dt:tmax;
nt = round(1+(tmax-tmin)/dt);
xmin = -1.0*pi;
xmax = +1.0*pi;
dx = 0.0001*pi;
nx = round(1+(xmax-xmin)/dx);
x = xmin:dx:xmax;
sum = 0;
for im = 0:N
    term = (a^2-1)^im*gamma(im+1/2)/(gamma(im+1)^2*gamma(N-im+1));
    sum = sum+term;
end
G = 2*sqrt(pi)*gamma(N+1)*sum/p;
norm = 1/sqrt(G);
nmin = 0;
nmax = 59;
f1 = norm*(cos(p*x)+1i*a*sin(p*x)).^(k*N);
az = f1.*conj(f1);
zz = simp(dx,nx,x,az);
y = sqrt(N*om)*x;
sum = zeros(nt,nx);
c2 = zeros(1,nmax+1);
```

```
c1 = zeros(1,nmax+1);
q = zeros(1,nmax+1);
p1 = (N*om/(pi))^(1/4);
e1 = exp(-(y.^2)/2);
for n = nmin:nmax
    E(n+1) = (n+1/2)*N*om;
    z = e1.*herm(n,y).*f1;
    c2(n+1) = 1/sqrt(2^n.*factorial(n));
    q = simp(dx,nx,x,z);
    c1(n+1) = c2(n+1)*q;
end
cn = p1.*c1;
for it = 1:nt
    for n = nmin:nmax
        e2(it) = exp(-1i*E(n+1)*t(it)/N);
        pre1(it) = cn(n+1)*c2(n+1)*p1*e2(it);
        term1(it,:) = pre1(it)*e1.*herm(n,y);
        sum(it,:) = sum(it,:)+term1(it,:);
    end
end
psi =  sum;
psilog = log(real(sum));
%f2 = log(real(f1));
contour(x/pi,t/pi,psilog,25)
set(gca, 'color', [0 0 0])
axis([-0.5 0.5 0 1])
```

```
%%%%%%%%%%%%%%%%%%%%%%%%%%%%%%%%%%%%%%%%%%%%%%%%%%%%%%%%%%%%%%%%%%%%%%%%
% Calculates the the wavepacket(cos px + i sin px)^N using the  %
% propagator for the Harmonic oscillator.                       %
% For a series of times displayed as a density map.             %
%%%%%%%%%%%%%%%%%%%%%%%%%%%%%%%%%%%%%%%%%%%%%%%%%%%%%%%%%%%%%%%%%%%%%%%%
clear
tmin = 0.000;
tmax = 0.04*pi;
dt = 0.001*pi;
t = tmin:dt:tmax;
nt = round(1+(tmax-tmin)/dt);
for it = 1:nt
    if t(it) == 0
        t(it) = 2*pi;
    end
end
N = 20;
a = 4;
om = 1.0;
p = 1.0;
k = 1.0;
xmin = -2.000;
xmax = +2.000;
for it = 1:nt
    dx = 0.005;
    nx = round(1+(xmax-xmin)/dx);
    x = xmin:dx:xmax;
    SUM = 0;
    for im = 0:N
        term = (a^2-1)^im*gamma(im+1/2)/(gamma(im+1)^2*gamma(N-im+1));
        SUM = SUM+term;
    end
    G = 2*sqrt(pi)*gamma(N+1)*SUM/p;
    norm = 1/sqrt(G);
    xpmin = -2.500;
    xpmax = +2.500;
    if t(it) >= 0.430*pi && t(it) <= 0.570*pi || t(it) >= 1.430*pi && t(it) <= 1.570*pi
        xpmin = -3.1500;
        xpmax = +3.1500;
    end
    dxp = 0.005;
    xprmin = xpmin;
    xprmax = xpmax;
    dxpr = dxp;
    npr = round(1+(xprmax-xprmin)/dxpr);
    xpr = xprmin:dxpr:xprmax;
    xpcmin = xpmin;
    xpcmax = xpmax;
    dxpc = dxp;
```

```
npc = round(1+(xpcmax-xpcmin)/dxpc);
xpc = xpcmin:dxpc:xpcmax;
Kern = zeros(3,3);
xj = zeros(nx,2);
f1 = zeros(1,nx);
f2 = zeros(1,nx);
f = zeros(1,nx);
qp = zeros(1,nx);
p1 = zeros(1,nx);
p2 = zeros(1,nx);
psi = zeros(1,nx);
psilog = zeros(1,nx);
f4 = zeros(1,nx);
f5 = zeros(1,nx);
qp1 = zeros(1,nx);
p3 = zeros(1,nx);
p4 = zeros(1,nx);
psi1 = zeros(1,nx);
psi2 = zeros(1,nx);
psilog1 = zeros(1,nx);
psilogt = zeros(1,nx);
xp = zeros(npr,npc);
for ipr = 1:npr
    for ipc = 1:npc
        xp(ipr,ipc) = xpr(ipr)+1i*xpc(ipc);
    end
end
q = zeros(npr,npc);
q = p*k*(1i*sin(p*xp)+a*cos(p*xp))./(cos(p*xp)+1i*a*sin(p*xp));
lhs = sin(om*t(it))*q;
for ix = 1:nx
    rhs = om*(x(ix)-xp*cos(om*t(it)));
    frac = (lhs-rhs);
    Sfrac = frac;
    for ij = 1:2
        [low,Arr] = min(abs(frac(:)));
        [ipr,ipc] = ind2sub(size(frac),Arr);
        for ixx = 1:3
            for iy = 1:3
                nX = ipr-2+ixx;
                nY = ipc-2+iy;
                if nX >= 1 && nX <= npr
                    if nY >= 1 && nY <= npc
                        Kern(ixx,iy) = str2num(sprintf('%.20f',Sfrac(nX,nY)));
                    end
                end
                if nX < 1 || nX > npr
                    Kern(ixx,iy) = str2num(sprintf('%.20f',Sfrac(ipr,ipc)));
                end
```

```
        if nY < 1 || nY > npc
            Kern(ixx,iy) = str2num(sprintf('%.20f',Sfrac(ipr,ipc)));
        end
    end
end
if ij <= 1
    SKern = Kern;
end
fipc = 0;
fipr = 0;
Fipr = 0;
Fipc = 0;
if Kern(2,2) < 0
    if Kern(1,2) > 0
        dyy = Kern(1,2)-Kern(2,2);
        dyy = dyy/99;
        Axx = Kern(2,2):dyy:Kern(1,2);
        [Low,Arr] = min(abs(Axx));
        [fipr] = -(ind2sub(size(Axx),Arr)-1);
        Fipr = fipr*dxpc/100;
        Fipc = fipc*dxpc/100*1i;
    end
    if Kern(3,2)>0
        dyy = Kern(3,2)-Kern(2,2);
        dyy = dyy/99;
        Axx = Kern(2,2):dyy:Kern(3,2);
        [Low,Arr] = min(abs(Axx));
        [fipr] = ind2sub(size(Axx),Arr)-1;
        Fipr = fipr*dxpc/100;
        Fipc = fipc*dxpc/100*1i;
    end
end
if Kern(2,2)>0
    if Kern(1,2)<0
        dyy = Kern(1,2)-Kern(2,2);
        dyy = dyy/99;
        Axx = Kern(2,2):dyy:Kern(1,2);
        [Low,Arr] = min(abs(Axx));
        [fipr] = -(ind2sub(size(Axx),Arr)-1);
        Fipr = fipr*dxpc/100;
        Fipc = fipc*dxpc/100*1i;
    end
    if Kern(3,2)<0
        dyy = Kern(3,2)-Kern(2,2);
        dyy = dyy/99;
        Axx = Kern(2,2):dyy:Kern(3,2);
        [Low,Arr] = min(abs(Axx));
        [fipr] = ind2sub(size(Axx),Arr)-1;
        Fipr = fipr*dxpc/100;
```

```
            Fipc = fipc*dxpc/100*1i;
        end
    end
    iq = ix-1;
    if ij <= 1
        xj(ix,1) = xp(ipr,ipc)+Fipc+Fipr;
    end
    if ij >= 2
        xj(ix,2) = xp(ipr,ipc)+Fipc+Fipr;
        if ipr-1 >= 1
            Test = frac(ipr-1,ipc);
            if Test == 10
                xj(ix,2) = NaN;
            end
        end
        if ipr+1 <= npr
            Test = frac(ipr+1,ipc);
            if Test == 10
                xj(ix,2) = NaN;
            end
        end
        if ipc-1 >= 1
            Test = frac(ipr,ipc-1);
            if Test == 10
                xj(ix,2) = NaN;
            end
        end
        if ipc+1 <= npc
            Test = frac(ipr,ipc+1);
            if Test == 10
                xj(ix,2) = NaN;
            end
        end
    end
    Sipr(ij) = ipr;
    Sipc(ij) = ipc;
    frac(ipr,ipc) = 10;
    if t(it) >= 0.032*pi && t(it)<=0.968*pi || t(it) >= 1.032*pi && t(it)<=1.968*p
        for Kfx = -5:5
            for Kfy = -5:5
                ipr1 = ipr+Kfx;
                ipc1 = ipc+Kfy;
                if ipr1 >= 1 && ipr1 <= npr
                    if ipc1 >= 1 && ipc1 <= npc
                        frac(ipr1,ipc1) = 10;
                    end
                end
            end
        end
```

```
        end
    end
end
for ix = 1:nx
    if ix+1 <= nx
        dif1 = abs(xj(ix,1)-xj(ix+1,1));
        dif2 = abs(xj(ix,1)-xj(ix+1,2));
        if dif2 <= dif1
            switch1 = xj(ix+1,1);
            switch2 = xj(ix+1,2);
            xj(ix+1,2) = switch1;
            xj(ix+1,1) = switch2;
        end
    end
end
Sortxj(:,1) = xj(:,2);
for ix = 1:nx
    if isnan(Sortxj(ix,1)) <= 0
        if ix+1 <= nx
            if isnan(Sortxj(ix+1,1)) >= 1
                xj(ix,2) = NaN;
            end
            if ix-1 >= 1
                if isnan(Sortxj(ix-1,1)) <= 0

                    xj(ix,2) = Sortxj(ix,1);
                end
            end
        end
    end
end
Sortxj(:,1) = xj(:,2);
for ix = 1:nx
    if isnan(Sortxj(ix,1)) <= 0
        if ix+10 <= nx
            A = [Sortxj(ix+2,1) Sortxj(ix+3,1) Sortxj(ix+4,1) Sortxj(ix+5,1) Sortxj(ix
            A = real(A);
            for tidy = 1:9
                if isnan(A(tidy))
                    A(tidy) = 0;
                end
            end
            xj(ix,2) = NaN;
            if sum(A) >= 1
                xj(ix,2) = Sortxj(ix,1);
            end
            if ix-3 >= 1
                if isnan(Sortxj(ix-3,1)) <= 0
                    xj(ix,2) = Sortxj(ix,1);
```

```
                    end
                end
            end
        end
    end
    for ix = 1:nx
        f1(ix) = cos(p*(xj(ix,1)))+1i*a*sin(p*(xj(ix,1)));
        f(ix) = f1(ix)^(k*N);
        qp(ix) = 1i*p^2*k*(1-a^2)/f1(ix)^2;
        p1(ix) = sqrt(om/(qp(ix)*sin(om*t(it))+om*cos(om*t(it))));
        r1 = (x(ix)^2+(xj(ix,1)^2))*cos(om*t(it))-2*x(ix)*(xj(ix,1));
        p2(ix) = exp(1i*N*om*r1/(2*sin(om*t(it))));
        psi(ix) = p1(ix)*f(ix)*p2(ix)*norm;
        psilog(ix) = log(real(psi(ix)));
        DensityGrid(it,ix) = psilog(ix);
    end
    for ix = 1:nx
        f4(ix) = cos(p*(xj(ix,2)))+1i*a*sin(p*(xj(ix,2)));
        f5(ix) = f4(ix)^(k*N);
        qp1(ix) = 1i*p^2*k*(1-a^2)/f4(ix)^2;
        p3(ix) = sqrt(om/(qp1(ix)*sin(om*t(it))+om*cos(om*t(it))));
        r2 = (x(ix)^2+(xj(ix,2)^2))*cos(om*t(it))-2*x(ix)*(xj(ix,2));
        p4(ix) = exp(1i*N*om*r2/(2*sin(om*t(it))));
        psi1(ix) = p3(ix)*f5(ix)*p4(ix)*norm;
        if isnan(psi1(ix))
            psi1(ix) = 0;
        end
        if t(it) <= 0.014*pi || t(it) >= 0.986*pi && t(it) <= 1.014*pi || t(it) >= 1.986*p
            psi1(ix) = 0;
        end
        psi2(ix) = psi(ix)+psi1(ix);
        psilog1(ix) = log(real(psi1(ix)));
        psilogt(ix) = log(real(psi2(ix)));
        DensityGrid1(it,ix) = psilog1(ix);
        DensityGridt(it,ix) = psilogt(ix);
    end
end
contour(x/pi,t/pi,Tree,50)
set(gca, 'color', [0 0 0])
axis([-0.5 0.5 0 2])
```

```
%%%%%%%%%%%%%%%%%%%%%%%%%%%%%%%%%%%%%%%%%%%%%%%%%%%%%%%%%%%%%%%%%%%%%%%%%%%%
% Calculates the wavefunction for the harmonic oscillator                     %
% according to Equation [5.4.25].                                             %
% These equations are valid in the small x and small t limit only.            %
% For a series of times displayed as a density map.                           %
%%%%%%%%%%%%%%%%%%%%%%%%%%%%%%%%%%%%%%%%%%%%%%%%%%%%%%%%%%%%%%%%%%%%%%%%%%%%
clear
a = 4.0;
N = 20;
om = 1.00;
k = 1;
p = 1;
xmin = -0.50*pi;
xmax = +0.50*pi;
dx = 0.001*pi;
nx = round(1+(xmax-xmin)/dx);
x = xmin:dx:xmax;
tmin = +0.001*pi;
tmax = +2.001*pi;
dt = 0.002*pi;
nt = round(1+(tmax-tmin)/dt);
t = tmin:dt:tmax;
eta = a*p*x;
Om = om/(a*p)^2;
N1 = factorial(N);
sum = 0;
for im = 0:N
    term = (a^2-1)^im*gamma(im+1/2)/(gamma(im+1)^2*gamma(N-im+1));
    sum = sum+term;
end
G = 2*sqrt(pi)*gamma(N+1)*sum;
sum = zeros(1,nx);
psa = zeros(1,nx);
psalog = zeros(1,nx);
p1 = zeros(1,nx);
s = zeros(2,nx);
e1 = zeros(1,nx);
for it = 1:nt
    tau(it) = (a*p)^2*t(it);
    ct = cos(Om*tau(it));
    st = sin(Om*tau(it));
    p1 = N1*((ct+1i*eta)/ct).^N;
    e1 = exp(-1i*N*Om*eta.^2*tan(Om*tau(it))/2);
    sum = zeros(1,nx);
    for m = 0:N/2;
        p2 = 1/(factorial(m)*factorial(N-2*m));
        term = p2*(-1i*st/(2*N*Om*ct))^m*(ct./(ct+1i*eta)).^(2*m);
        sum = sum+term;
    end
```

```
    psa(it,:) = p1.*sum.*e1/sqrt(G*ct);
    psalog(it,:) = log(real(psa(it,:)));
end
contour(x,t,psalog,50)
set(gca, 'color', [0 0 0])
```

```
%%%%%%%%%%%%%%%%%%%%%%%%%%%%%%%%%%%%%%%%%%%%%%%%%%%%%%%%%%%%%%%%%%%%%%%%%%%%%%%
% Calculates psi(x,t) using Equation [5.5.13]. It reads                        %
% in x, t, omega and calculates eta, tau and Omega. Then it works out the      %
% wavefunction. For a series of times displayed as a density map.              %
%%%%%%%%%%%%%%%%%%%%%%%%%%%%%%%%%%%%%%%%%%%%%%%%%%%%%%%%%%%%%%%%%%%%%%%%%%%%%%%
clear
tmin = +0.001*pi;
tmax = +0.041*pi;
dt = 0.002*pi;
nt = round(1+(tmax-tmin)/dt);
t = tmin:dt:tmax;
xmin = -0.50*pi;
xmax = +0.50*pi;
dx = 0.001*pi;
nx = round(1+(xmax-xmin)/dx);
x = xmin:dx:xmax;
p = 1;
k = 1;
a = 4.0;
N = 20;
Nk = N*k;
N1 = factorial(Nk);
om = 1.0;
Om = om/(a*p)^2;
eta = a*p*x;
deta = a*p*dx;
tau = a^2*p^2*t;
suma = 0;
for im = 0:Nk
    term = (a^2-1)^im*gamma(im+1/2)/(gamma(im+1)^2*gamma(Nk-im+1));
    suma = suma+term;
end
G = 2*sqrt(pi)*gamma(Nk+1)*suma;
for it = 1:nt
    ct = cos(Om*tau(it));
    st = sin(Om*tau(it));
    d = sqrt(1-eta.^2/ct^2+2*1i*(eta-2*k*st/Om)/ct);
    s(1,:) = 0.5*(eta(:)/ct+1i-1i*d(:));
    s(2,:) = 0.5*(eta(:)/ct+1i+1i*d(:));
    for ix = 1:nx
        for is = 1:2
            uta(is,ix) = Om*((eta(ix)^2+s(is,ix)^2)*ct-2*eta(ix)*s(is,ix));
        end
    end
    Phi(1,:) = -1i*k*log(1+1i*s(1,:))+uta(1,:)/(2*st);
    Phi(2,:) = -1i*k*log(1+1i*s(2,:))+uta(2,:)/(2*st);
    eiphi(1,:) = exp(1i*N*Phi(1,:));
    eiphi(2,:) = exp(1i*N*Phi(2,:));
    dq(1,:) = -1i*k./((1+1i*s(1,:)).^2);
```

```
    dq(2,:) = -1i*k./((1+1i*s(2,:)).^2);
    psu(1,:) = eiphi(1,:).*sqrt(Om./(Om*ct+st*dq(1,:)));
    psu(2,:) = eiphi(2,:).*sqrt(Om./(Om*ct+st*dq(2,:)));
    if (it >= 1) && (it <= 8)
        psu(2,:) = 0;
    end
    if (it >= 9) && (it <= 14)
        for ifix = 725:1001
            psu(2,ifix) = 0;
        end
    end
    psb(it,:) = (psu(1,:)+psu(2,:))/sqrt(G);
    psb1(it,:) = psu(1,:)/sqrt(G);
    psb2(it,:) = psu(2,:)/sqrt(G);
    psv1(it,:) = log(real(psb1(it,:)));
    psv2(it,:) = log(real(psb2(it,:)));
    psv(it,:) = log(real(psb(it,:)));
end
contour(x/pi,t,psv,75)
set(gca, 'color', [0 0 0])
```